

Chesapeake Bay Sediment Flux Model

Dominic M. Di Toro

Edward C. Davis Professor of Civil and Environmental Engineering
Department of Civil and Environmental Engineering
University of Delaware
Newark, DE 19716



Tech Transfer Workshop

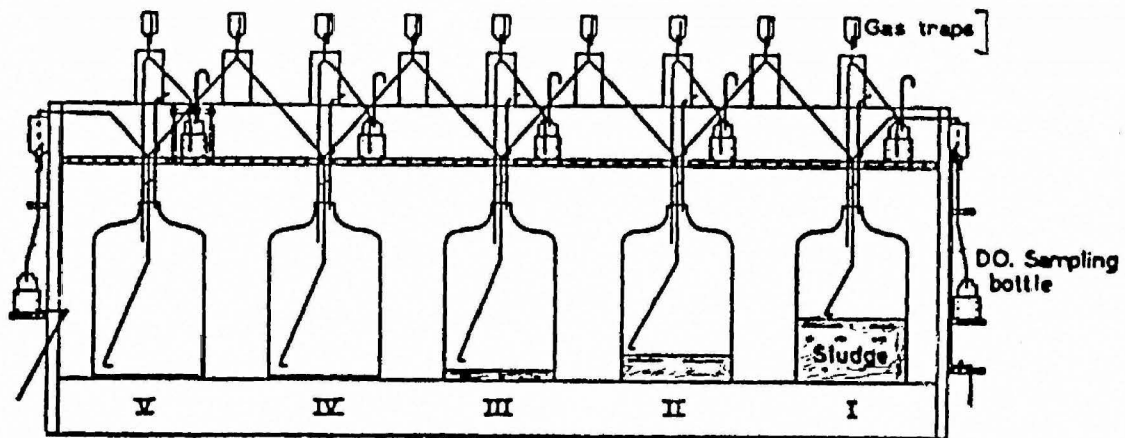
March 12 – 14th, 2019

IAN Annapolis Office, Large Conference Room.

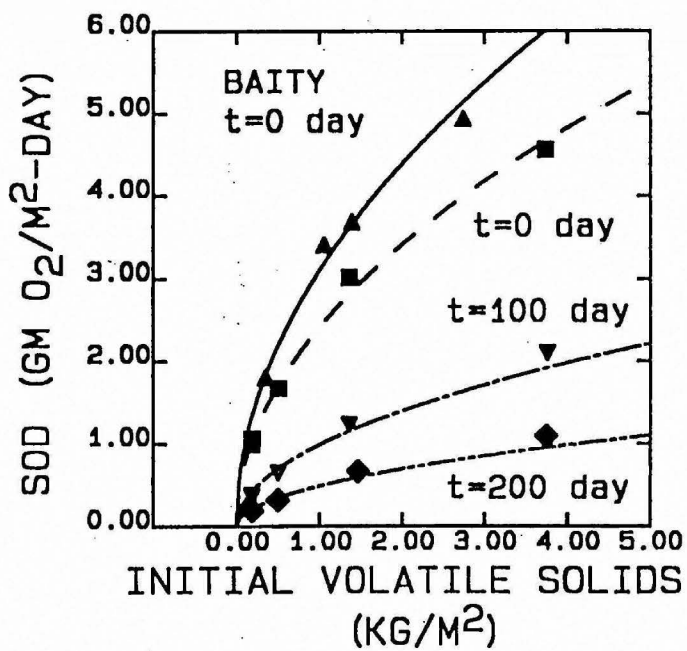
Address: 429 4th Street, Annapolis, MD 21403

Sediment Oxygen Demand

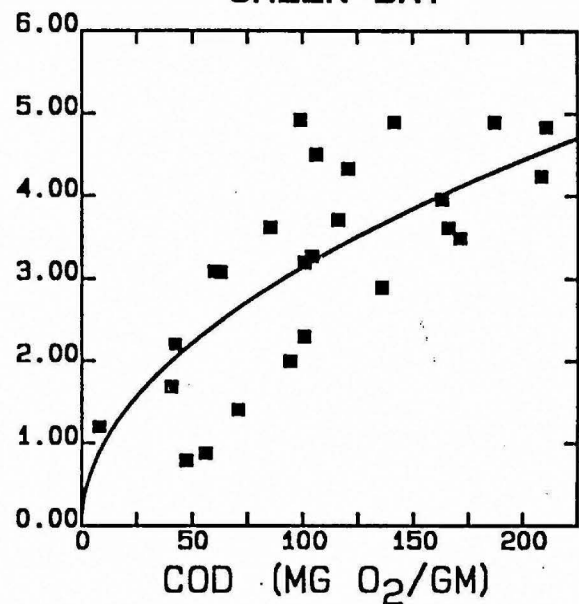
Fair, Moore, and Thomas 1941



FAIR, MOORE, & THOMAS



GREEN BAY



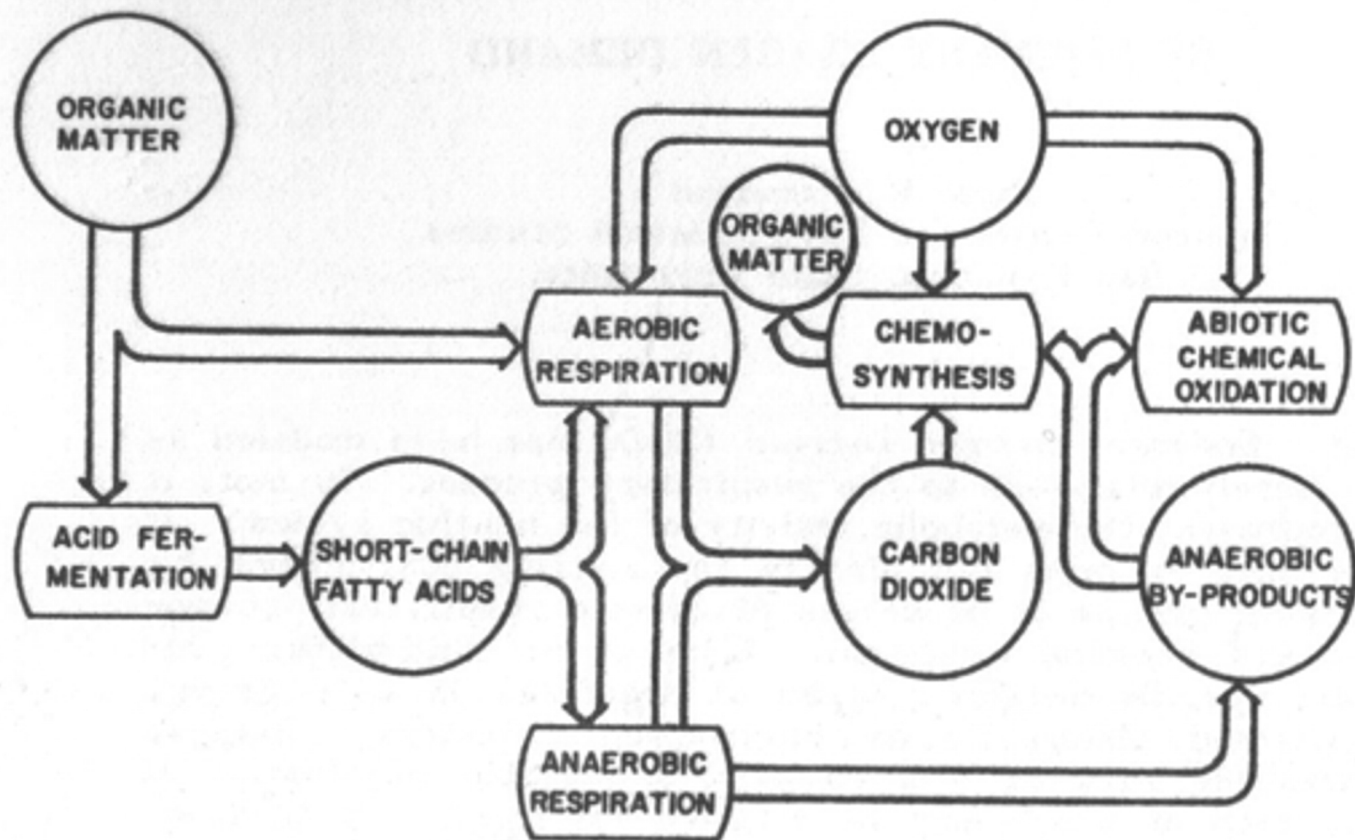


Figure 1. The relationship among oxygen-consuming and anaerobic benthic processes. Aerobic respiration and chemosynthesis are both oxygen-consuming processes, but the latter is accompanied by carbon dioxide uptake while respiration produces carbon dioxide. Oxidation of sulfides, ferrous, manganous, etc., by chemosynthetic organisms has not been distinguished from abiotic chemical oxidation.

Pamatmat (1986). Problems with empirical models of sediment oxygen demand. Sediment Oxygen Demand. Processes, Modeling and Measurement. K. J. Hatcher., Institute of Natural Resources, University of Georgia, Athens, GA.: 23-37.

TABLE 1. Oxygen-Consuming Processes in Sediment and Environmental Variables that Affect Sediment Oxygen Uptake

Oxygen-Consuming Processes	Environmental Variables
Biological Oxidation	Oxygen Pressure
Aerobic Respiration	Temperature
$(\text{CH}_2\text{O})_n + \text{CO}_2$	Salinity
Sulfide Oxidation	Light
$\text{S}^{2-} \rightarrow \text{S}^0 + \text{S}_2\text{O}_3^{2-} + \text{SO}_4^{2-}$	Hydrostatic Pressure
Nitrification	Turbulence
$\text{NH}_3 + \text{NO}_2^- + \text{NO}_3^-$	
Iron Oxidation	Sediment Properties
$\text{Fe}^{2+} \rightarrow \text{Fe}^{3+}$	Grain size
	Organic matter content
Methane Oxidation	
$\text{CH}_4 \rightarrow \text{CH}_3\text{OH} + \text{CO}_2$	Rate of Organic Matter Supply
	Primary productivity
Abiotic Chemical Oxidation	Sedimentation rate
$\text{S}^{2-} \rightarrow \text{SO}_4^{2-}$	Organic pollution
$\text{Fe}^{2+} \rightarrow \text{Fe}^{3+}$	Chemical Pollution
	Industrial
$\text{Mn}^{2+} \rightarrow \text{Mn}^{4+}$	Agricultural
	Domestic
Others	Community Structure

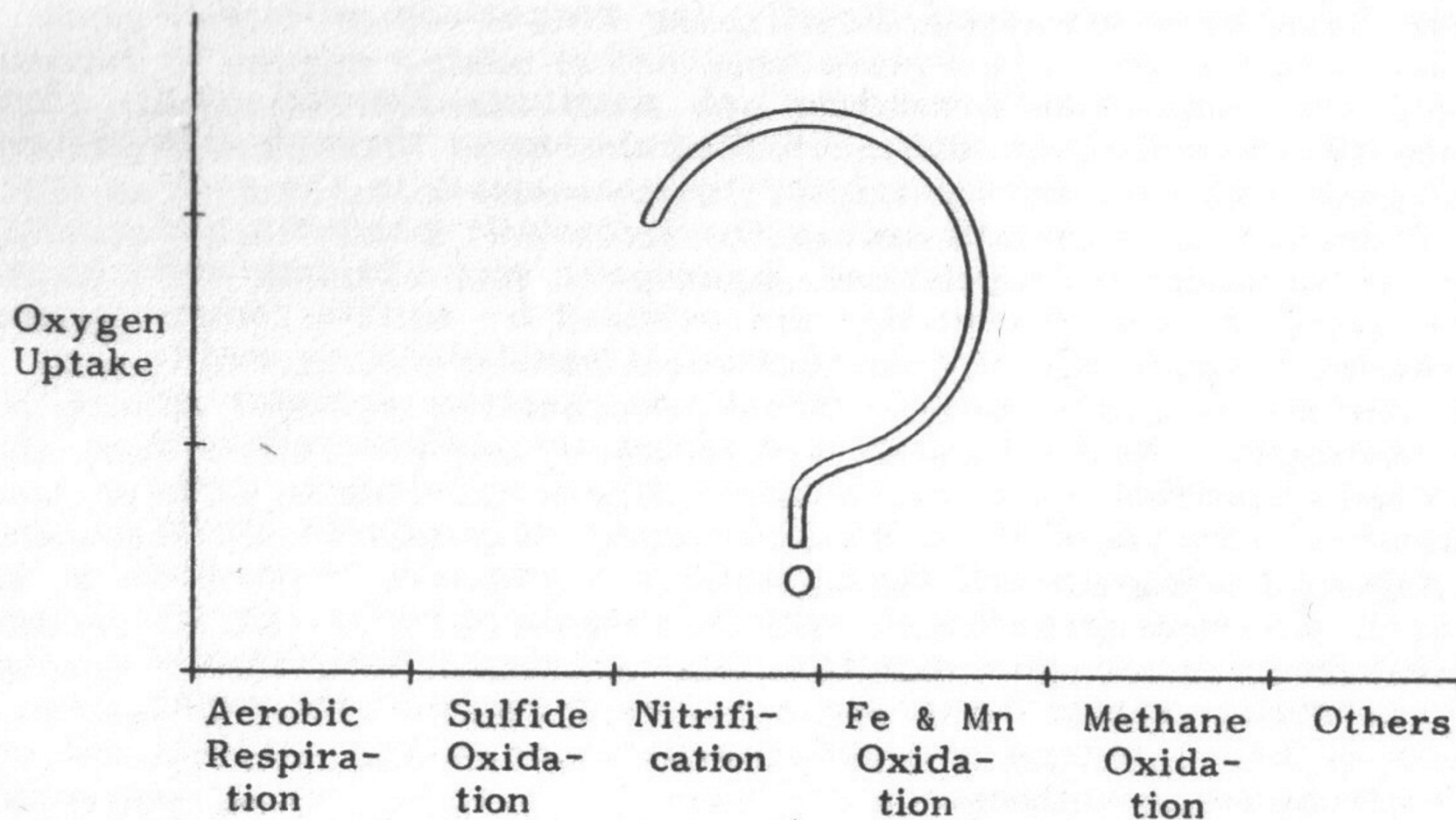


Figure 2. Curve summarizing present knowledge of SOD as an integral of the different oxygen consuming processes.

Pamatmat (1986). Problems with empirical models of sediment oxygen demand. Sediment Oxygen Demand. Processes, Modeling and Measurement. K. J. Hatcher., Institute of Natural Resources, University of Georgia, Athens, GA.: 23-37.

Sediment Flux Model

Sediment Diagenesis = Sediment Flux

- Flux of organic matter to the sediment is the source
- Fluxes are proportional to the stoichiometry of the decaying organic matter (Redfield stoichiometry)



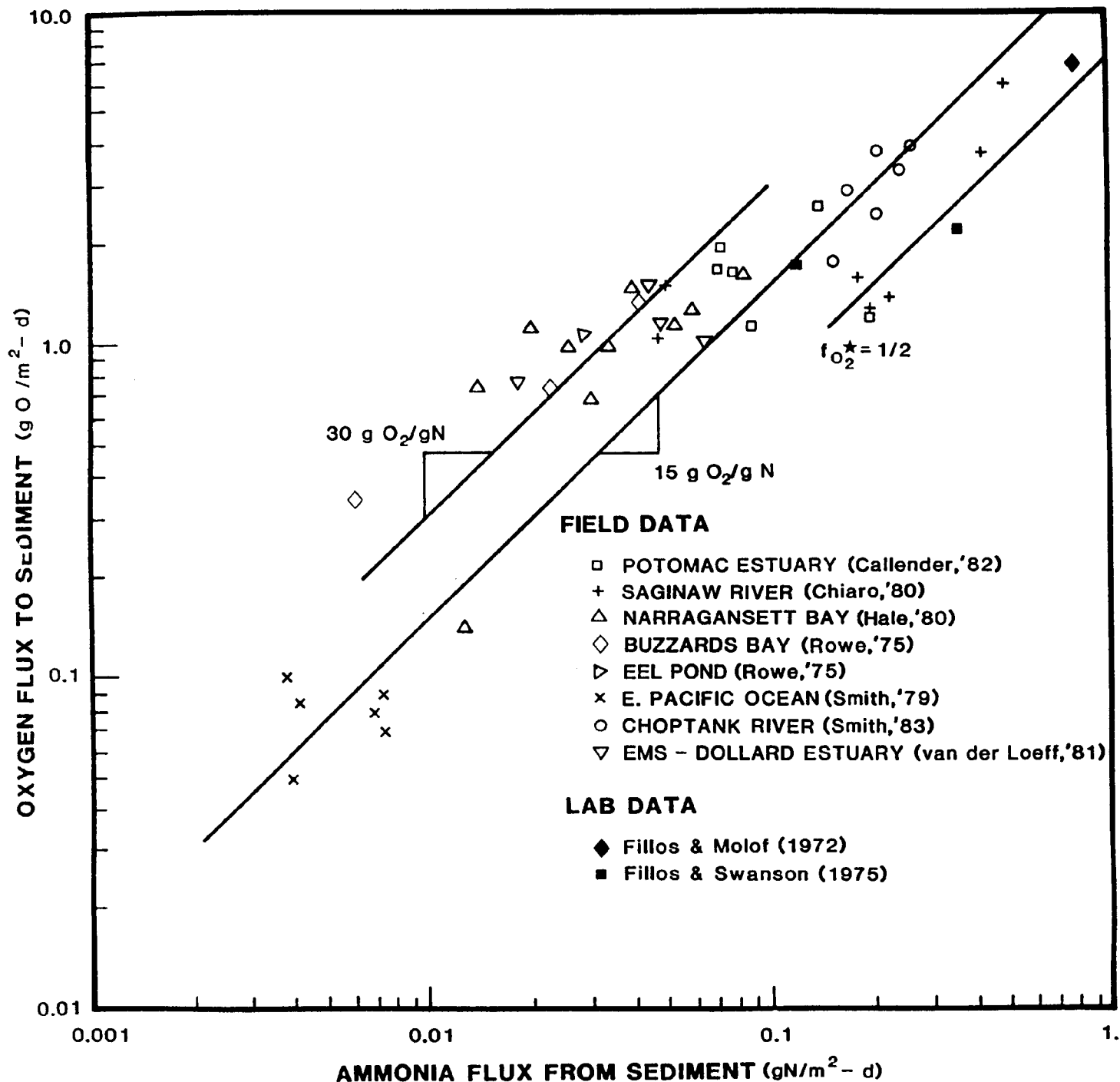
Ratio of fluxes

$$\frac{\text{SOD}}{\text{NH}_3} = \frac{106 (\text{O}_2) 32 (\text{gO}_2/\text{mol})}{16 (\text{N}) 14 (\text{gN}/\text{mol})} = 15.1 \text{ gO}_2/\text{g N}$$

Organic carbon oxidized by O_2
Ammonia conservative

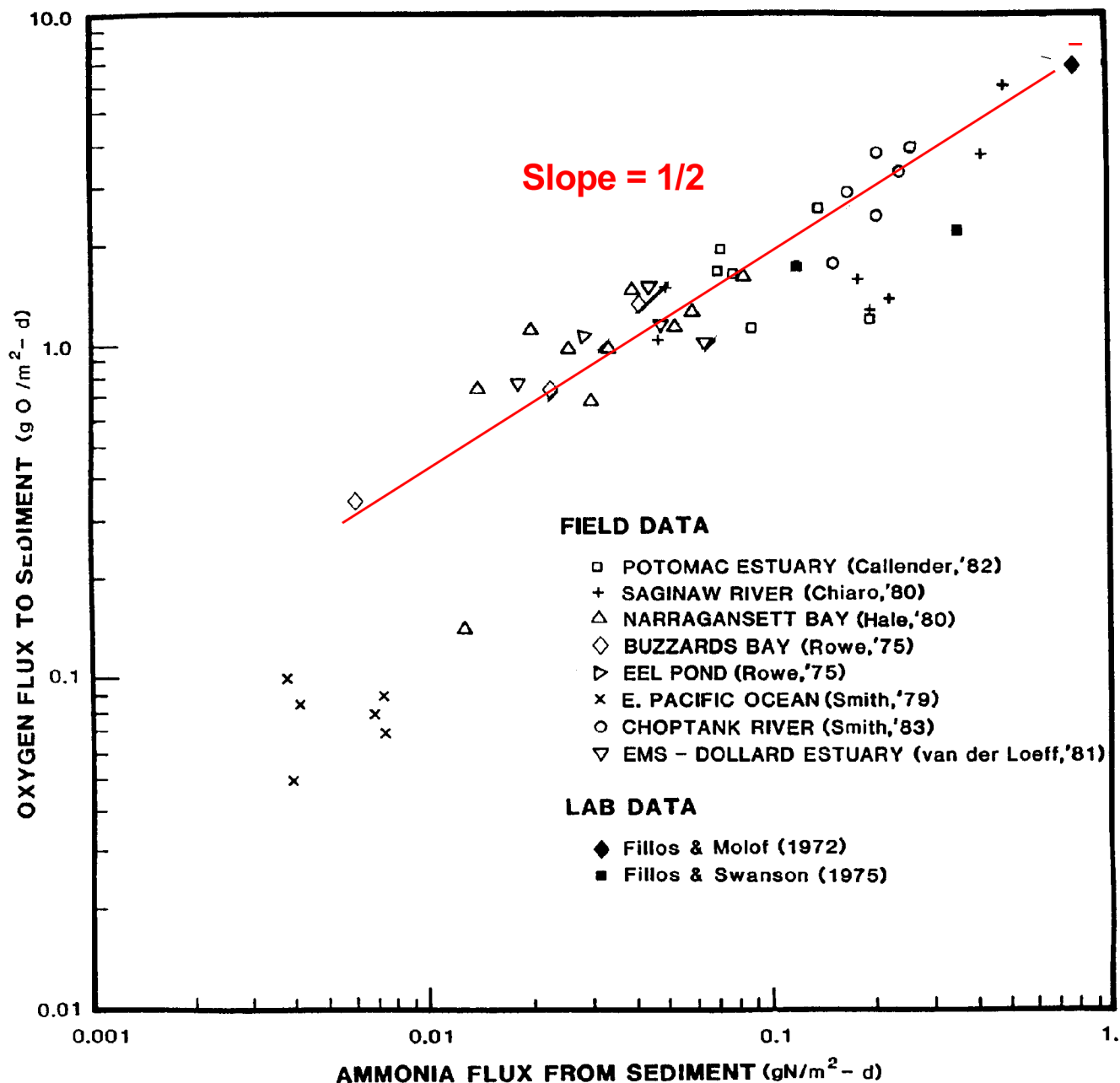
STOICHIOMETRIC FLUX RELATIONSHIP

(DIRECT MEASUREMENTS)

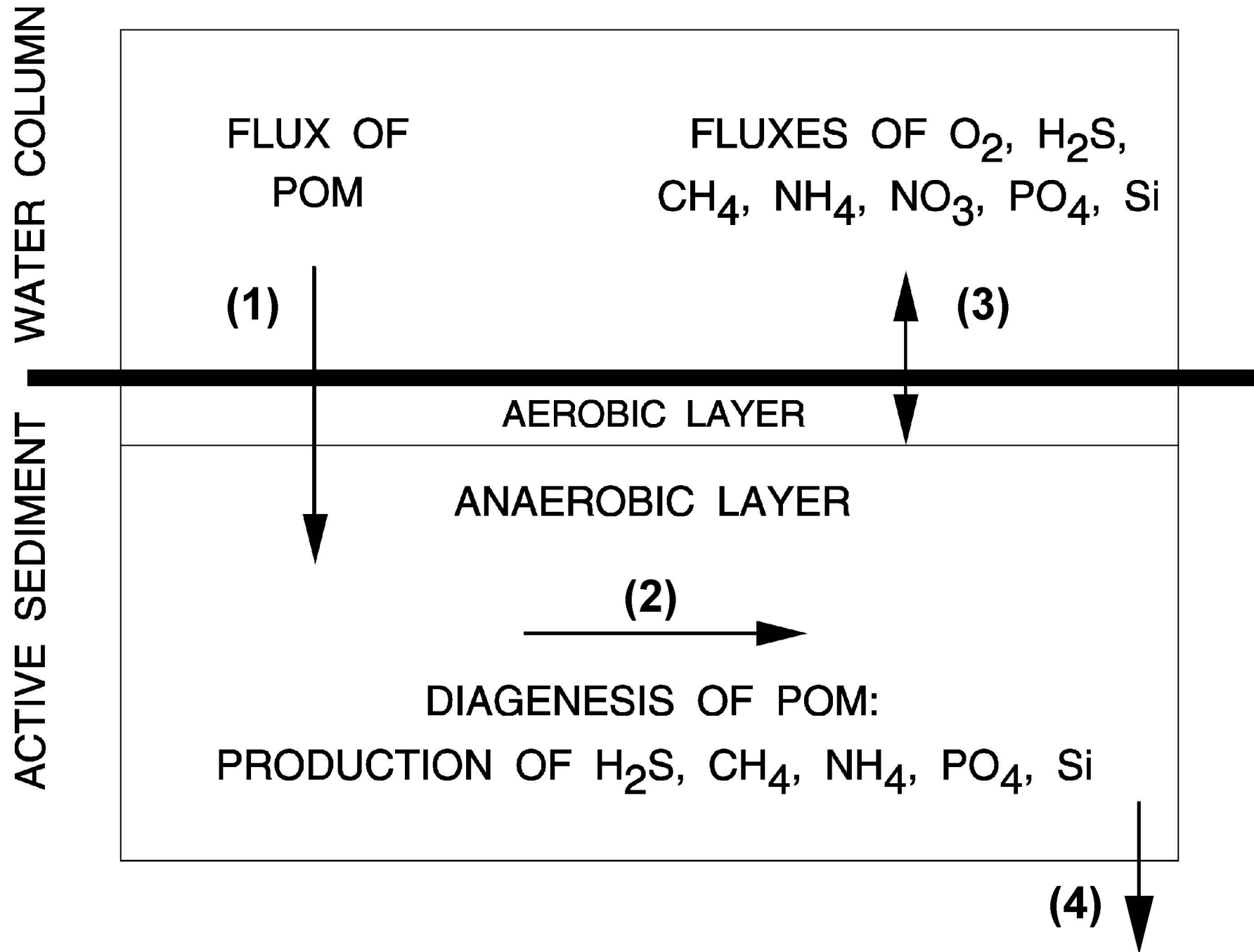


STOICHIOMETRIC FLUX RELATIONSHIP

(DIRECT MEASUREMENTS)

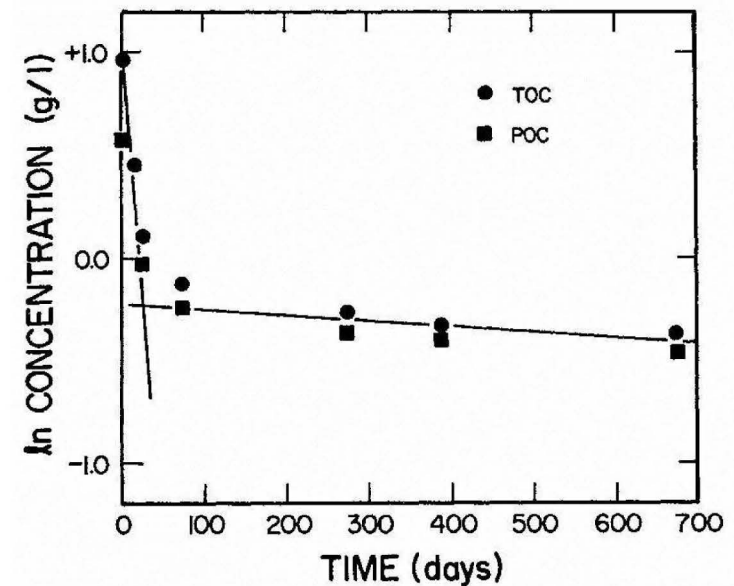
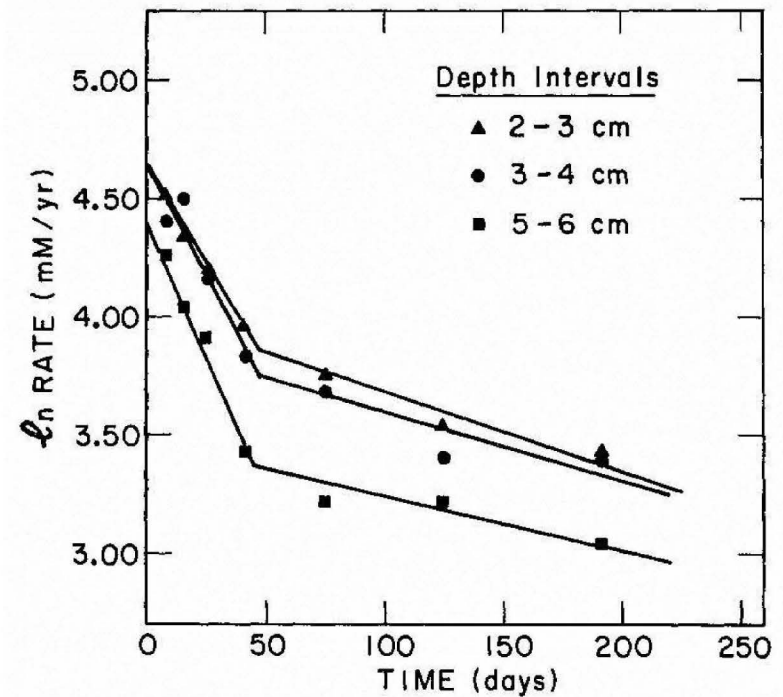
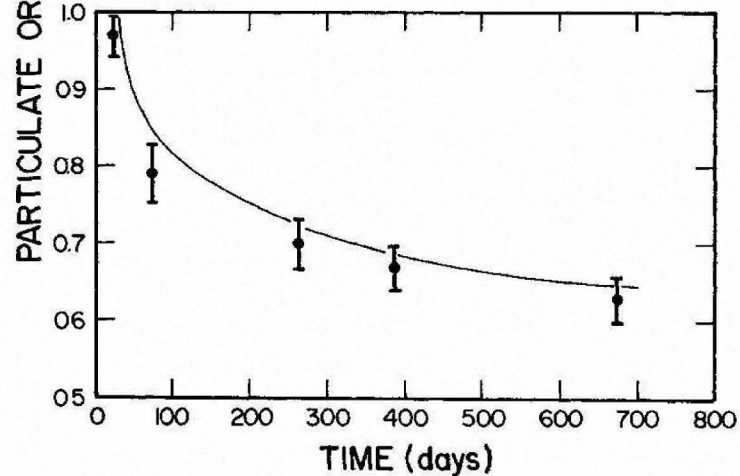
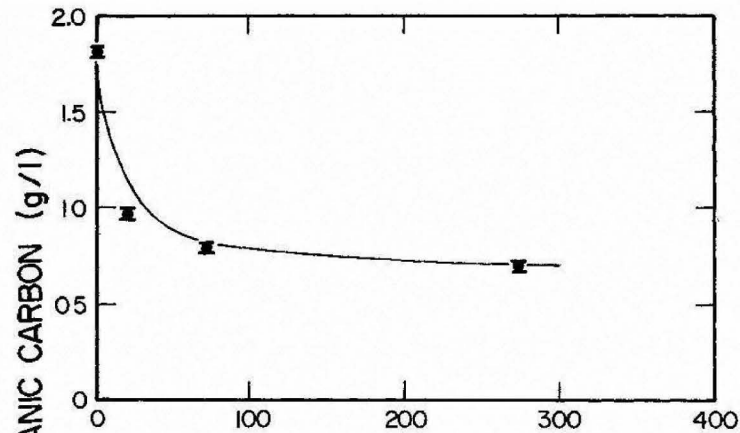


Schematic of Sediment Flux Model



Decay of Organic Matter

$$G_T(t) = G_{01}[\exp(-k_1 t)] + G_{02}[\exp(-k_2 t)] + G_{NR}$$



The Role of Sedimentary Organic Matter
in Bacterial Sulfate Reduction:

The G Model Tested

Westrich and Berner

Limnology and Oceanography, Vol. 29, No. 2, pp. 236-249

Sediment Diagenesis Model - Three G Model

- Diagenesis is the decay or decomposition of POM in the sediment bed
- The SFM uses Berner's 3G model framework, essentially splitting the deposited POM into labile (G_1), refractory (G_2), and inert (G_3) pools

<u>POC</u>	<u>G_1</u>	<u>G_2</u>	<u>G_3</u>
f_{POC}	0.65	0.20	0.15
k_{diag} (/day)	0.035	0.0018	0.0
1 "e-folding" (days)	28	555	
2 (Temp correction)	1.10	1.15	

θ	$Q_{10} = k(10)/k(20)$
1.068	0.518
1.100	0.386
1.150	0.247
$k_{10} = k_{20} \theta^{(-10)}$	

POC Mass Balance Equation

$$H \frac{dPOC_i}{dt} = f_{POC_i} J_{POC} - w_2 POC_i - H \cdot k_{POC_i} \theta_{POC_i} POC_i$$

where

H = depth of sediment (10 cm)

POC_i = concentration of POC in pool G_i

f_{POCi} = fraction of deposited POC going to G_i

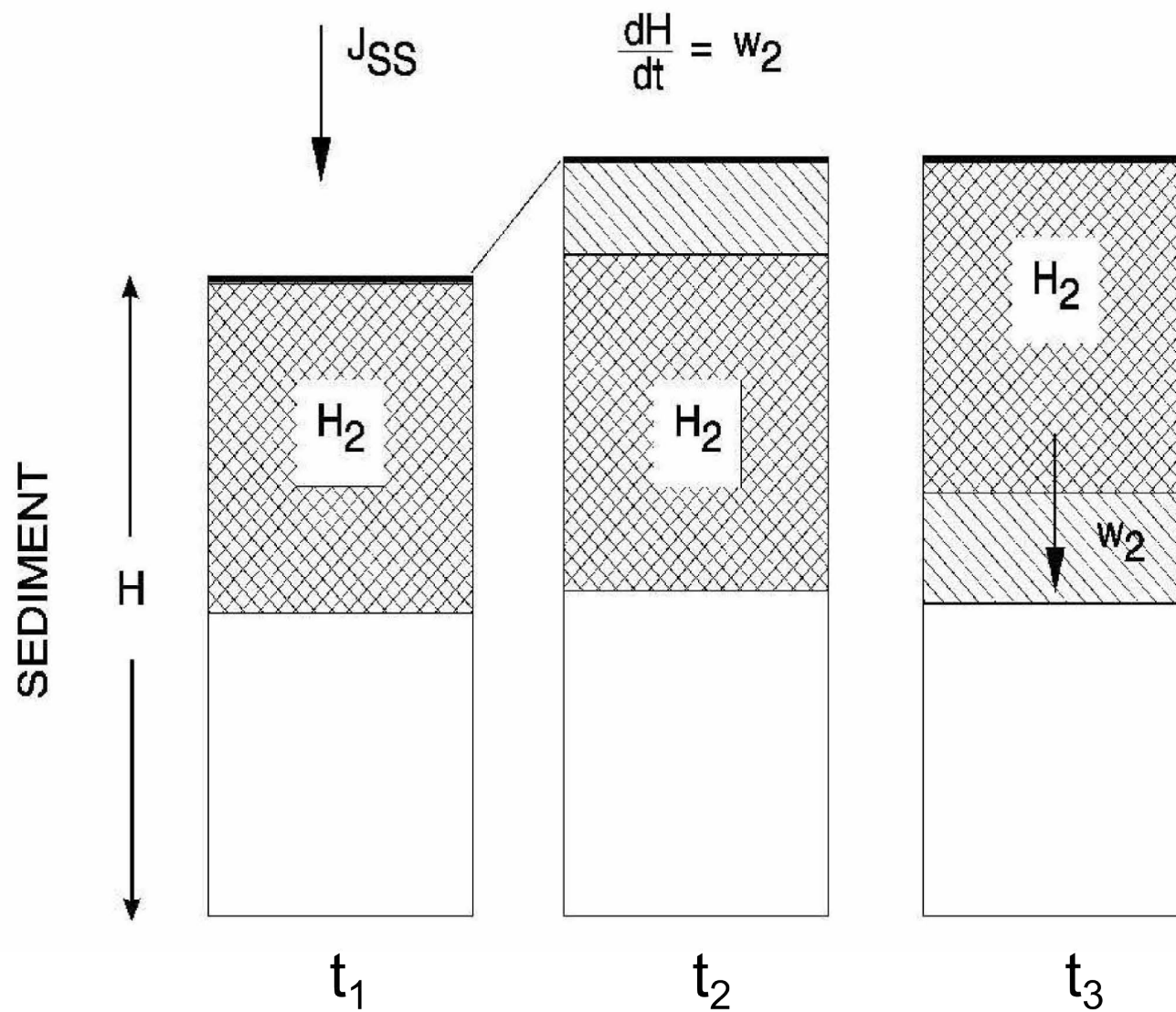
J_{POC} = deposition rate of POC (g C/m²-day)

w₂ = burial rate of organic matter (m/day)

k_{POCi} = diagenesis or decay rate of POC_i

2_{POCi} = temperature correction factor

Model of Sediment Loss by Burial



Steady State Solution for POC Concentrations

$$H \frac{dPOC_i}{dt} = f_{POC_i} J_{POC} - w_2 POC_i - H \cdot k_{POC_i} \theta_{POC_i} POC_i$$

- Rate of diagenesis

$$J_C = \sum_{i=1}^2 H \cdot k_{POC_i} \theta_{POC_i} POC_i$$

Solutions

$$G_1 \text{ and } G_2 \quad POC_i = \frac{f_{POC_i} J_{POC}}{k_i H + w_2}$$

$$G_3 \quad POC_i = \frac{f_{POC_i} J_{POC}}{w_2}$$

Magnitudes of the Parameters Resulting Concentrations

$$G_1 \text{ and } G_2 \quad POC_i = \frac{f_{POC_i} J_{POC}}{k_i H + w_2} \quad G_3 \quad POC_i = \frac{f_{POC_i} J_{POC}}{w_2}$$

What is the range in w_2 ?

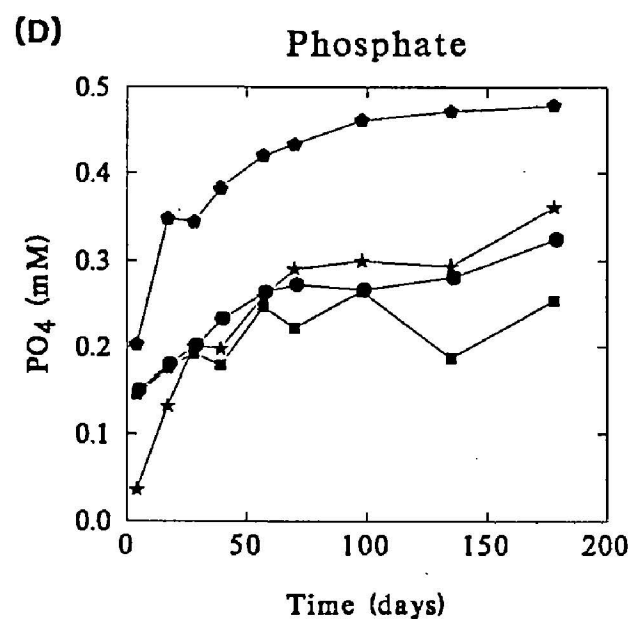
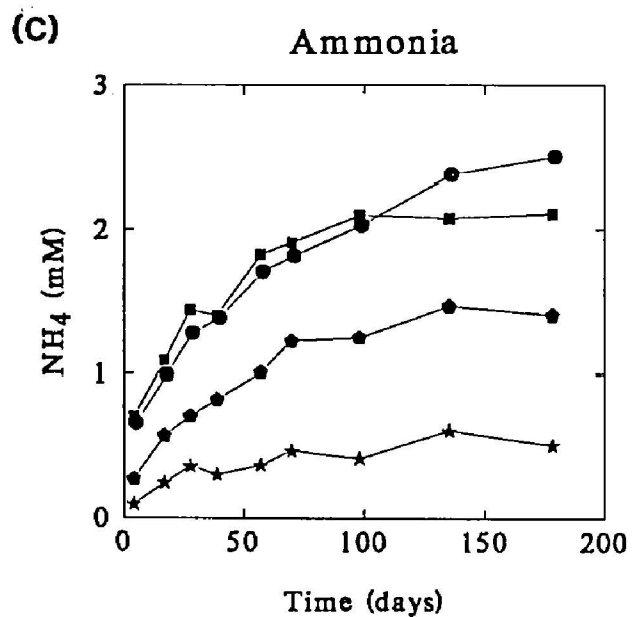
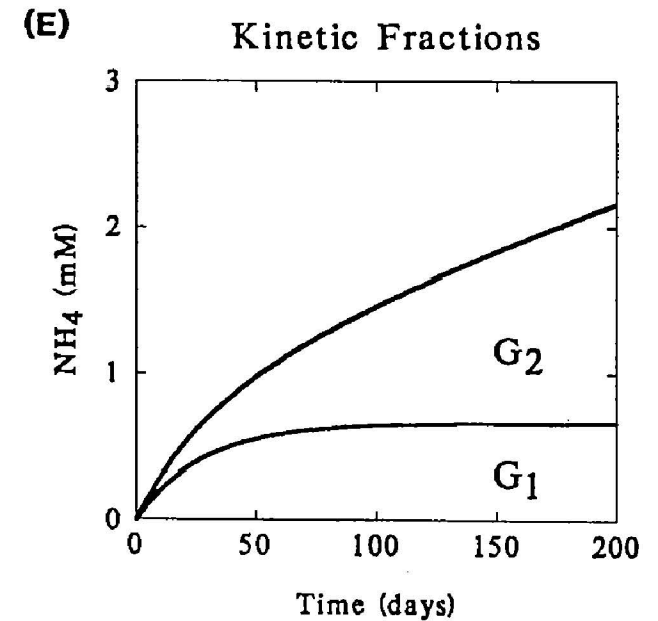
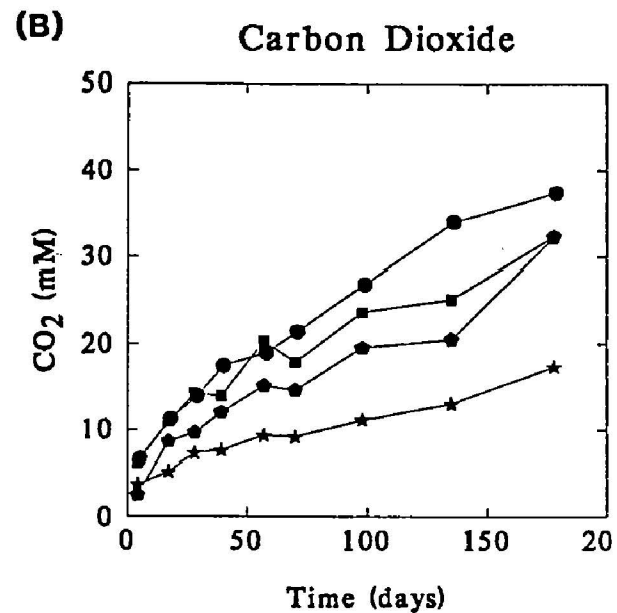
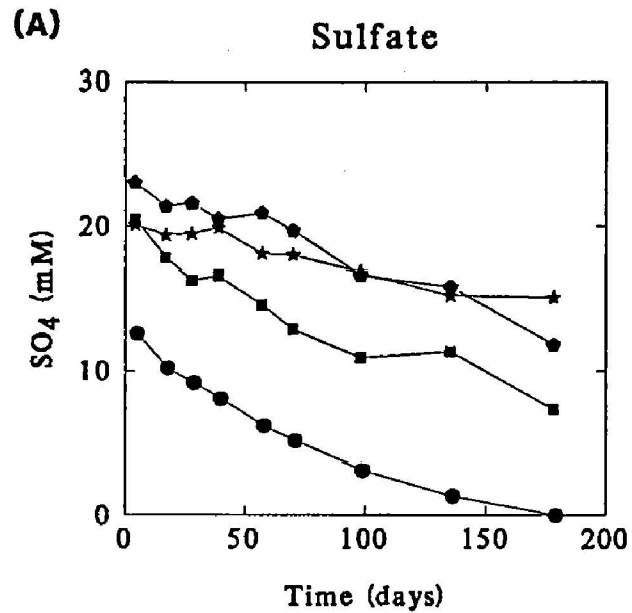
	ocean	bays-estuaries	“high deposition”
w_2 (cm/yr)	0.001-0.01	0.01-1	1-10
	G_1	G_2	
$k_i H$ (cm/yr)	130	6.6	Burial << Diagenesis

From these coefficients $POC_i = f_{POC_i} J_{POC} / k_i H$

Time to equilibrium: POC_1 . 3-4 months POC_2 . 5-6 years

$POC_3 = 40$ years for $w_2 = 0.25$ cm/yr

Sediment Mineralization Experiments



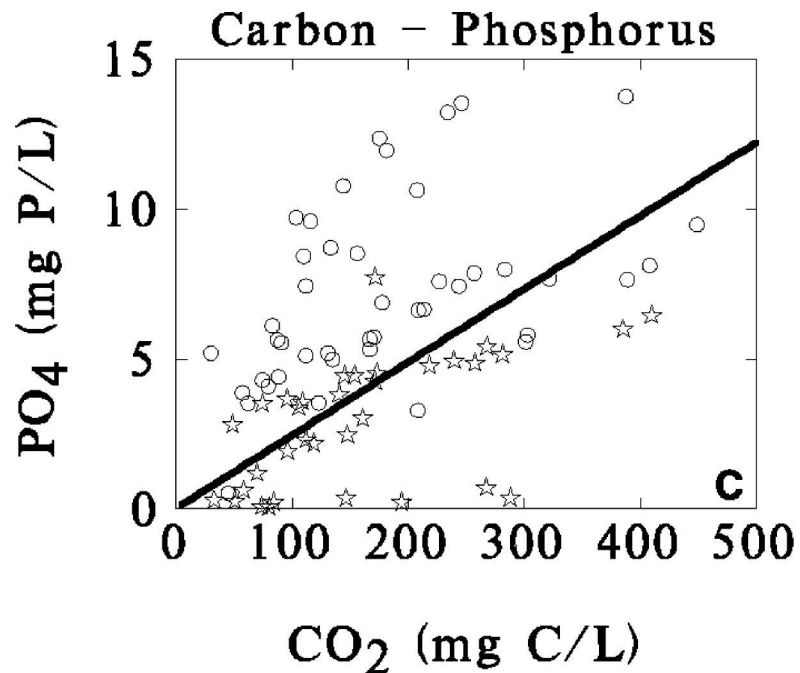
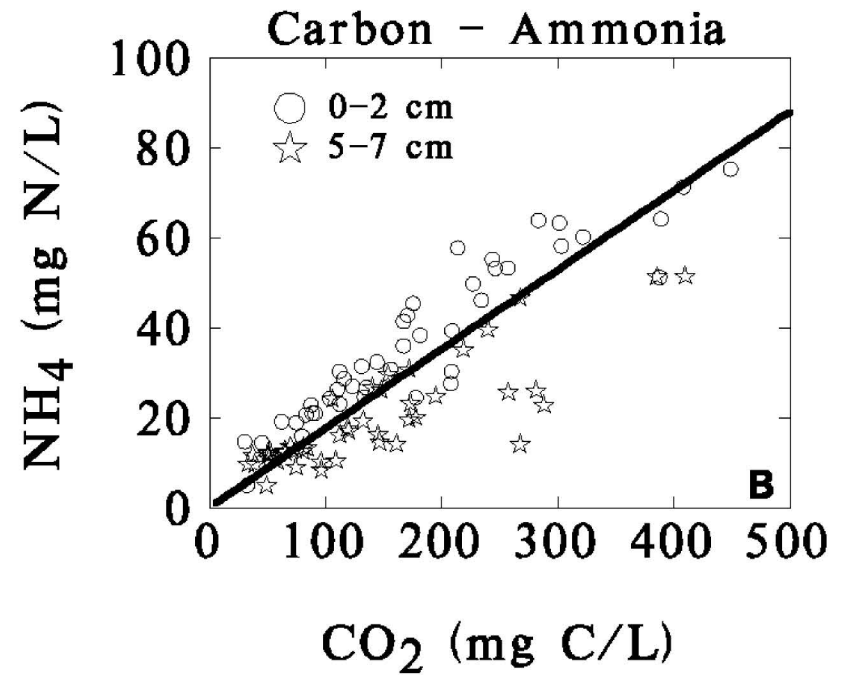
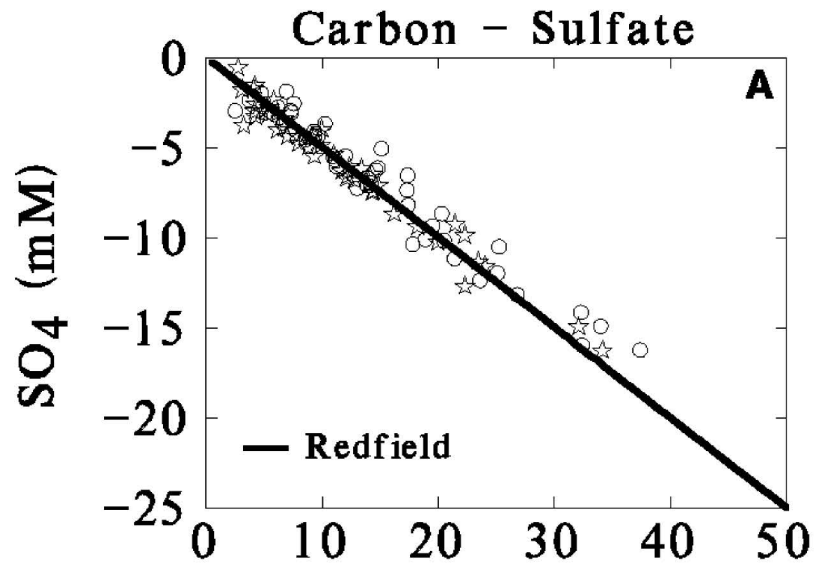
Sediment/Water
= 1:3

Legend

- Station 17
- Station 21
- ★ Station 25
- ◆ Station 26

Data from Burdige, 1991

Diagenesis Stoichiometry



Redfield Stiochiometry



Ammonia Flux Model

WATER COLUMN

\uparrow $\text{NH}_4(0)$

\downarrow $\text{NH}_4(1)$

SURFACE MASS TRANSFER: K_{L01}

AEROBIC

LAYER 1

DIAGENESIS: $\text{PON} \xrightarrow{J_{N1}} \text{NH}_4$

REACTION: $\text{NH}_4 \xrightarrow{K_{\text{NH}_4,1}} \text{NO}_3$

H_1

DIFFUSION: K_{L12}

SEDIMENT

ANAEROBIC

LAYER 2

DIAGENESIS: $\text{PON} \xrightarrow{J_{N2}} \text{NH}_4$

REACTION: NONE

H_2



Aerobic Layer

$$H_1 \frac{d[\text{NH}_4(1)]}{dt} = -k_{\text{NH}_4,1} [\text{NH}_4(1)] H_1 \\ - K_{\text{L}01} ([\text{NH}_4(1)] - [\text{NH}_4(0)]) \\ + K_{\text{L}12} ([\text{NH}_4(2)] - [\text{NH}_4(1)]) + J_{\text{N}1}$$

Anaerobic Layer

$$H_2 \frac{d[\text{NH}_4(2)]}{dt} = \\ - K_{\text{L}12} ([\text{NH}_4(2)] - [\text{NH}_4(1)]) + J_{\text{N}2}$$

- H_1 and H_2 = depths of the aerobic (1) and anaerobic (2) layers
- $[\text{NH}_4(0)]$, $[\text{NH}_4(1)]$, and $[\text{NH}_4(2)]$ = ammonia concentrations in overlying water (0), layers (1) and (2)
- $k_{\text{NH}_4,1}$ = nitrification rate constant in aerobic layer

Solution

$$0 = -k_{\text{NH}_4,1}[\text{NH}_4(1)]H_1 - K_{\text{L}01}([\text{NH}_4(1)] - [\text{NH}_4(0)]) + J_{\text{N}1} + J_{\text{N}2}$$

Ammonia concentrations

$$[\text{NH}_4(1)] = \frac{J_{\text{N}} + K_{\text{L}01}[\text{NH}_4(0)]}{K_{\text{L}01} + k_{\text{NH}_4,1}H_1}$$

$$[\text{NH}_4(2)] = \frac{J_{\text{N}}}{K_{\text{L}12}} + [\text{NH}_4(1)]$$

where $J_{\text{N}} = J_{\text{N}1} + J_{\text{N}2}$

Ammonia flux

$$J[\text{NH}_4] = K_{\text{L}01}([\text{NH}_4(1)] - [\text{NH}_4(0)])$$

or

$$J[\text{NH}_4] = J_{\text{N}} \frac{K_{\text{L}01}}{K_{\text{L}01} + k_{\text{NH}_4,1}H_1} - [\text{NH}_4(0)] \left(\frac{1}{K_{\text{L}01}} + \frac{1}{k_{\text{NH}_4,1}H_1} \right)^{-1}$$

- K_{L01} = mass transfer coefficient between overlying water and aerobic layer
- K_{L12} = mass transfer coefficient between H_1 and H_2
- J_{N1} and J_{N2} = sources of ammonia layers 1,2 from diagenesis of PON

Surface Mass Transfer Coefficient K_{L01}

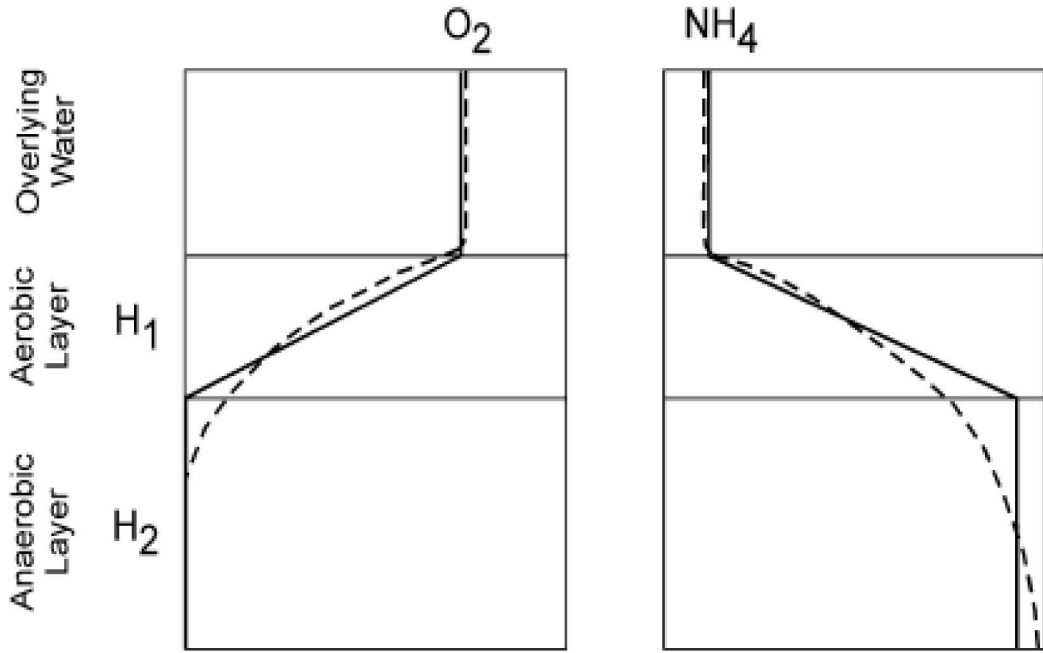


Figure 2: Schematic diagram of the idealized vertical profiles of oxygen and ammonia.

$$\begin{aligned}
 J[\text{NH}_4] &= -D_{\text{NH}_4} \left. \frac{d[\text{NH}_4(z)]}{dz} \right|_{z=0} \\
 &\simeq -D_{\text{NH}_4} \frac{[\text{NH}_4(0)] - [\text{NH}_4(H_1)]}{H_1} = \\
 &\quad -K_{L01,\text{NH}_4} ([\text{NH}_4(0)] - [\text{NH}_4(H_1)])
 \end{aligned}$$

where

$$K_{L01,\text{NH}_4} = \frac{D_{\text{NH}_4}}{H_1}$$

surface mass transfer coefficient, D_{NH_4} = diffusion coefficient

Surface Mass Transfer Coefficient K_{L01}

Similar argument for the SOD

$$\begin{aligned}\text{SOD} &= D_{O_2} \left. \frac{d[O_2(z)]}{dz} \right|_{z=0} \\ &\simeq D_{O_2} \frac{[O_2(0)] - [O_2(H_1)]}{H_1} \\ &= \frac{D_{O_2}}{H_1} [O_2(0)] \\ &= K_{L01, O_2} ([O_2(0)])\end{aligned}$$

where

$$K_{L01, O_2} = \frac{D_{O_2}}{H_1}$$

Therefore

$$K_{L01, O_2} = \frac{\text{SOD}}{[O_2(0)]} \triangleq s$$

a measured quantity

Depth of the Aerobic Zone, and Reaction Velocities

Need $k_{\text{NH}_4,1}H_1$

$$H_1 = D_{\text{O}_2} \frac{[\text{O}_2(0)]}{\text{SOD}} = \frac{D_{\text{O}_2}}{s}$$

Reaction rate-depth product $k_{\text{NH}_4,1}H_1s$

$$k_{\text{NH}_4,1}H_1 = \frac{D_{\text{O}_2}k_{\text{NH}_4,1}}{s}$$

Define *reaction velocity*

$$\kappa_{\text{NH}_4,1} = \sqrt{D_{\text{O}_2}k_{\text{NH}_4,1}}$$

Ammonia flux

$$J[\text{NH}_4] = J_{\text{N}} \frac{s^2}{s^2 + \kappa_{\text{NH}_4,1}^2} [\text{NH}_4(0)] \left(\frac{1}{s} + \frac{s}{\kappa_{\text{NH}_4,1}^2} \right)^{-1}$$

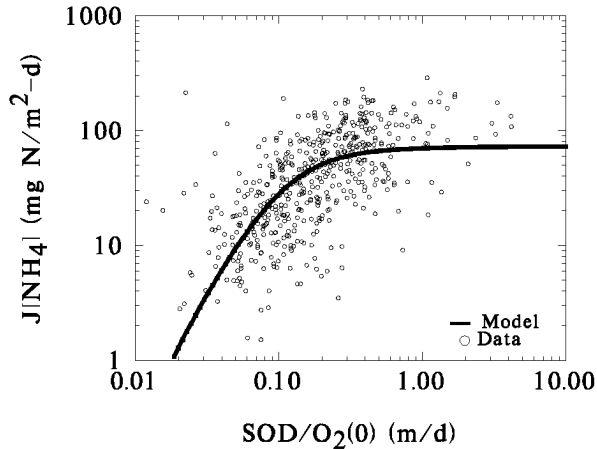


Fig. 3.5 Ammonia flux versus $s = \text{SOD}/[\text{O}_2(0)]$ for all stations and times in the Chesapeake Bay data set.

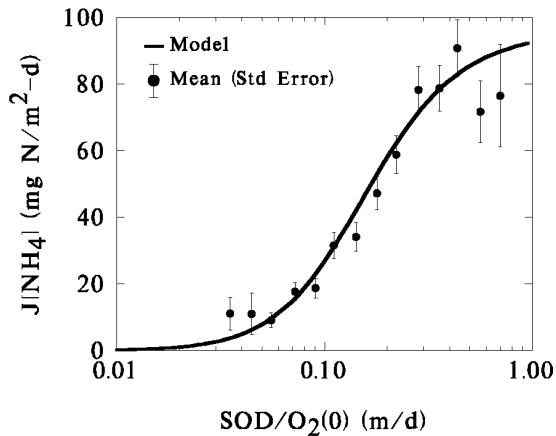


Fig. 3.6 Comparison of model calculation to data grouped into 0.1 \log_{10} intervals of s .

Nitrate Flux Model

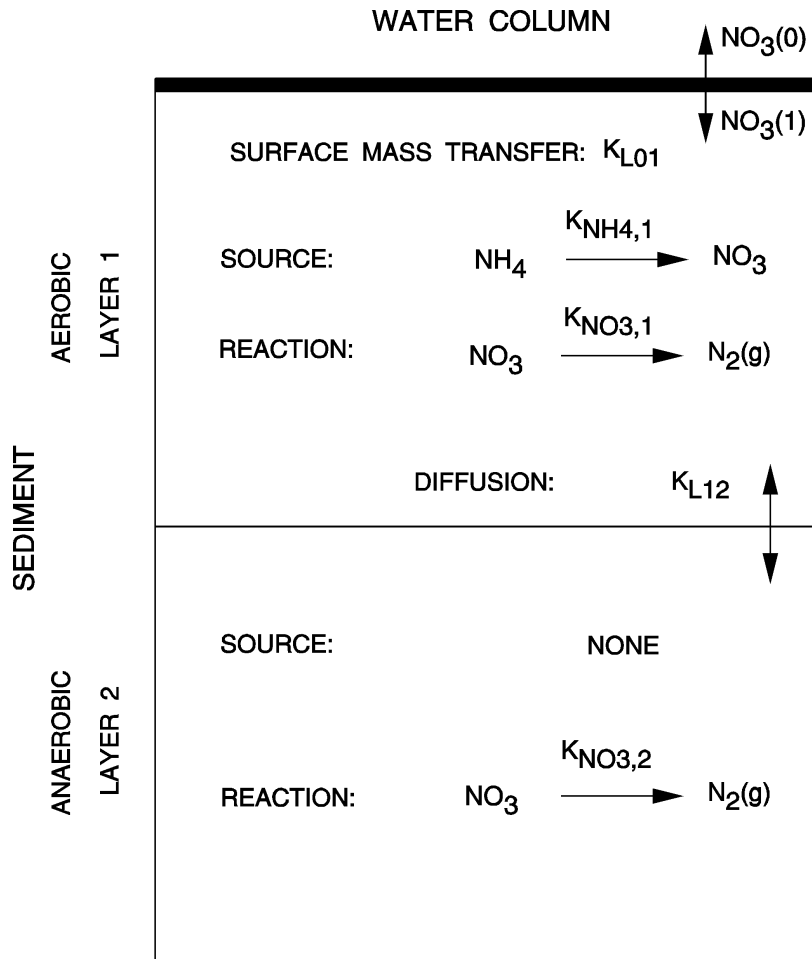


Figure 1: Schematic model of nitrate model

Aerobic Layer

$$H_1 \frac{d[\text{NO}_3(1)]}{dt} = -k_{\text{NO}_3,1}[\text{NO}_3(1)]H_1 \\ -K_{\text{L}01}([\text{NO}_3(1)] - [\text{NO}_3(0)]) \\ +K_{\text{L}12}([\text{NO}_3(2)] - [\text{NO}_3(1)]) \\ +S[\text{NO}_3]$$

Anaerobic Layer

$$H_2 \frac{d[\text{NO}_3(2)]}{dt} = -k_{\text{NO}_3,2}[\text{NO}_3(2)]H_2 \\ -K_{\text{L}12}([\text{NO}_3(2)] - [\text{NO}_3(1)])$$

where $S[\text{NO}_3]$ = nitrate from ammonia nitrification

Solutions

$$[\text{NO}_3(1)] =$$

$$\frac{S[\text{NO}_3] + K_{L01}[\text{NO}_3(0)]}{k_{\text{NO}_3,1}H_1 + K_{L01} + \left(\frac{1}{k_{\text{NO}_3,2}H_2} + \frac{1}{K_{L12}} \right)^{-1}}$$

$$[\text{NO}_3(2)] = [\text{NO}_3(1)] \frac{K_{L12}}{k_{\text{NO}_3,2} + K_{L12}}$$

where

$$\kappa_{\text{NO}_3,1} = \sqrt{D_{\text{NO}_3} k_{\text{NO}_3,1}}$$

$$\kappa_{\text{NO}_3,2} = k_{\text{NO}_3,2}H_2$$

$$\kappa_{\text{NO}_3,2}^* = \left(\frac{1}{\kappa_{\text{NO}_3,2}} + \frac{1}{K_{L12}} \right)^{-1}$$

So that

$$[\text{NO}_3(1)] = \frac{S[\text{NO}_3] + s[\text{NO}_3(0)]}{\kappa_{\text{NO}_3,1}^2/s + s + \kappa_{\text{NO}_3,2}^*}$$

$$[\text{NO}_3(2)] = [\text{NO}_3(1)] \frac{K_{L12}}{\kappa_{\text{NO}_3,2} + K_{L12}}$$

Nitrate Source

$$\begin{aligned} S[\text{NO}_3] &= J_{\text{N}} + s[\text{NH}_4(0)] - s[\text{NH}_4(1)] \\ &= J_{\text{N}} - s([\text{NH}_4(1)] - [\text{NH}_4(0)]) \\ &= J_{\text{N}} - J[\text{NH}_4] \end{aligned}$$

Nitrate flux

$$J[\text{NO}_3] = s([\text{NO}_3(1)] - [\text{NO}_3(0)])$$

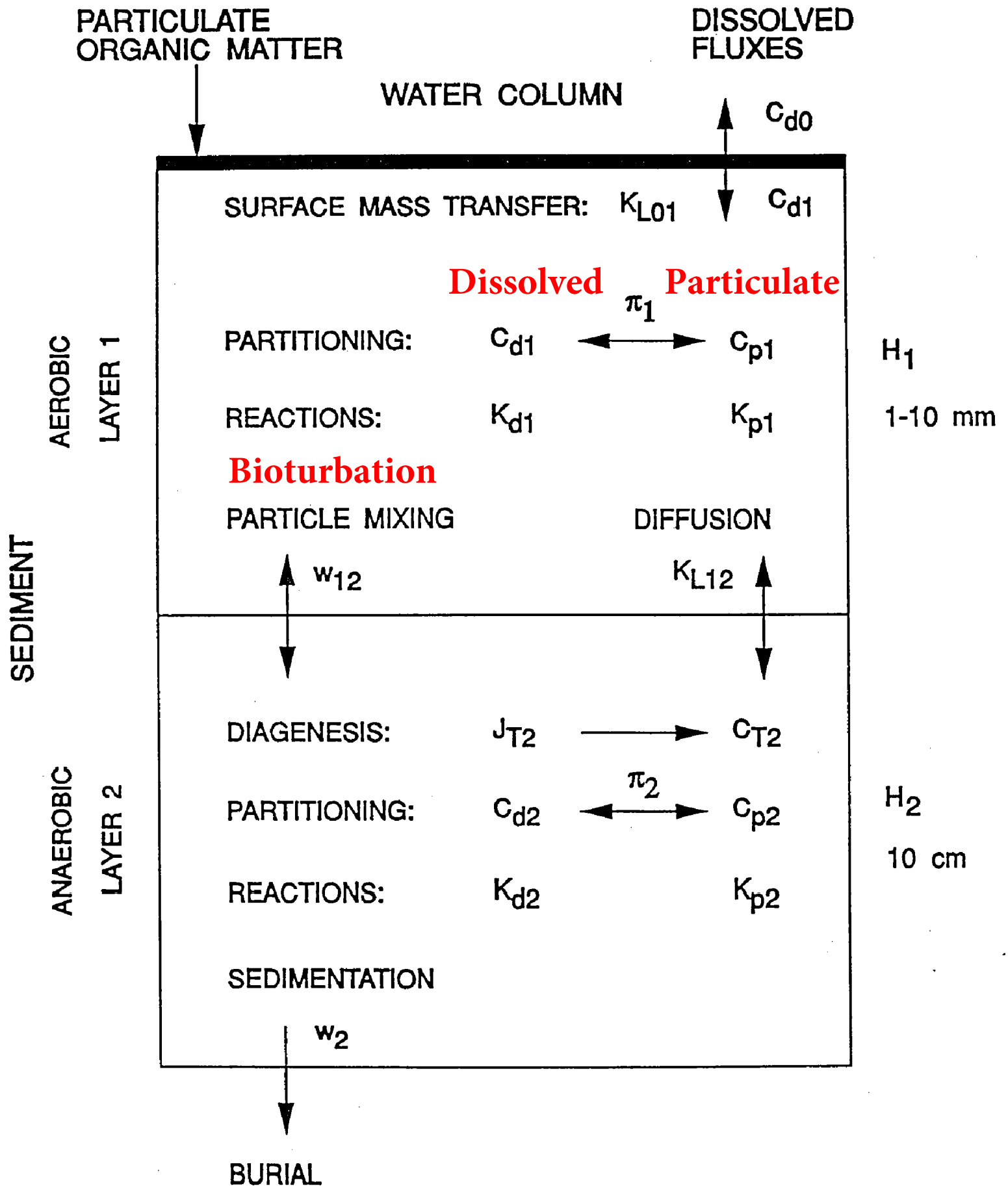
Solution

$$\begin{aligned} J[\text{NO}_3] &= \left(\frac{s^2}{\kappa_{\text{NO}_3,1}^2/s + s + \kappa_{\text{NO}_3,2}^*} - s \right) [\text{NO}_3(0)] \\ &\quad + \left(\frac{s(J_{\text{N}} - J[\text{NH}_4])}{\kappa_{\text{NO}_3,1}^2/s + s + \kappa_{\text{NO}_3,2}^*} \right) \end{aligned}$$

Two parts

1. Due to overlying water $[\text{NO}_3]$
2. Due to nitrification $J_{\text{N}} - J[\text{NH}_4]$

SEDIMENT FLUX MODEL



Reactions

	Diagenesis	Partitioning	Reaction
NH ₄	PON -> NH ₄	Small	NH ₄ + O ₂ -> NO ₃
NO ₃			NO ₃ + POC -> N ₂ (g)
H ₂ S	POC -> H ₂ S	H ₂ S <-> FeS(s)	H ₂ S + O ₂ -> FeS + O ₂ ->
PO ₄	POP -> PO ₄	PO ₄ <-> PIP(s) $\pi_1 > \pi_2$ $\pi_1 = f[O_2(0)]$	
Si	PSi -> DSi	PSi <-> DSi	$k_{Si}P_{Si}$ (DSi - Si _{sat})
SOD			NH ₄ + O ₂ -> H ₂ S + O ₂ -> FeS + O ₂ ->

Transport Mechanisms

Surface Mass Transfer	Particle Mixing	Diffusion
K _{L01}	w ₁₂	K _{L12}
K _{L01} = SOD / O ₂ (0)	G ₁ Carbon, O ₂ (0), T	T

Distribution Between Particulate and Dissolved Concentrations

C_d = bulk dissolved mg P / L water

C_p = bulk particulate mg P/ L water

m = particle conc. kg SS/L

q_p = particulate conc. mg P/kg SS

$$q_p = C_p / m$$

Partitioning Model

$$q_p = K_p C_d$$

K_p = partition coefficient (L / kg SS)

$$\text{"Pie"} = K_p$$

Sediment Bioturbation

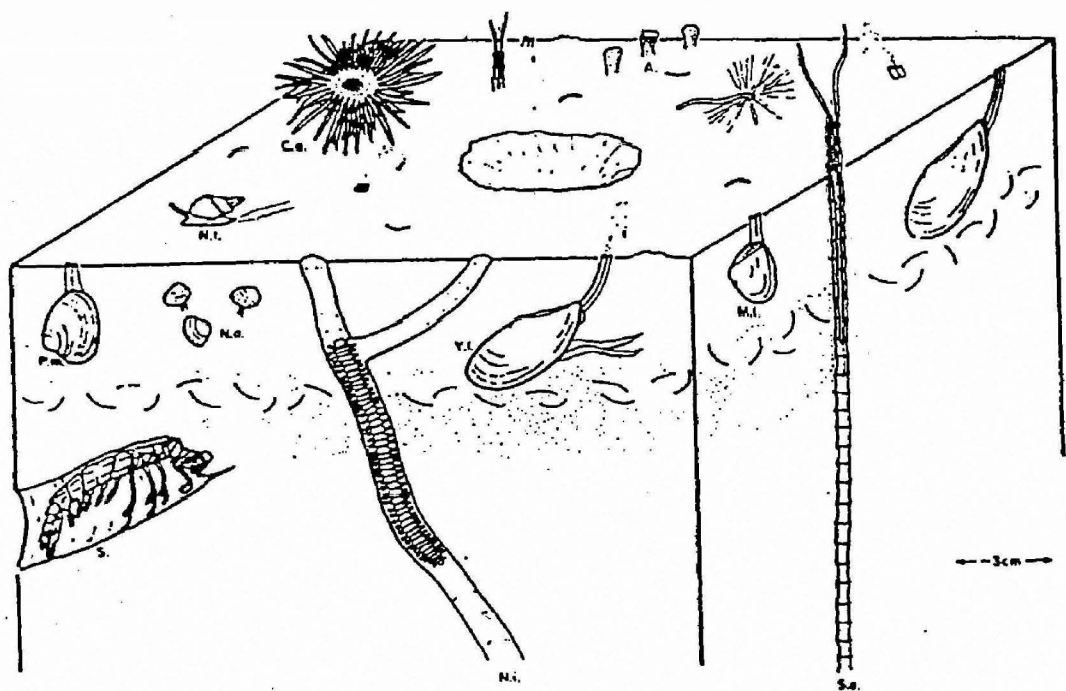
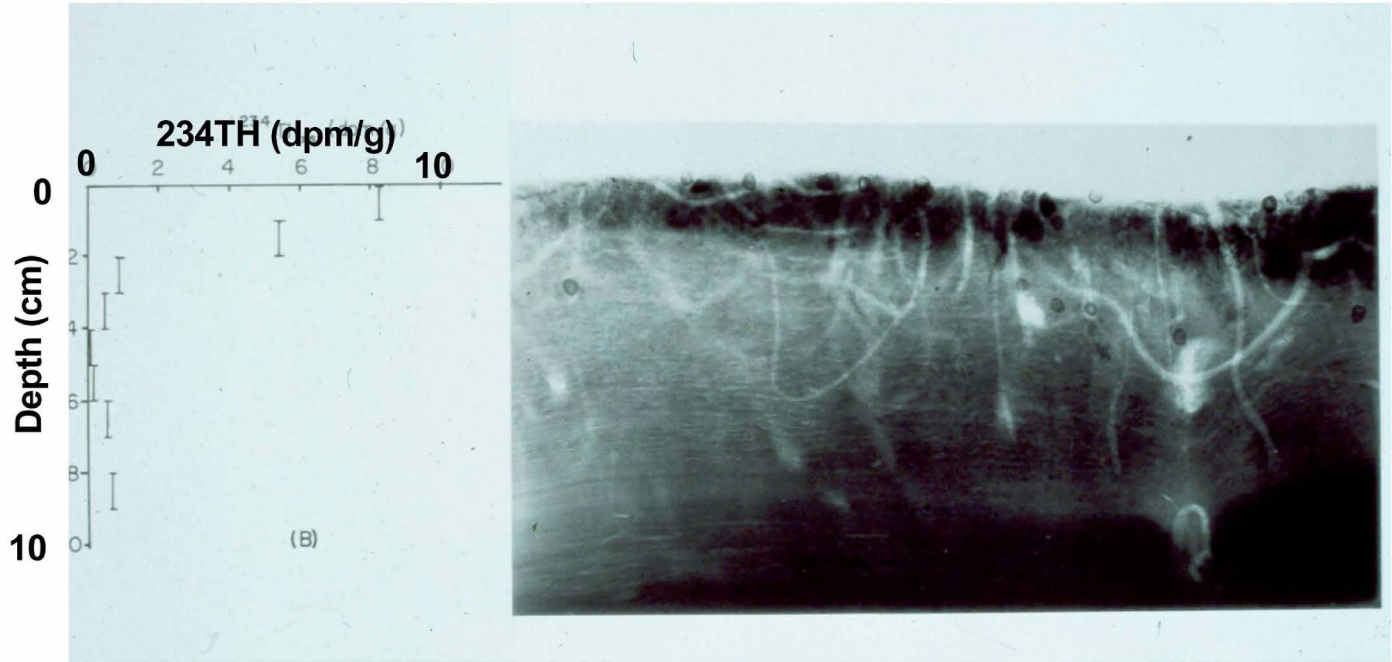
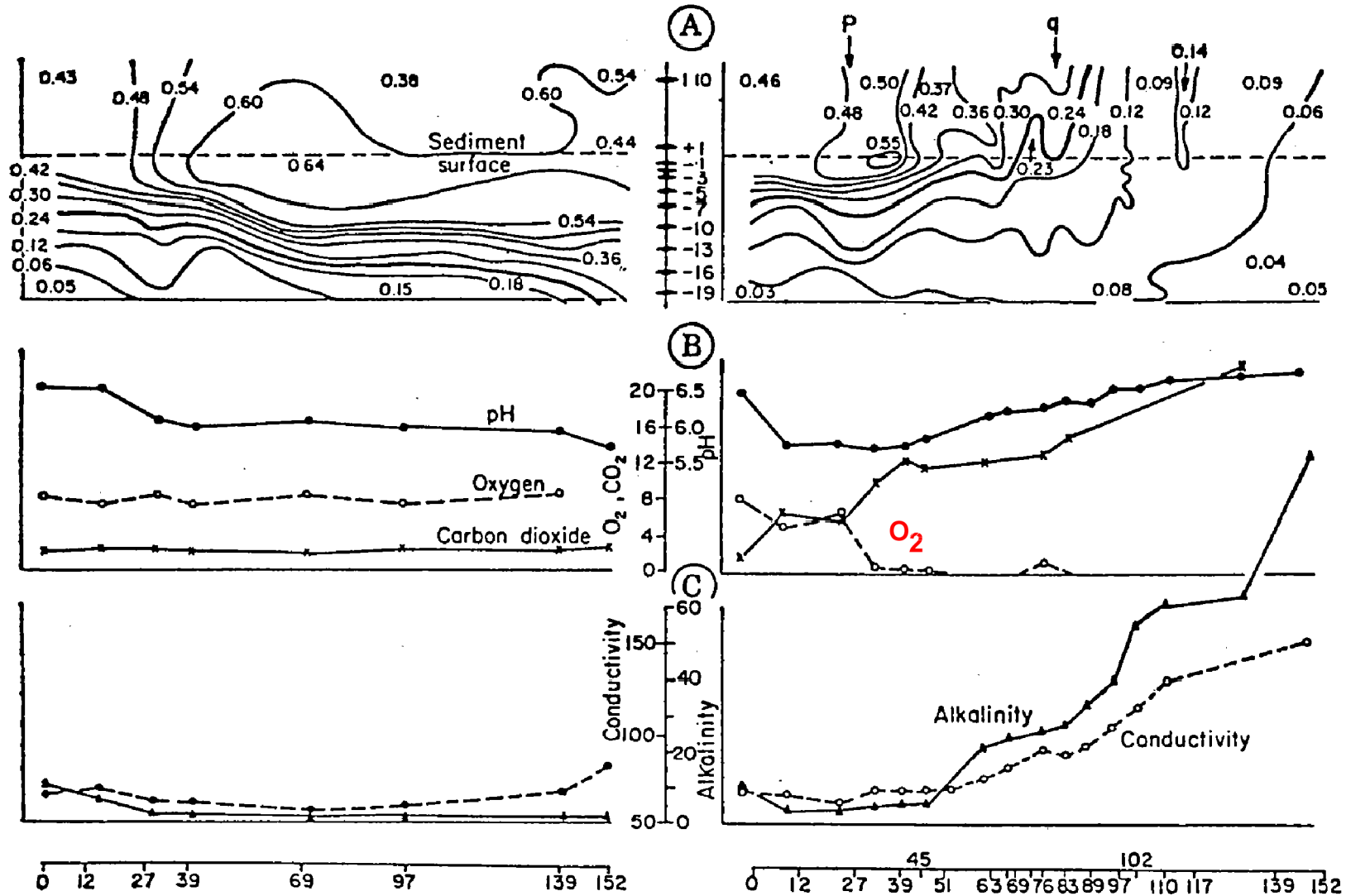


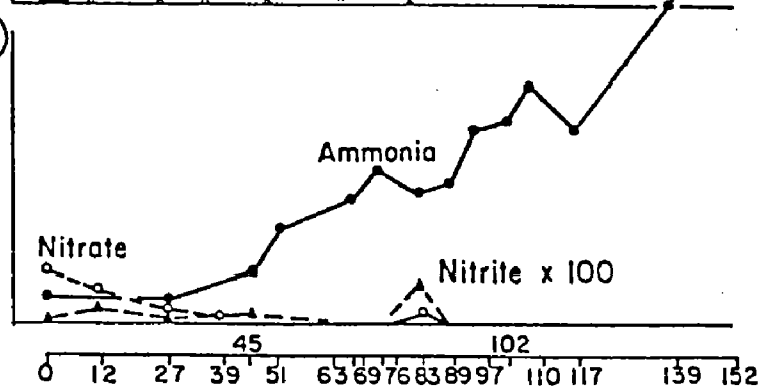
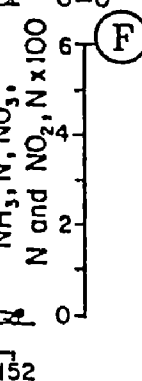
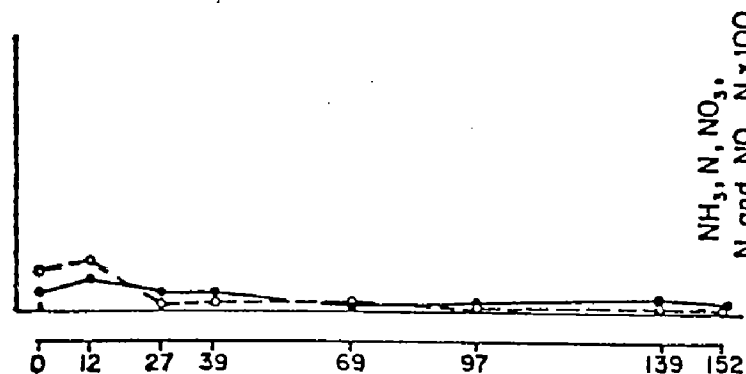
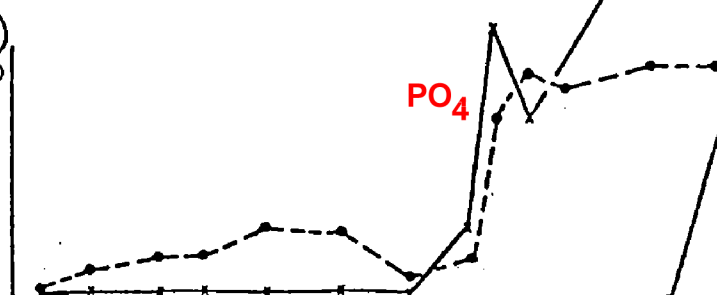
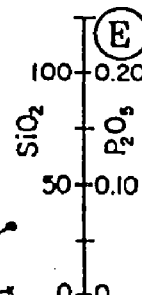
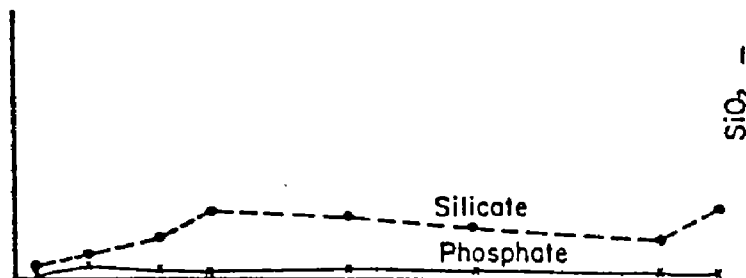
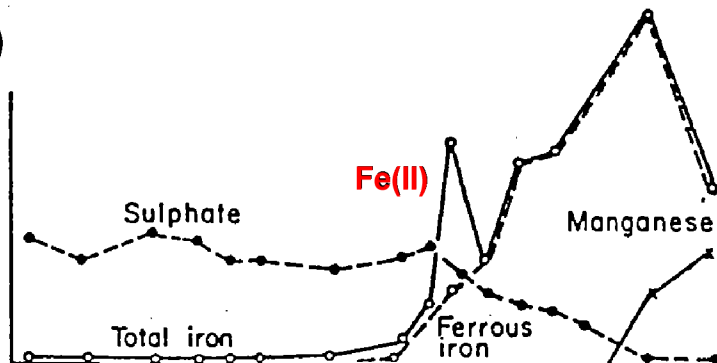
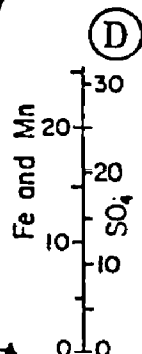
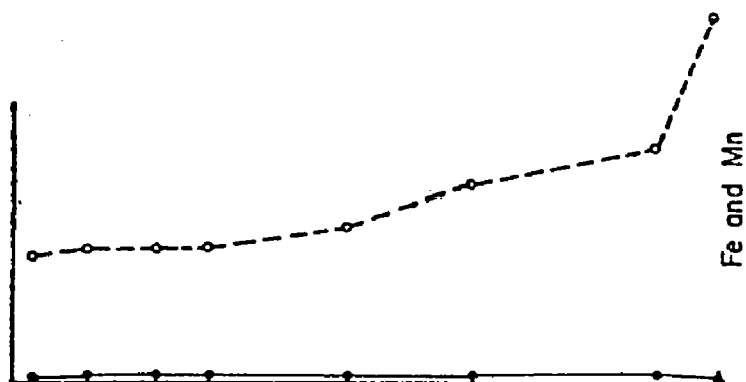
FIG. 6. Schematic drawing of major fauna at NWC: C.a., *Ceriantheopsis americanus*; P.m., *Pitar morrhuana*; and S., *Squilla*; all other abbreviations as in Fig. 3.

Aller, R.C. (1980)



Mortimer Experiments 1941-1942





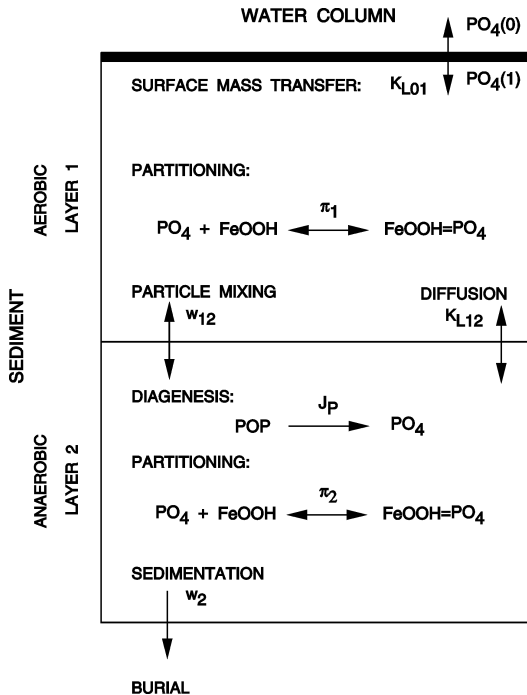


Fig. 6.1 Schematic diagram of the phosphorus flux model.

Phosphorus Flux Model

$$\begin{aligned}
 H_1 \frac{d[\text{PO}_4(1)]_T}{dt} = & s([\text{PO}_4(0)] - f_{d1}[\text{PO}_4(1)]_T) \\
 & + w_{12}(f_{p2}[\text{PO}_4(2)]_T - f_{p1}[\text{PO}_4(1)]_T) \\
 & + K_{L12}(f_{d2}[\text{PO}_4(2)]_T - f_{d1}[\text{PO}_4(1)]_T) \\
 & - w_2[\text{PO}_4(1)]_T
 \end{aligned} \tag{6.1a}$$

$$\begin{aligned}
 H_2 \frac{d[\text{PO}_4(2)]_T}{dt} = & -w_{12}(f_{p2}[\text{PO}_4(2)]_T - f_{p1}[\text{PO}_4(1)]_T) \\
 & - K_{L12}(f_{d2}[\text{PO}_4(2)]_T - f_{d1}[\text{PO}_4(1)]_T) \\
 & + w_2([\text{PO}_4(1)]_T - [\text{PO}_4(2)]_T) + J_P
 \end{aligned} \tag{6.1b}$$

H_1 and H_2 are the depths of the aerobic (1) and anaerobic (2) layers

$[\text{PO}_4(0)]$ is the dissolved phosphate concentration in the overlying water

$[\text{PO}_4(1)]_T$ and $[\text{PO}_4(2)]_T$ are the total phosphate concentrations in layers 1 and 2

f_{d1} , and f_{d2} are the dissolved fractions in layers 1 and 2

f_{p1} and f_{p2} are the particulate fractions in layers 1 and 2

s is the surface mass transfer coefficient between the overlying water and the aerobic layer

K_{L12} is the mass transfer coefficient between the aerobic and anaerobic layers

w_{12} is the particle mixing velocity between the aerobic and anaerobic layers

w_2 is the burial velocity

J_P is the source of phosphate from the diagenesis of particulate organic phosphorus POP

$$J[\text{PO}_4] \approx J_P \frac{s f_{d1}}{s f_{d1} + w_2 \left(\frac{K_{L12} f_{d1} + s f_{d1}}{K_{L12} f_{d2}} \right)} = \frac{s}{s + w_2 \left(\frac{K_{L12} + s}{K_{L12} f_{d2}} \right)}$$

The dissolved f_d and particulate f_p fractions are computed from the partitioning equations

$$f_d = \frac{\phi}{1 + m_1 \pi_1 / \phi} \quad (5.2a)$$

$$f_p = \frac{m_1 \pi_1 / \phi}{1 + m_1 \pi_1 / \phi} \quad (5.2b)$$

where the solids concentrations are m_1 and m_2 , and the partition coefficients are π_1 and π_2 , respectively. Note that the solids concentration partition coefficient products: $m_1 \pi_1$ and $m_2 \pi_2$ determine the extent of partitioning. The concentrations of dissolved and particulate chemical are obtained as products of these fractions and the total concentrations C_{T1} and C_{T2} .

$$\pi_1 = \pi_2(\Delta\pi_{\text{PO}_4,1}) \quad [\text{O}_2(0)] > [\text{O}_2(0)]_{\text{crit,PO}_4} \quad (6.19)$$

However, if oxygen falls below a critical concentration, $[\text{O}_2(0)] < [\text{O}_2(0)]_{\text{crit,PO}_4}$, then

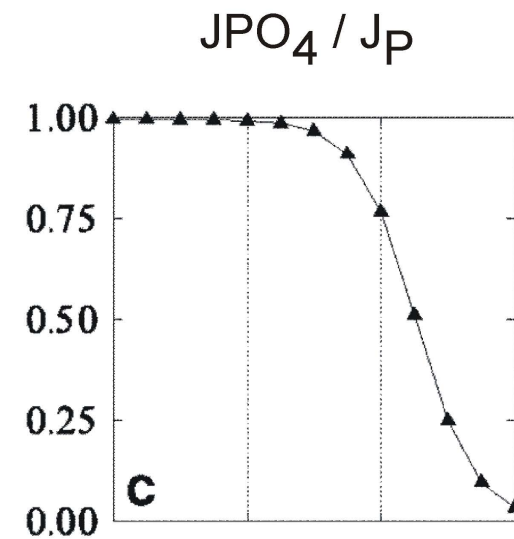
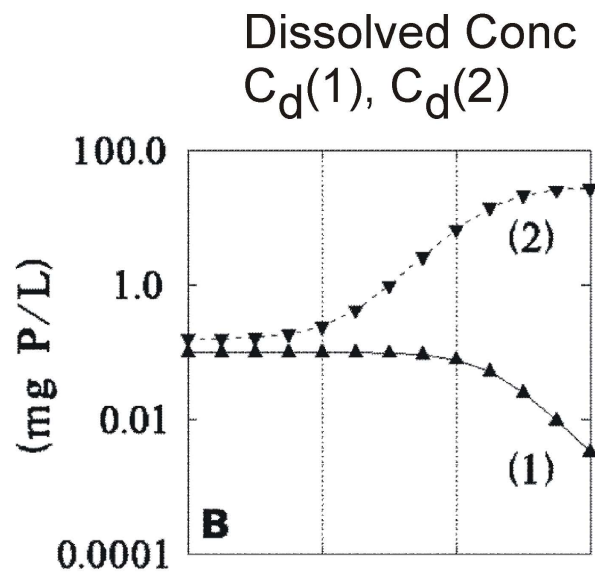
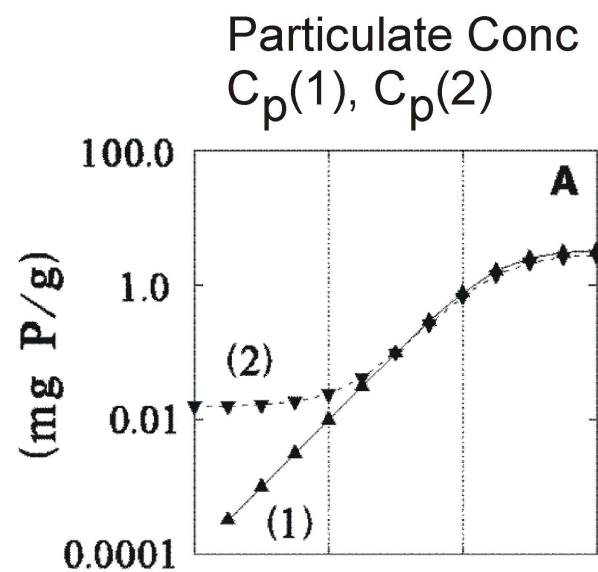
$$\pi_1 = \pi_2(\Delta\pi_{\text{PO}_4,1})^{\beta_{\text{PO}_4}} \quad [\text{O}_2(0)] \leq [\text{O}_2(0)]_{\text{crit,PO}_4} \quad (6.20)$$

where

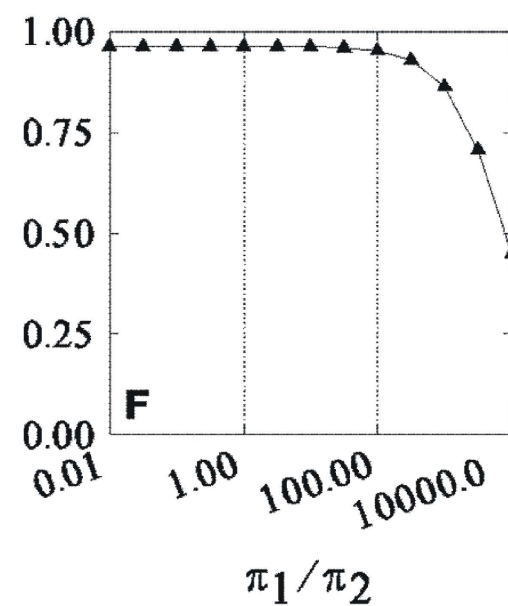
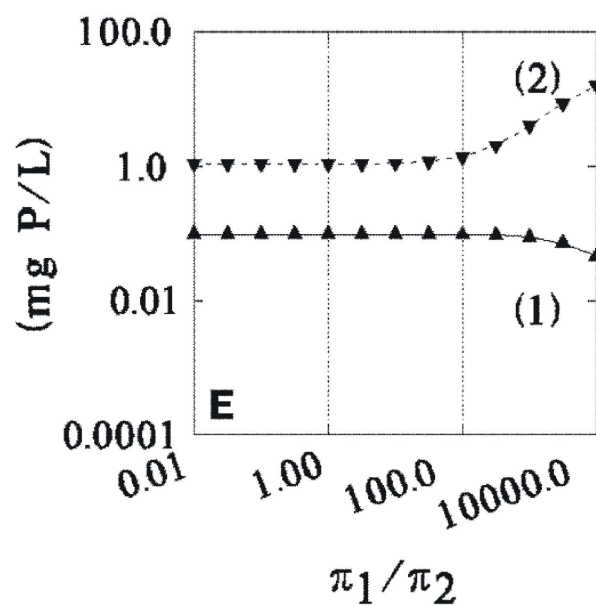
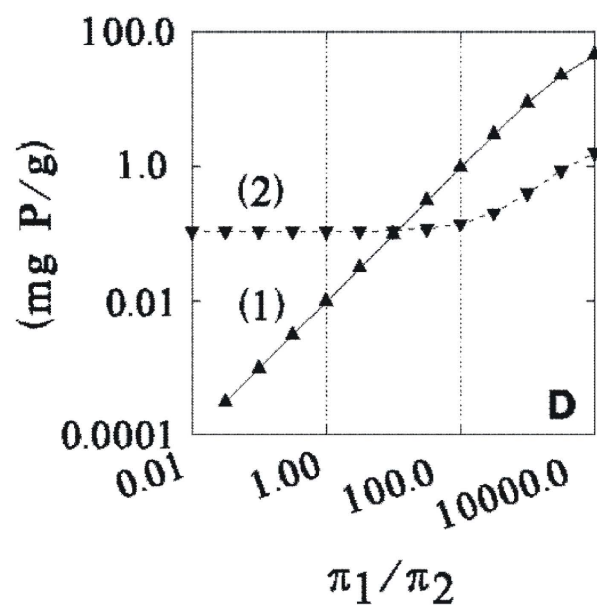
$$\beta_{\text{PO}_4} = \frac{[\text{O}_2(0)]}{[\text{O}_2(0)]_{\text{crit,PO}_4}} \quad (6.21)$$

Eq. (6.20) smoothly reduces the aerobic layer partition coefficient to that in the anaerobic layer as $[\text{O}_2(0)]$ goes to zero.

With Particle Mixing



Without Particle Mixing



Ratio of Layer 1 to Layer 2 Paratition Coefficient

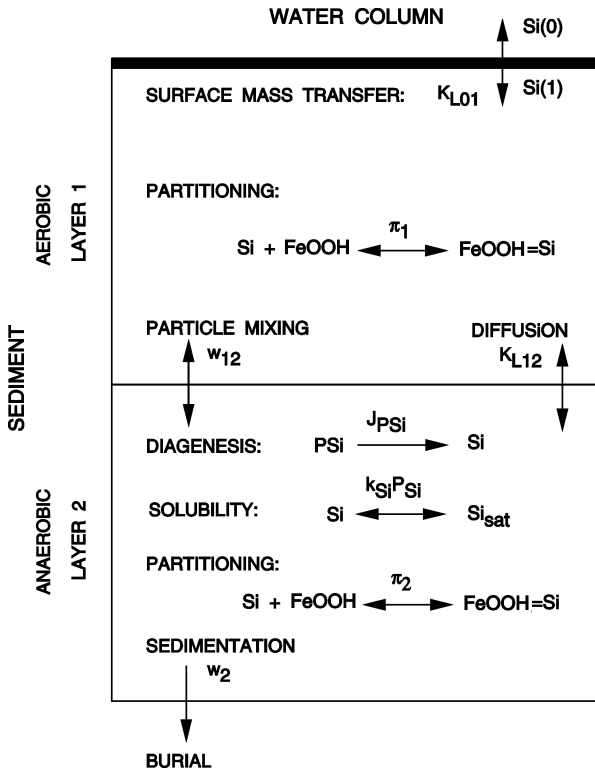


Fig. 7.1 Schematic diagram of the silica flux model.

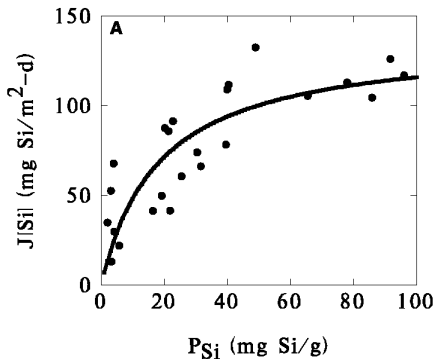


Fig. 7.3 (A) Silica flux versus particulate silica concentration versus distance along the axis of Chesapeake Bay.

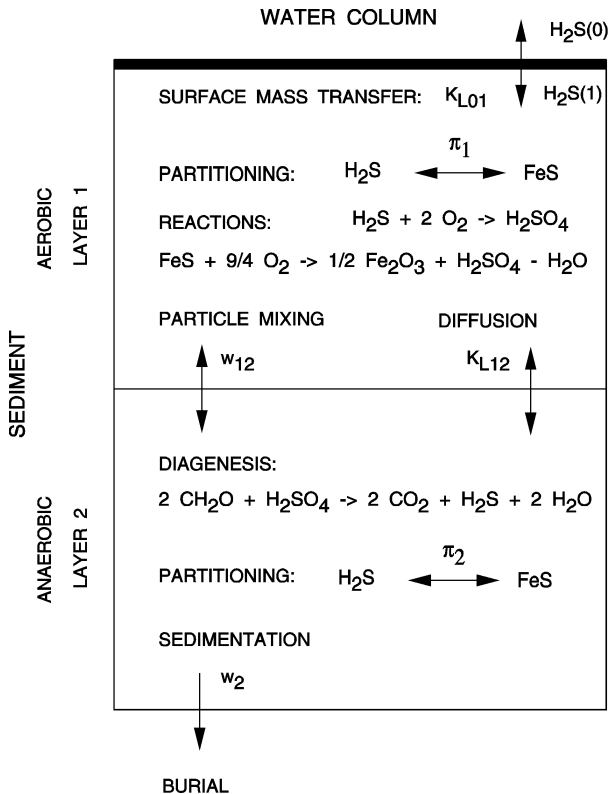


Fig. 9.1 Schematic diagram of the sulfide oxidation model.

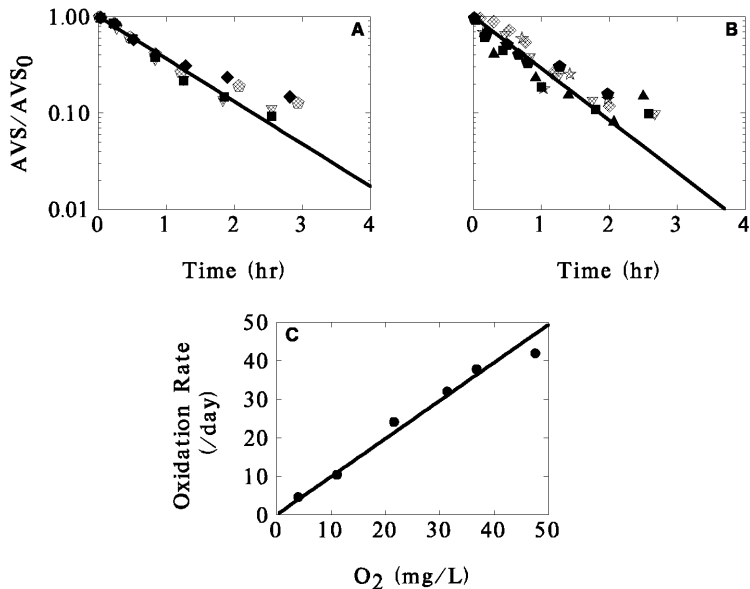


Fig. 9.2 Kinetics of FeS(s) oxidation for (A) Jamacia Bay and (B) Van Cortlandt Pond sediments (Di Toro et al., 1996a). (C) Effect of dissolved oxygen concentration on the oxidation rate (Nelson, 1978).

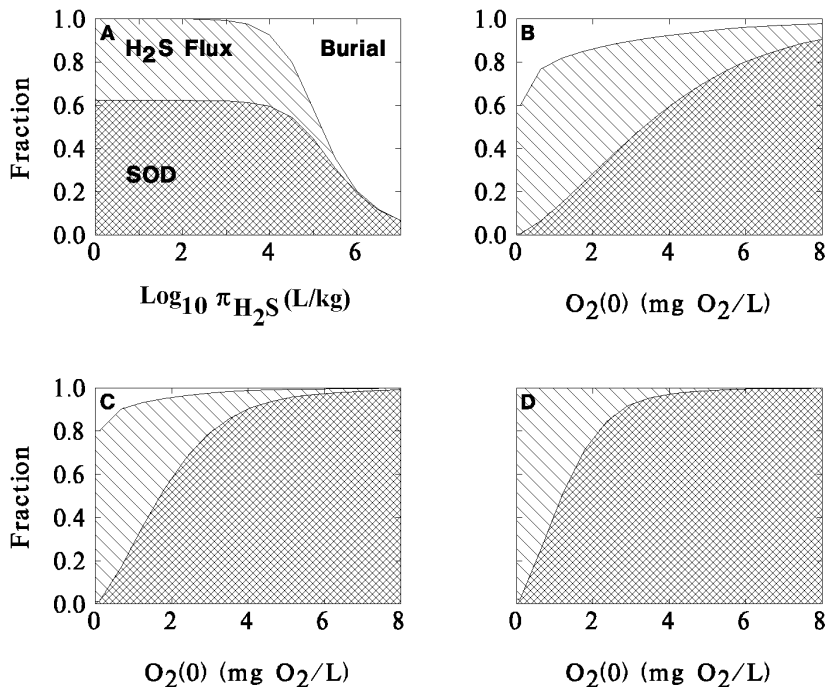


Fig. 9.3 (A) Effect of partition coefficients and (B) overlying water dissolved oxygen with increasing particulate sulfide oxidation rate (C-D) on the fraction of J_C that is oxidized as SOD J_{ox} , diffuses to the overlying water as an H_2S flux J_{aq} , or is buried J_{br} . See Table 9.1 for parameter values.

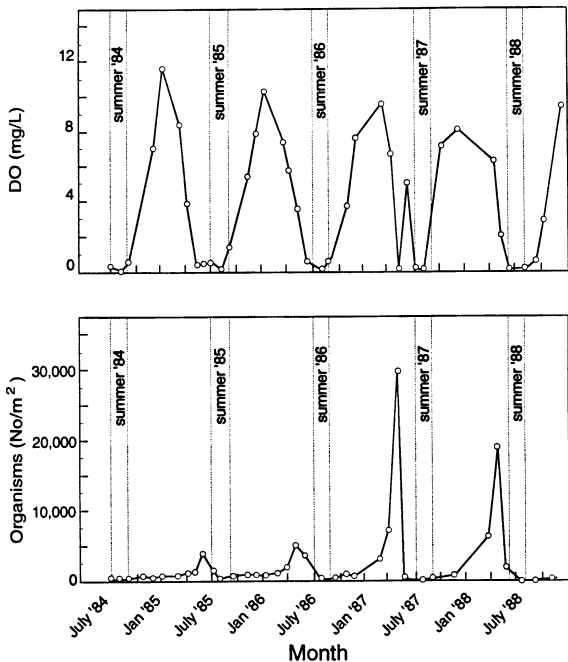


Fig. 13.4 Benthic organism density and bottom water dissolved oxygen for a deep water station in Chesapeake Bay. Data from Versar (1990).

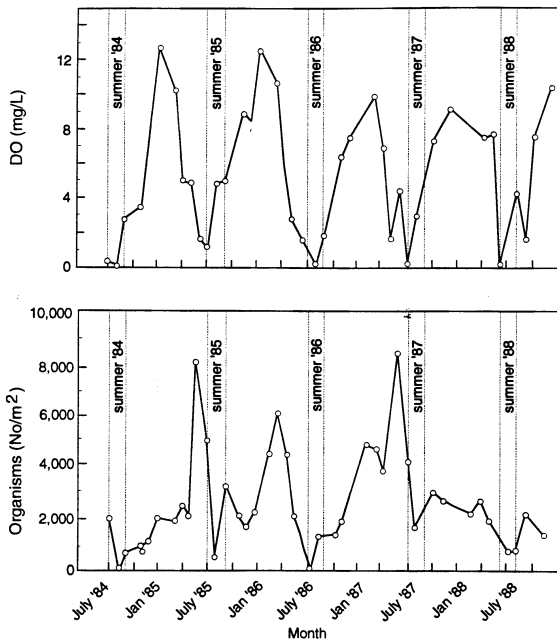
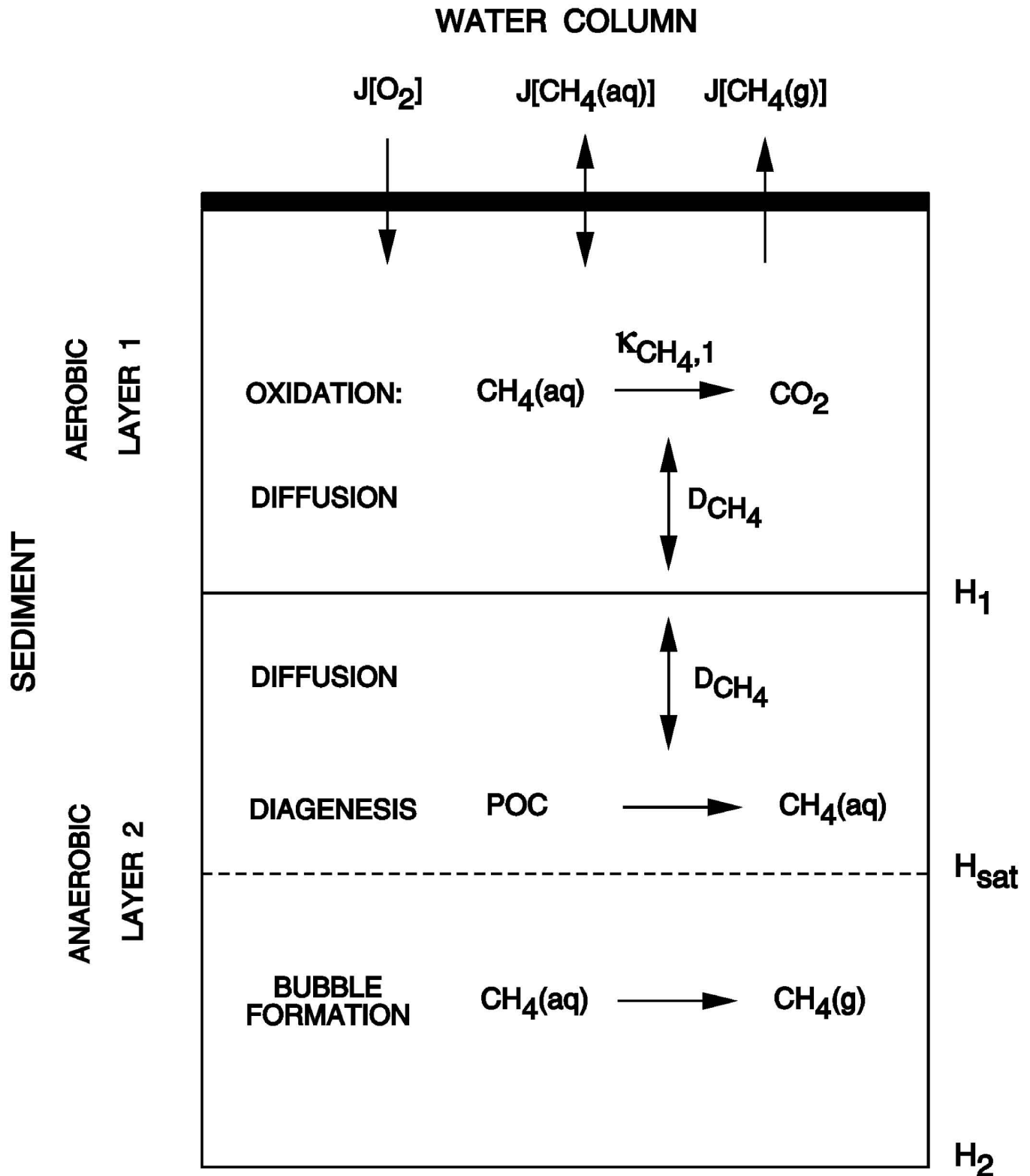


Fig. 13.5 Benthic organism density and bottom water dissolved oxygen for a station near the deep trough in Chesapeake Bay. Data from Versar (1990).

Methane Model



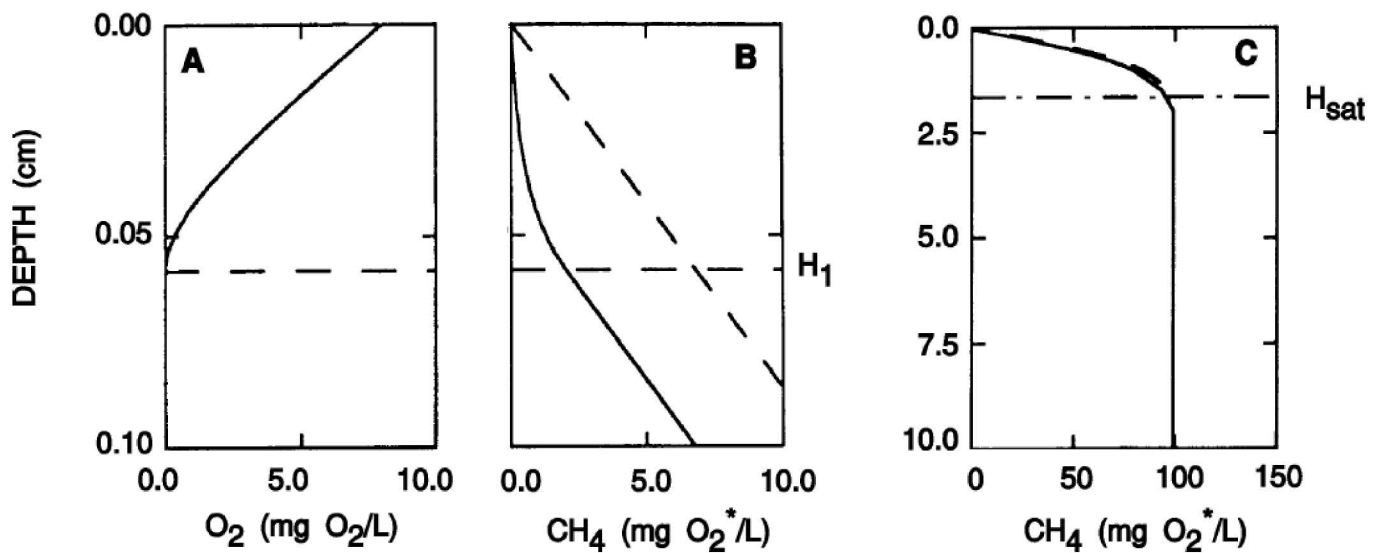


Fig. 10.2 Interstitial water concentrations profiles of dissolved oxygen and methane versus depth. (A) $\text{O}_2(z)$ from $z = 0$ to $z = 1$ mm. (B) $\text{CH}_4(\text{aq})$ from $z = 0$ to $z = 1$ mm. (C) $\text{CH}_4(\text{aq})$ from $z = 0$ to $z = 10$ cm. Dashed lines are for $\kappa_{\text{CH}_4,1} = 0$. Aerobic zone depth H_1 and depth of methane saturation H_{sat} are shown. Parameter values are given in Table 10.1.

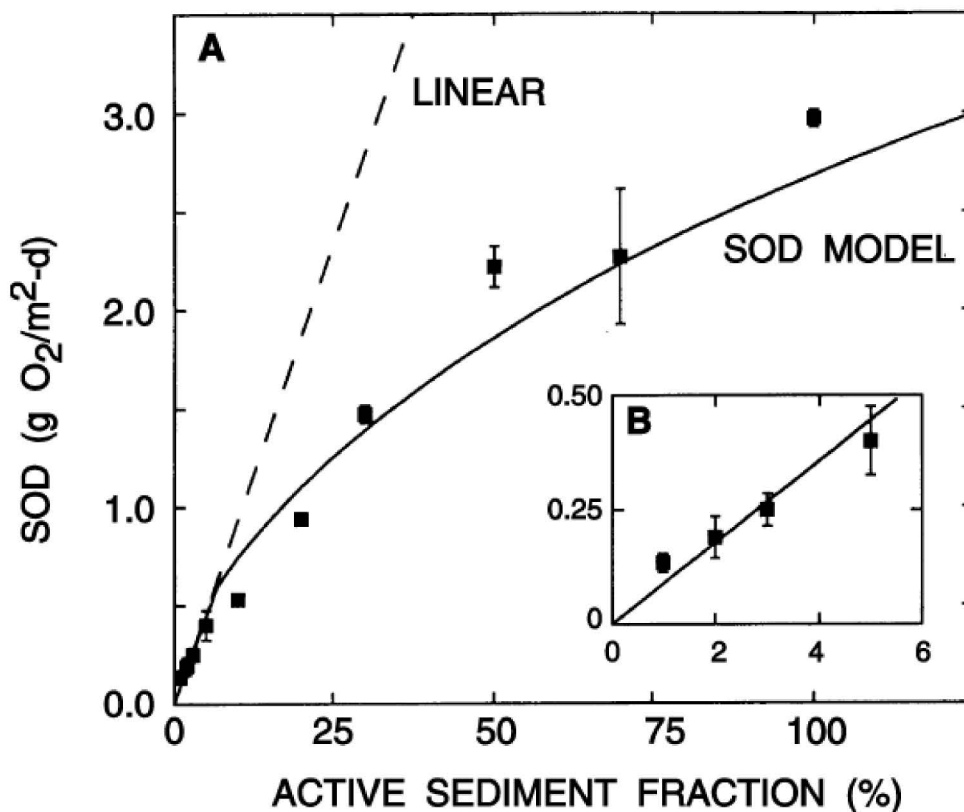


Fig. 10.3 Sediment dilution experiment. SOD versus percent of Milwaukee River sediment in the mixture. Data (mean \pm standard deviation). SOD model (solid lines computed using Eqs. (10.43)). Parameters are listed in Table 10.3. Axes and labels for the inset Fig. B are the same as (A). Dashed line in (A) is an extrapolation of the linear portion of the model result, shown in the inset figure (B).

SOD and Ammonia Flux vs Gas Flux

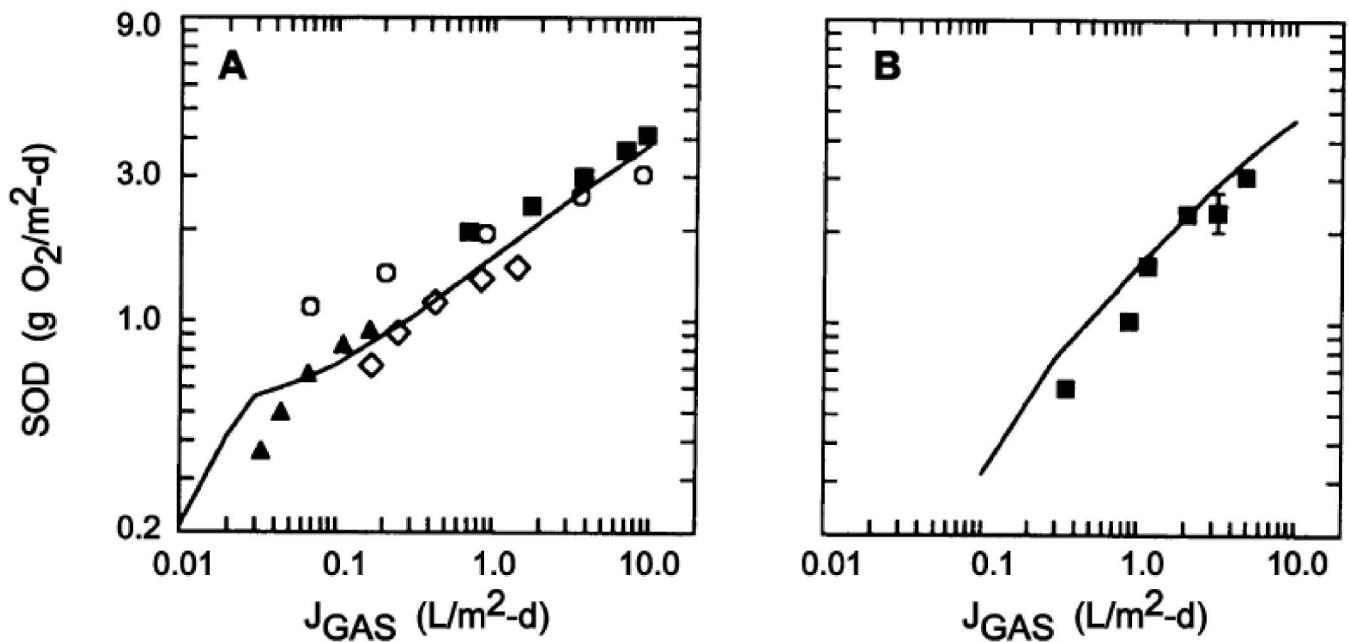


Fig. 10.4 SOD versus total gas flux. (A) Fair et al. (1941) Reactor depth (cm) = 1.42(▲), 2.55(■), 4.75(□), 10.2(◇). (B) Sediment dilution experiment. Lines are computed using Eqs. (10.43, 10.55, 10.56). Parameter values given in Table 10.3.

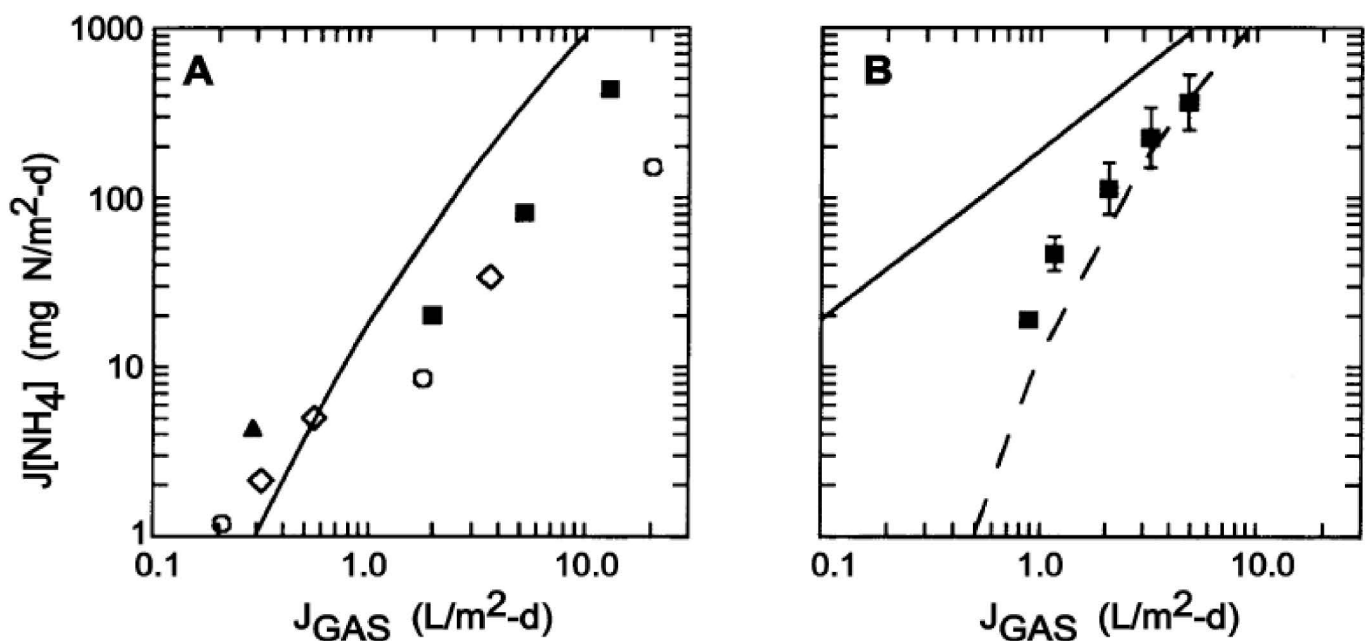


Fig. 10.5 Ammonia flux versus total gas flux. (A) Fair et al. (1941) data. Reactor depth (cm) = 1.42(▲), 2.55(■), 4.75(□), 10.2(◇). (B) Sediment dilution experiment. Anaerobic (solid line) and aerobic (dashed line) flux. Lines are computed using Eqs. (10.43a, 10.55, 10.56). Parameter values given in Table 10.3.

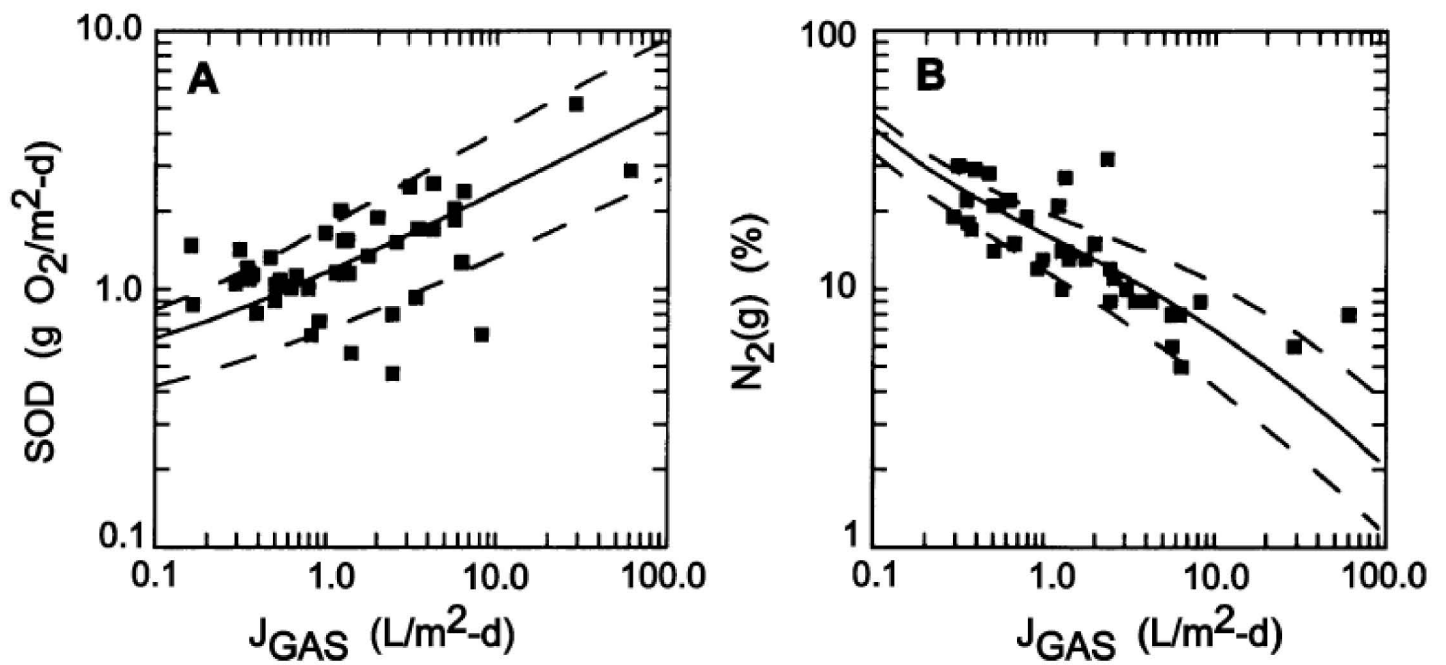
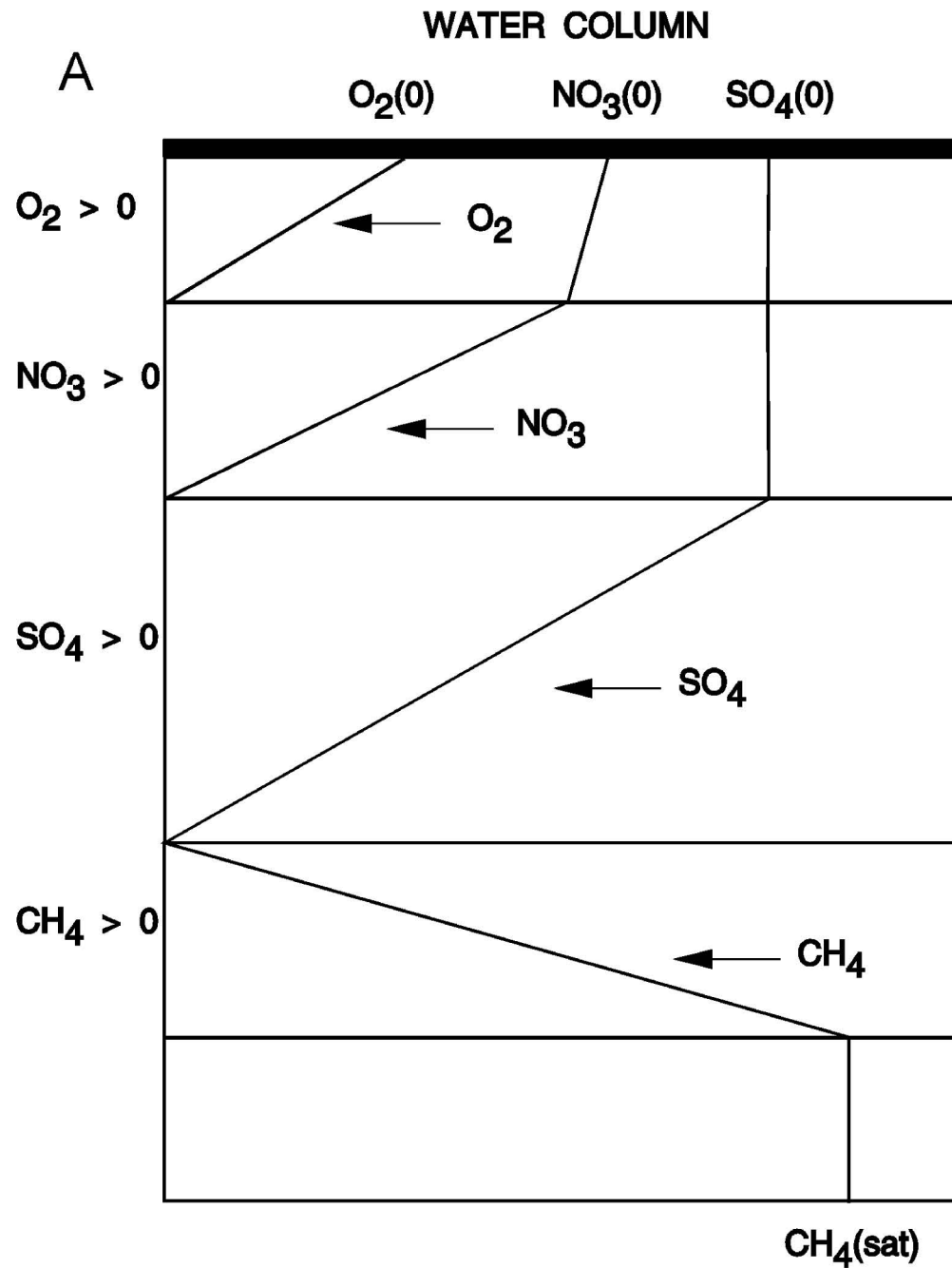
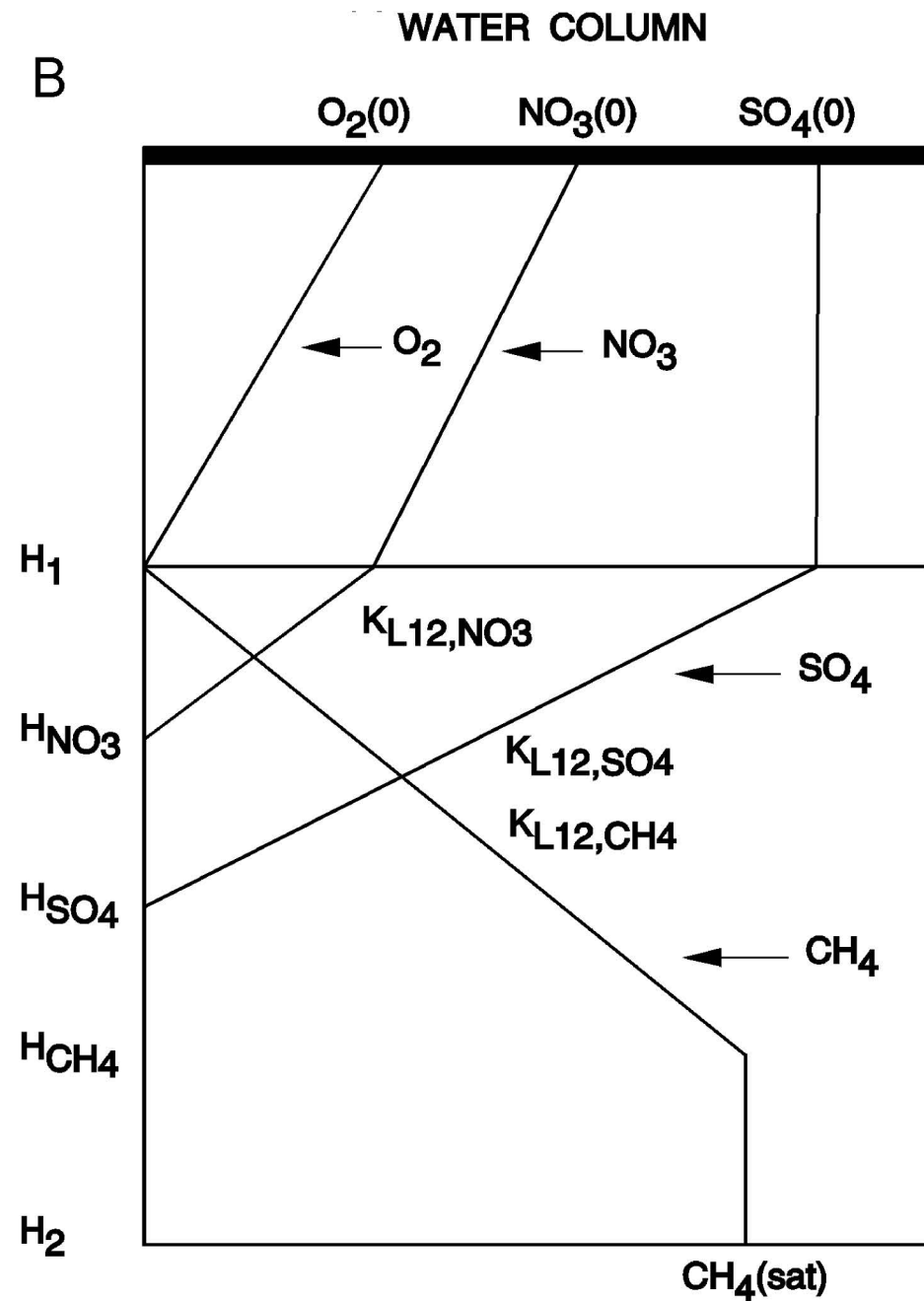


Fig. 10.6 Milwaukee River (A) SOD and (B) percent nitrogen gas versus total gas flux. Lines are computed using Eqs. (10.43, 10.55–10.56). Parameter values given in Table 10.3. Model results are evaluated using the median (solid) and the median plus and minus the standard deviation (dashed) of DO, temperature, and methane saturation concentration, given in Table 10.4.

Multilayer Model



Two Layer Model



Example Computations

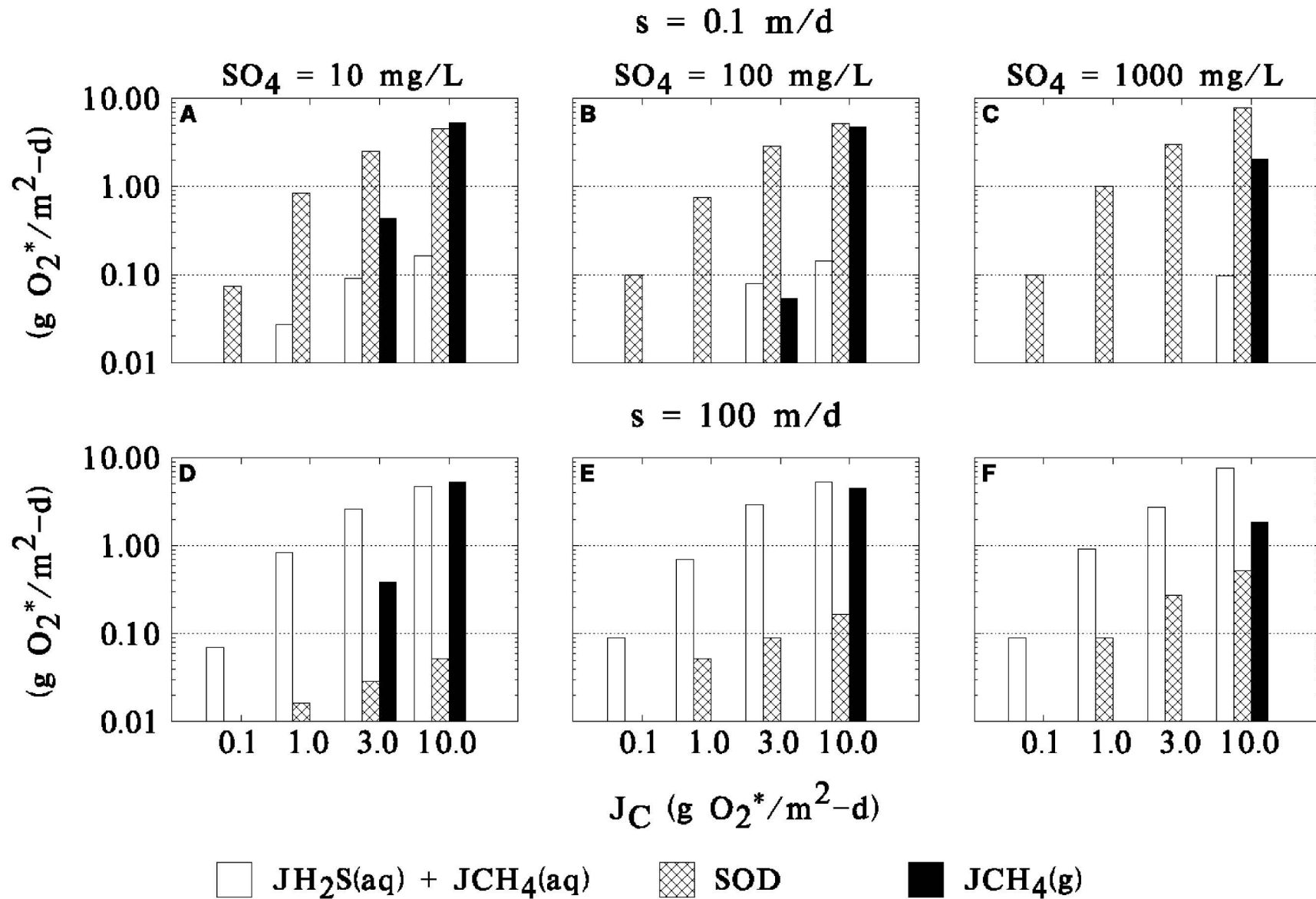
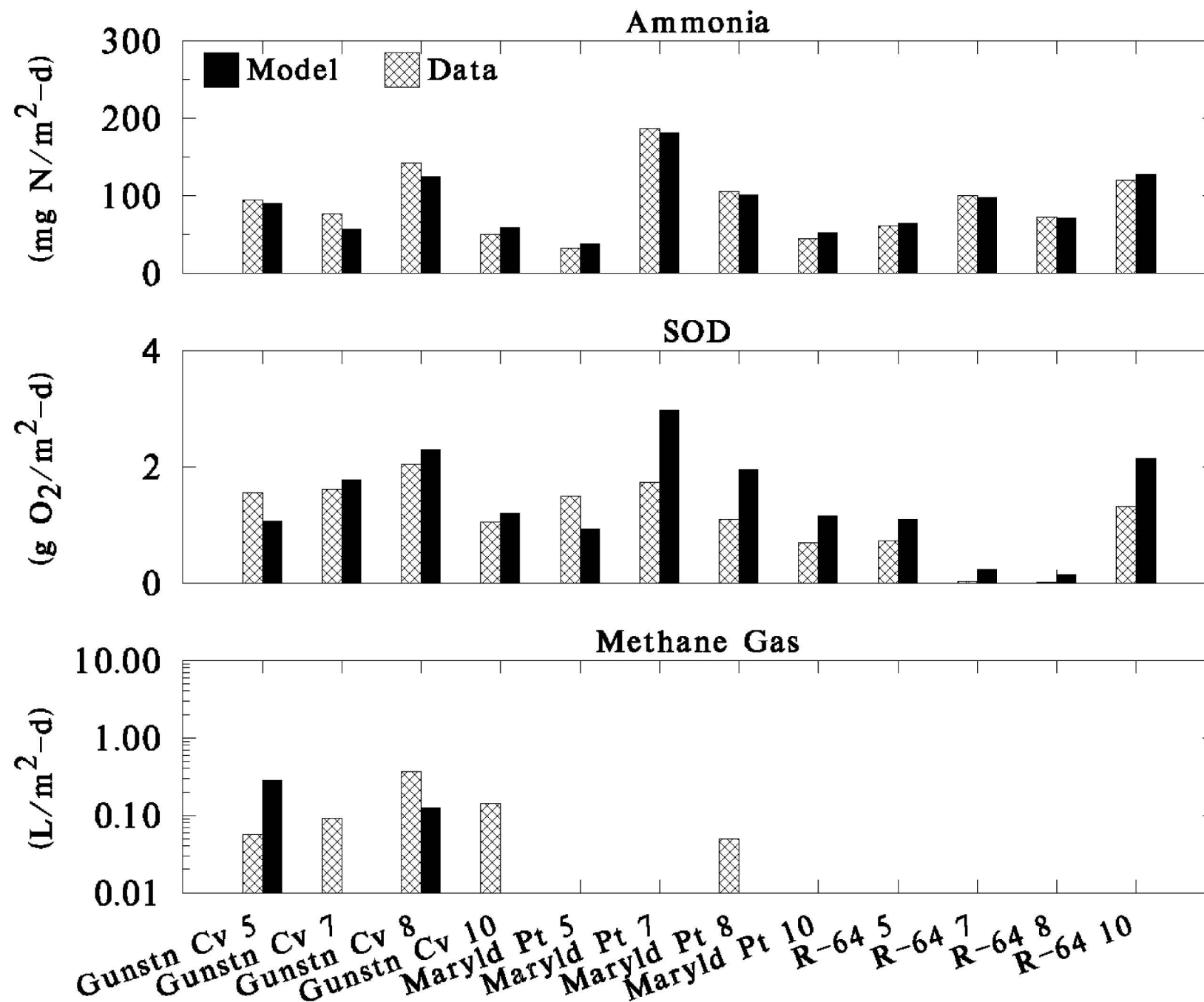
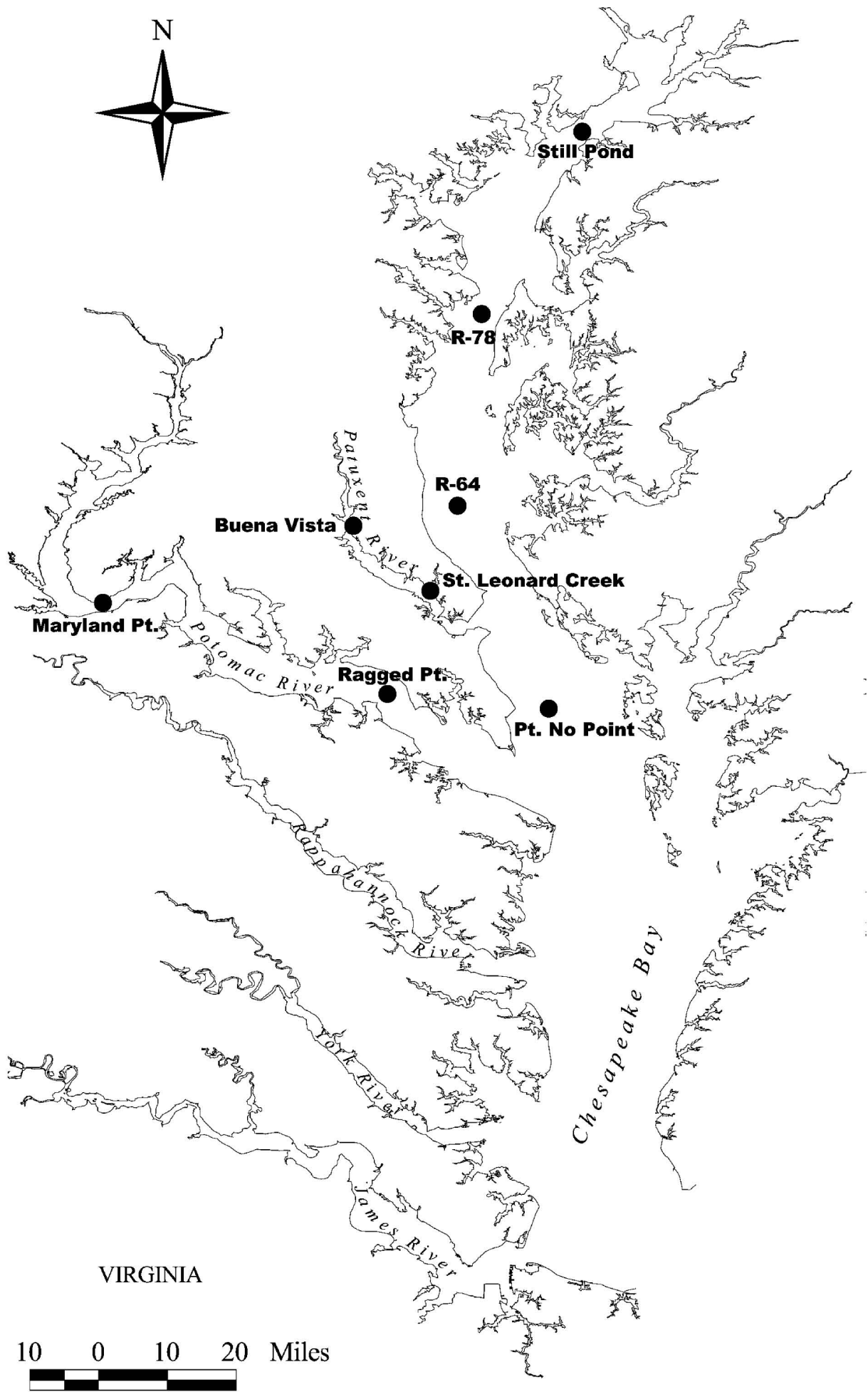


Fig. 11.7 Computed SOD, sulfide, and methane flux as a function of the surface mass transfer coefficient s (top and bottom rows), overlying water sulfate concentration $[\text{SO}_4(0)]$ (the three columns), and carbon diagenesis J_C (abscissa).

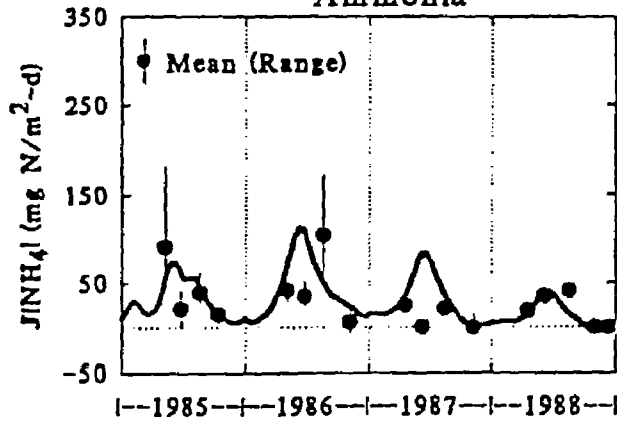
Model - Data Comparisons



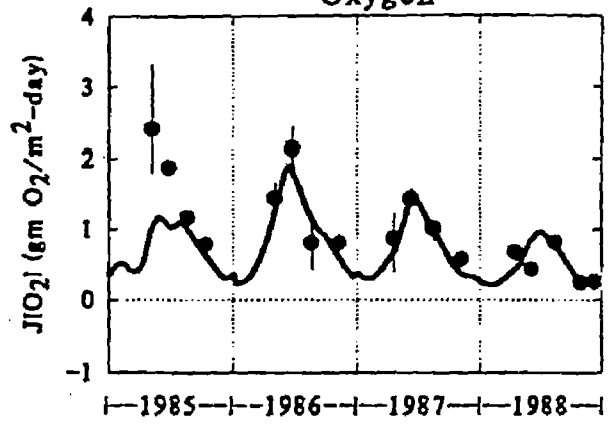


Still Pond

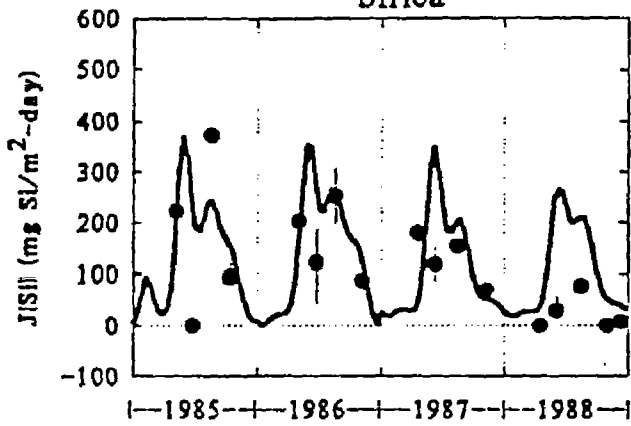
Ammonia



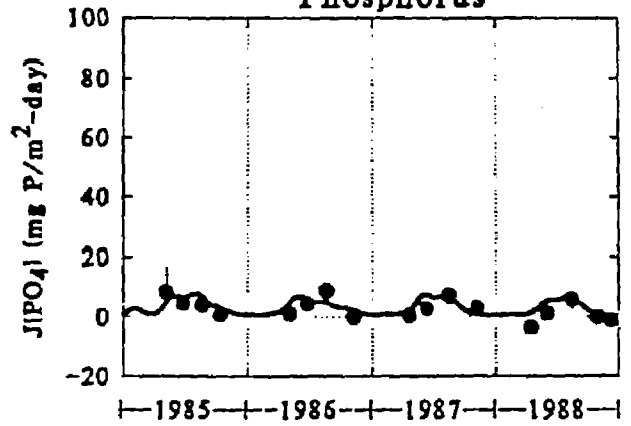
Oxygen



Silica

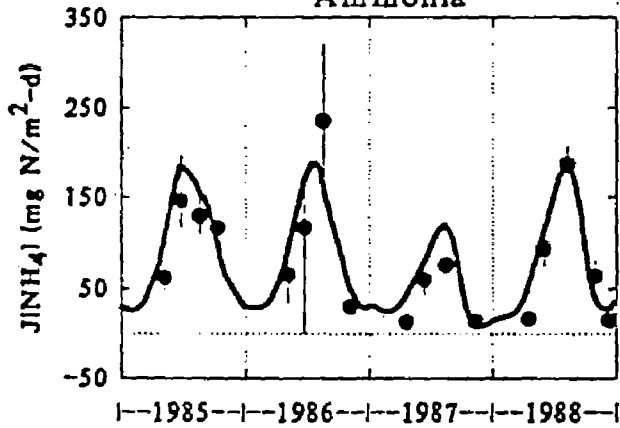


Phosphorus

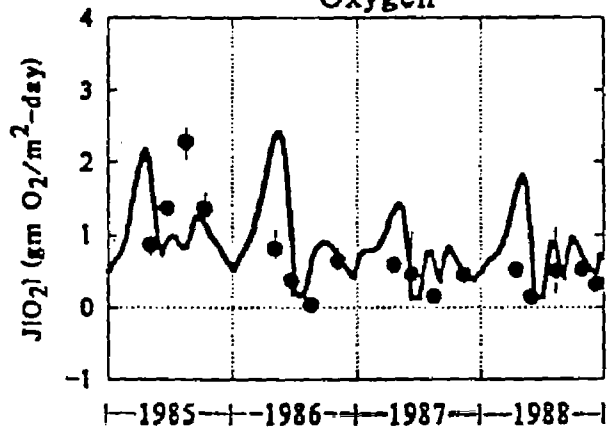


R-64

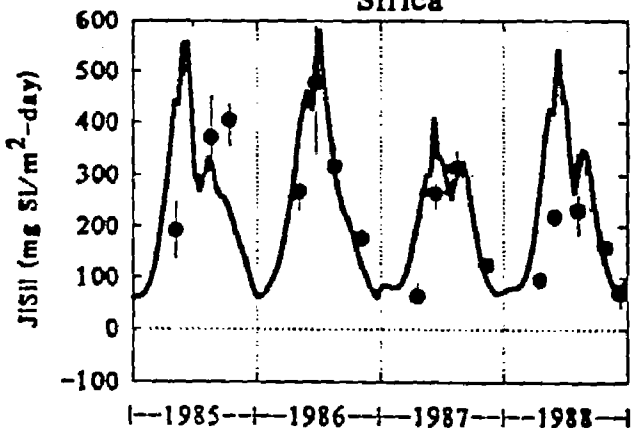
Ammonia



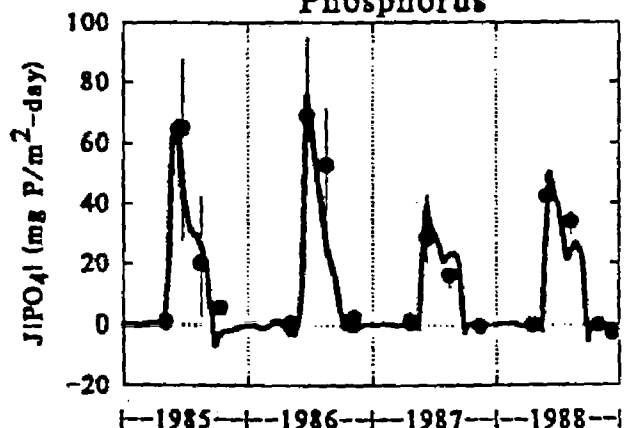
Oxygen

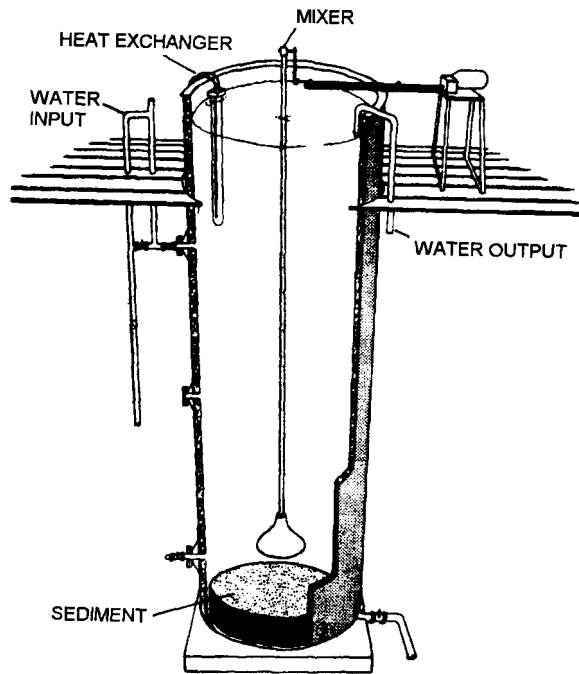
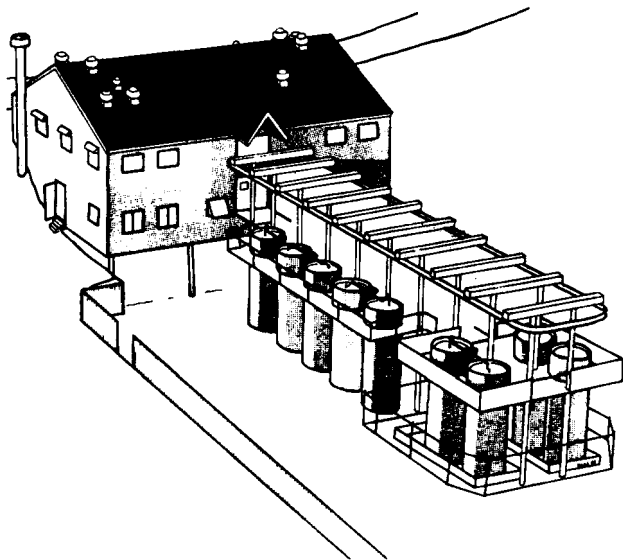


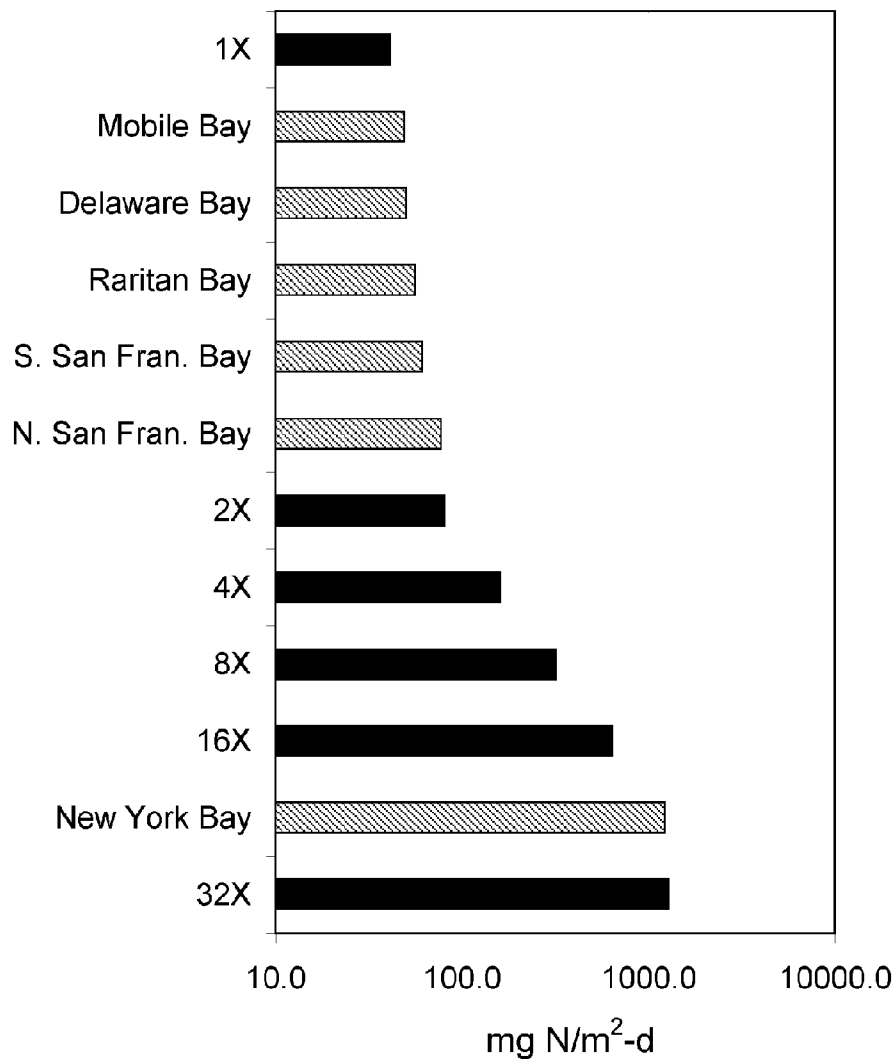
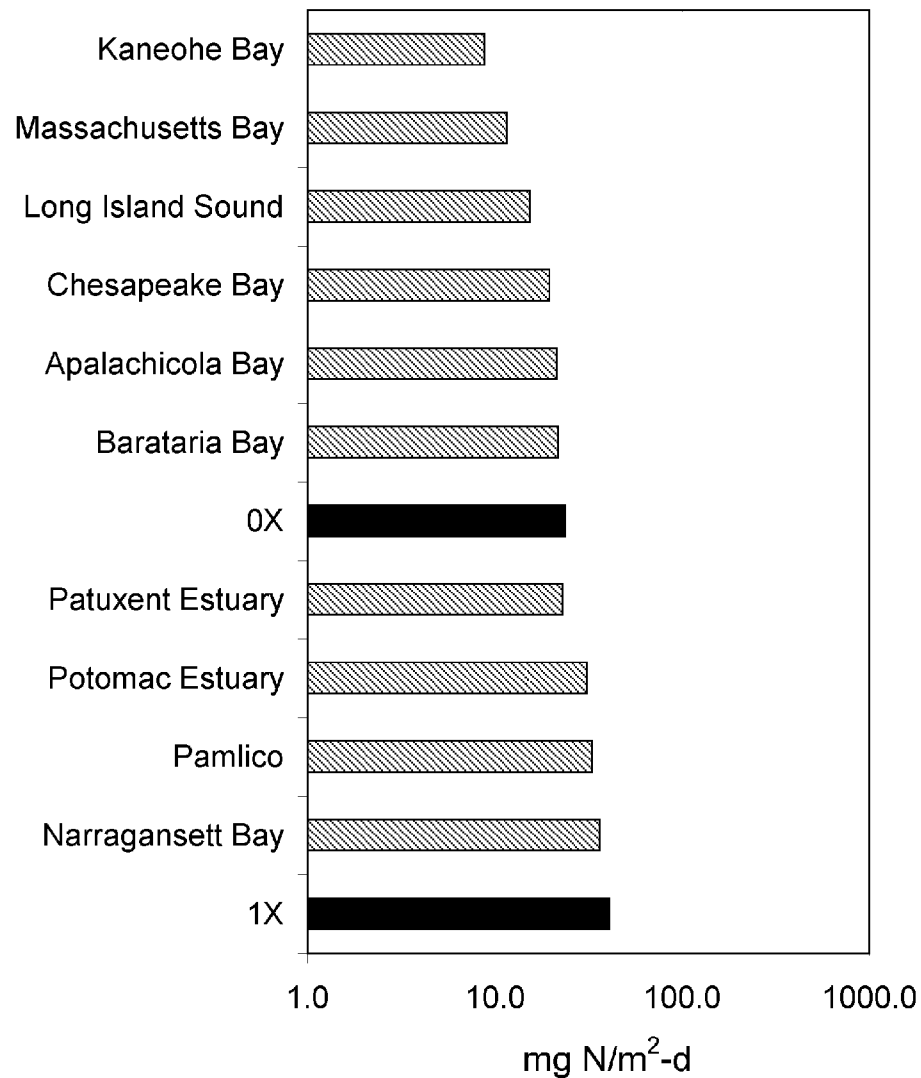
Silica



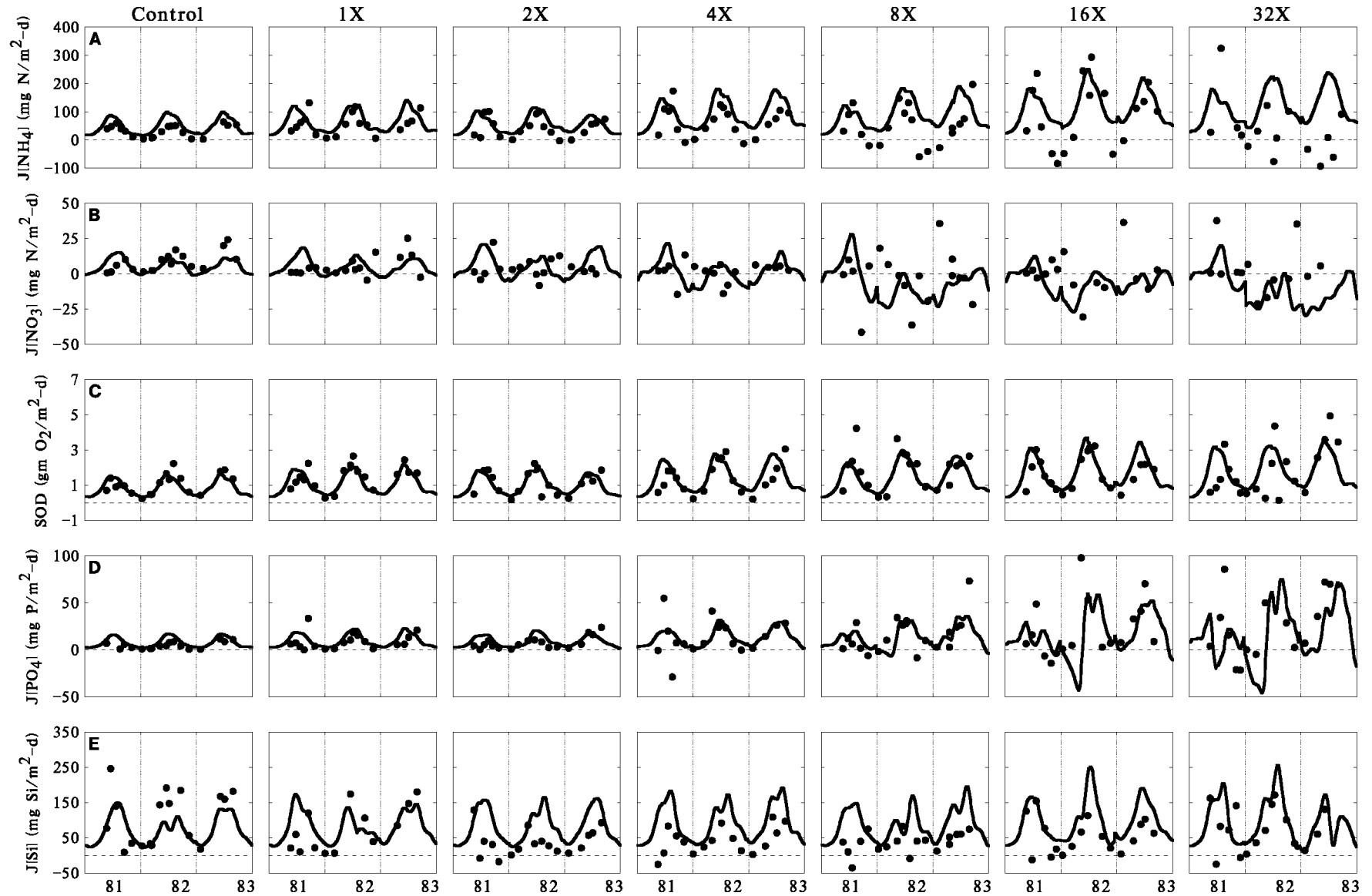
Phosphorus







Sediment Flux Model Validation (MERL Mesocosm)



Chesapeake Bay Ammonia Flux Calibration

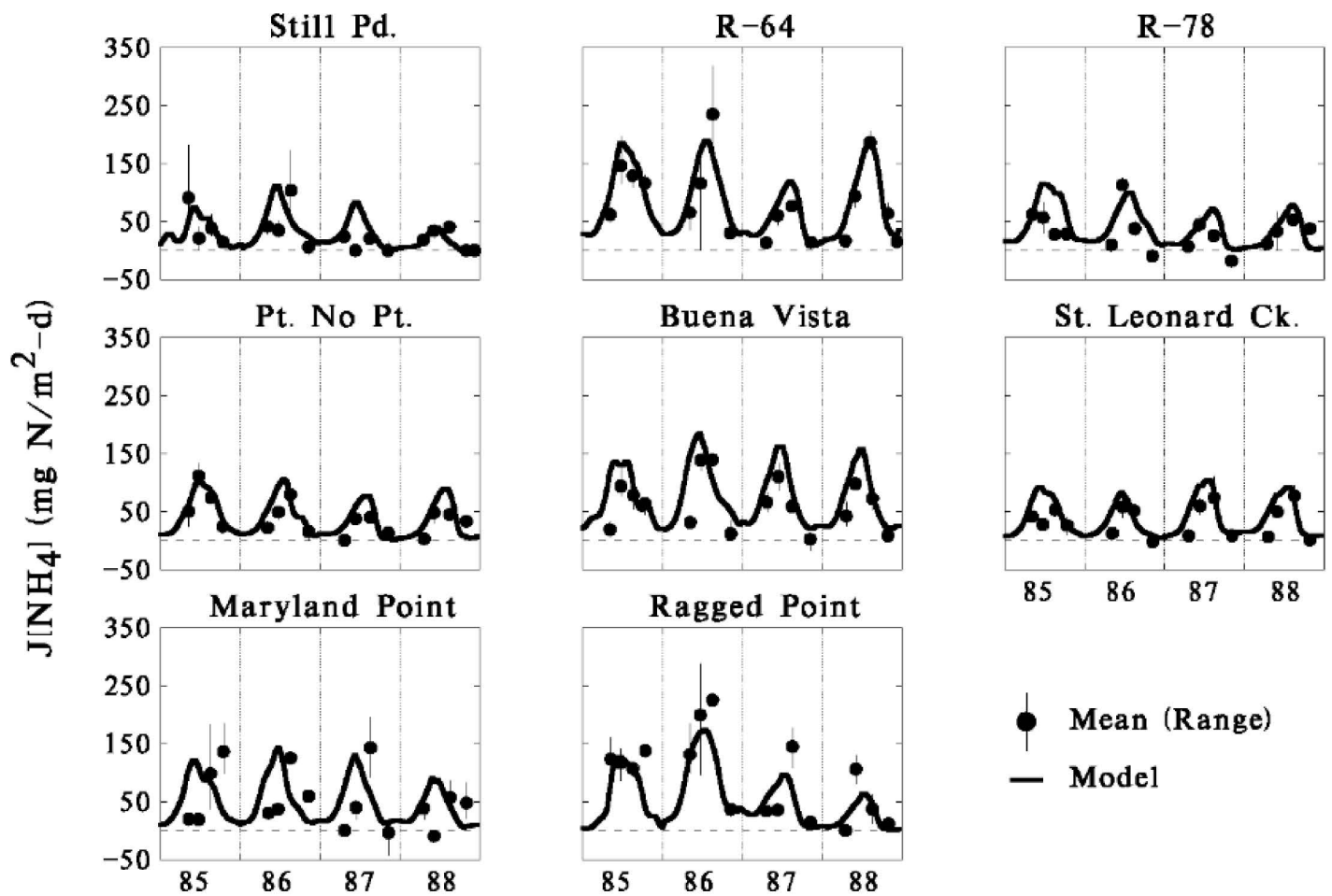
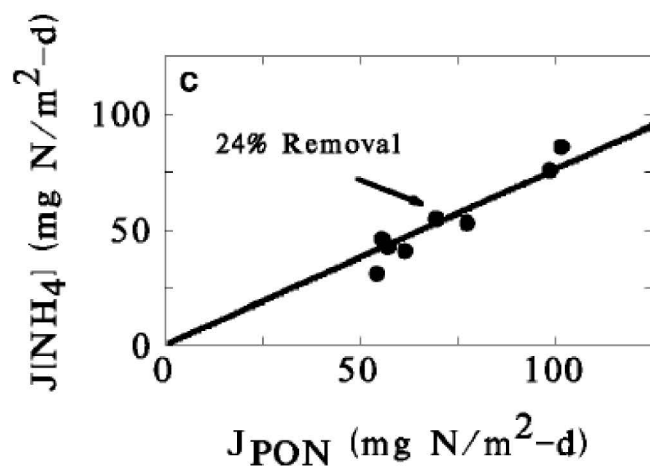
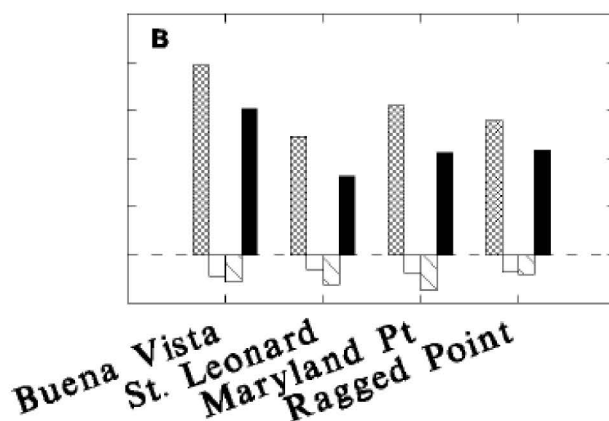
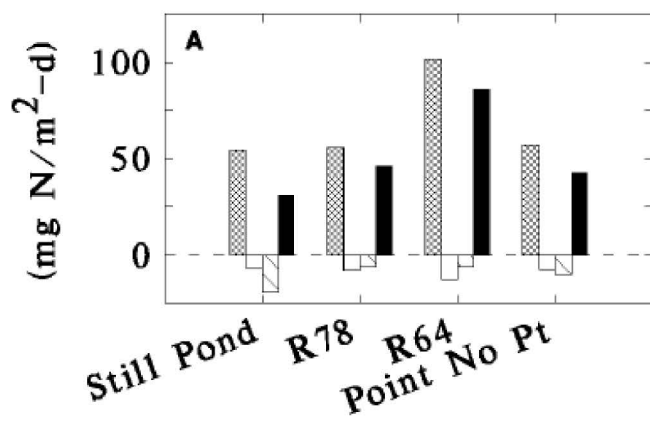
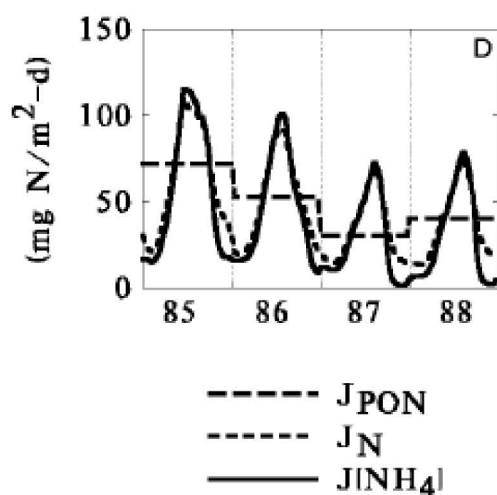
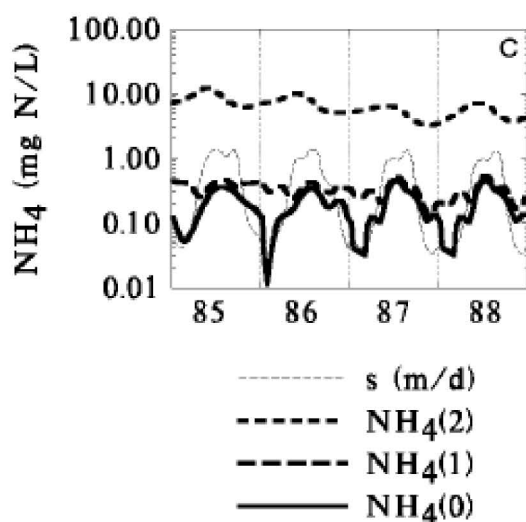
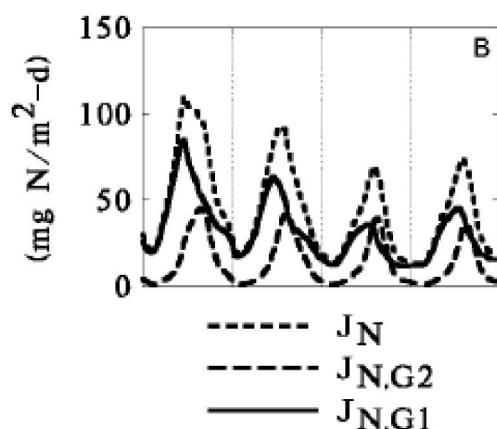
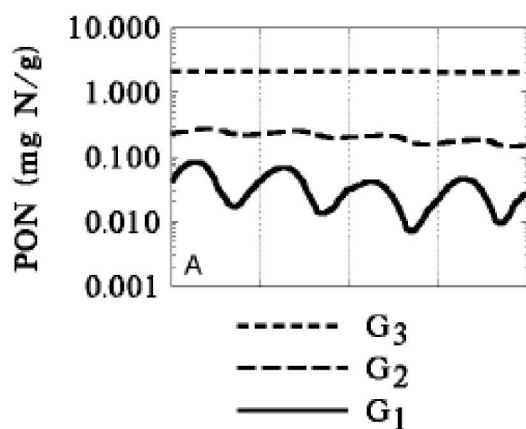


Table 12.6 Yearly Average Particulate Organic Nitrogen Depositional Fluxes J_{PON} ($\text{mg N/m}^2\text{-d}$)

Station	1985	1986	1987	1988
Point No Point	66.6	61.3	34.1	50.0
R-64	114.2	110.0	50.0	110.0
R-78	71.7	52.2	30.0	40.0
Still Pond	57.0	80.0	47.4	30.0
St. Leo	64.0	47.1	72.3	57.9
Buena Vista	97.5	120.0	90.0	90.0
Ragged Point	75.0	125.0	40.0	30.0
Maryland Point	82.5	81.0	77.9	60.0

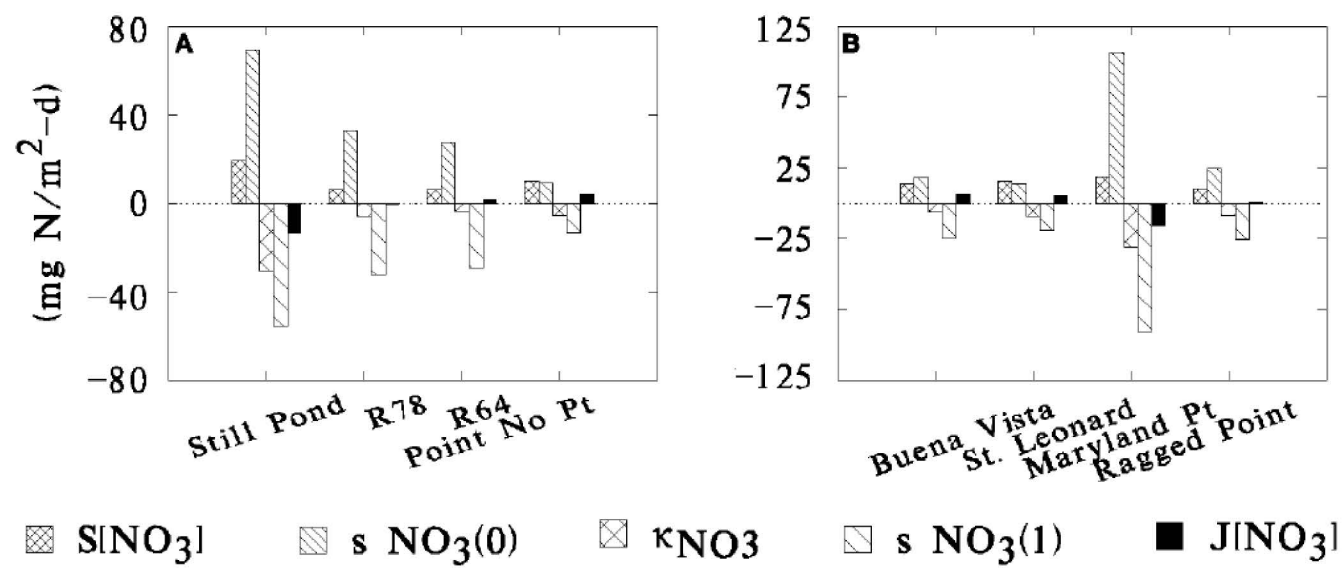
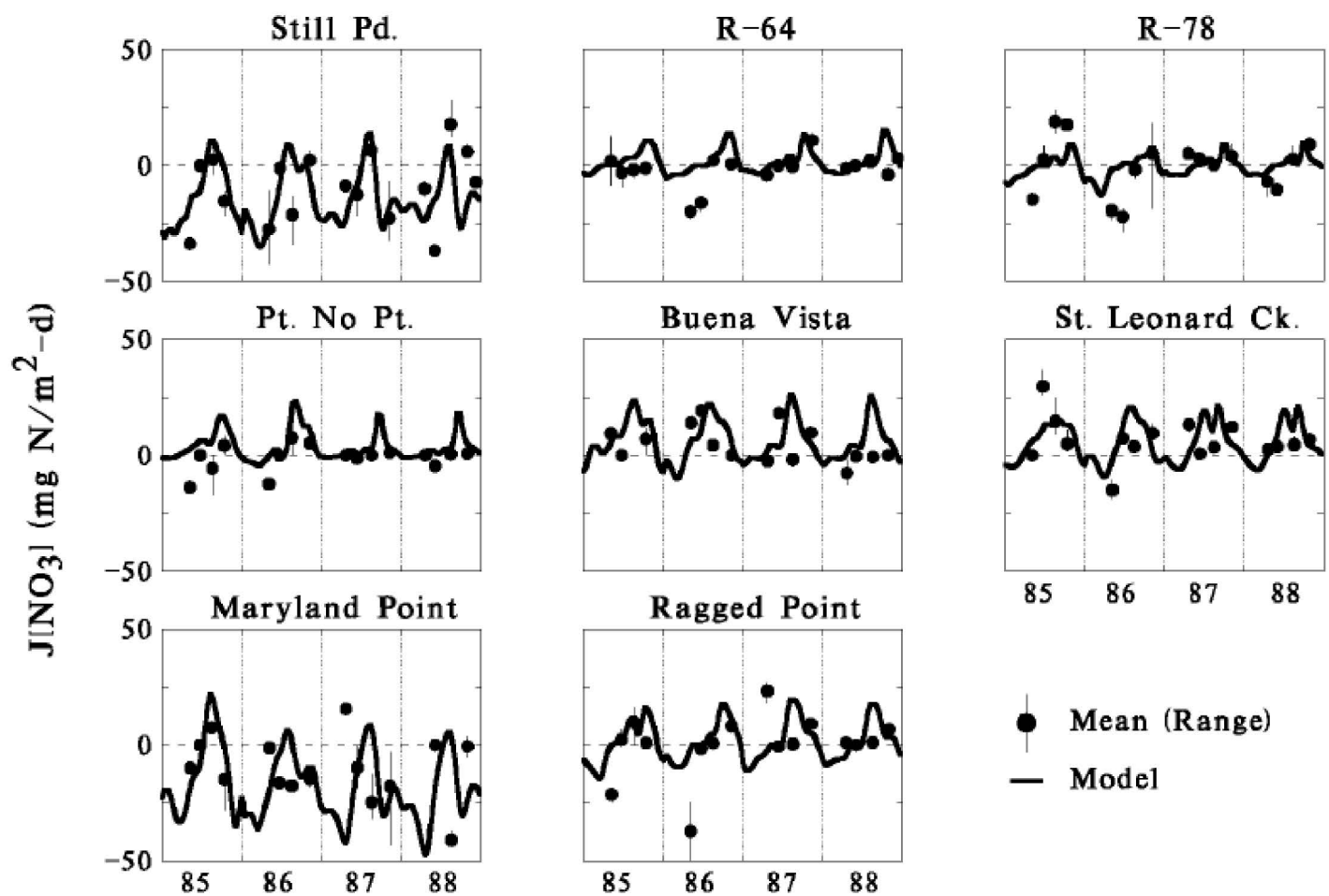
Ammonia Flux - Components



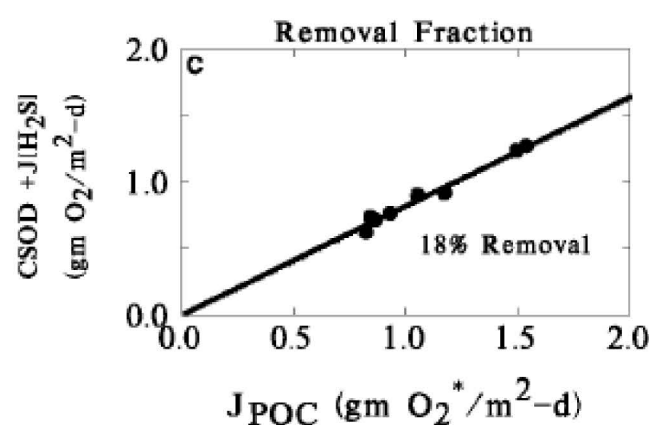
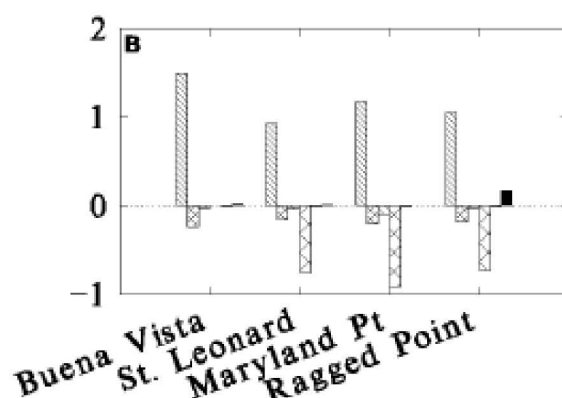
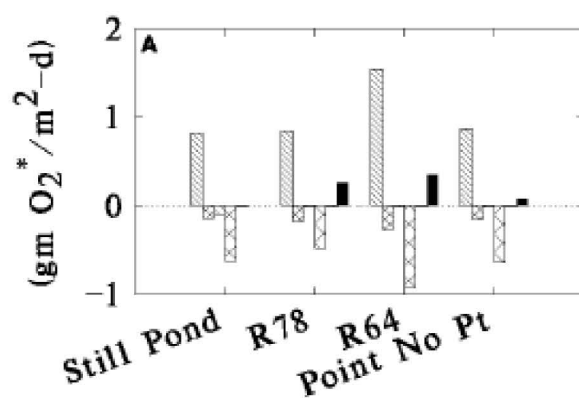
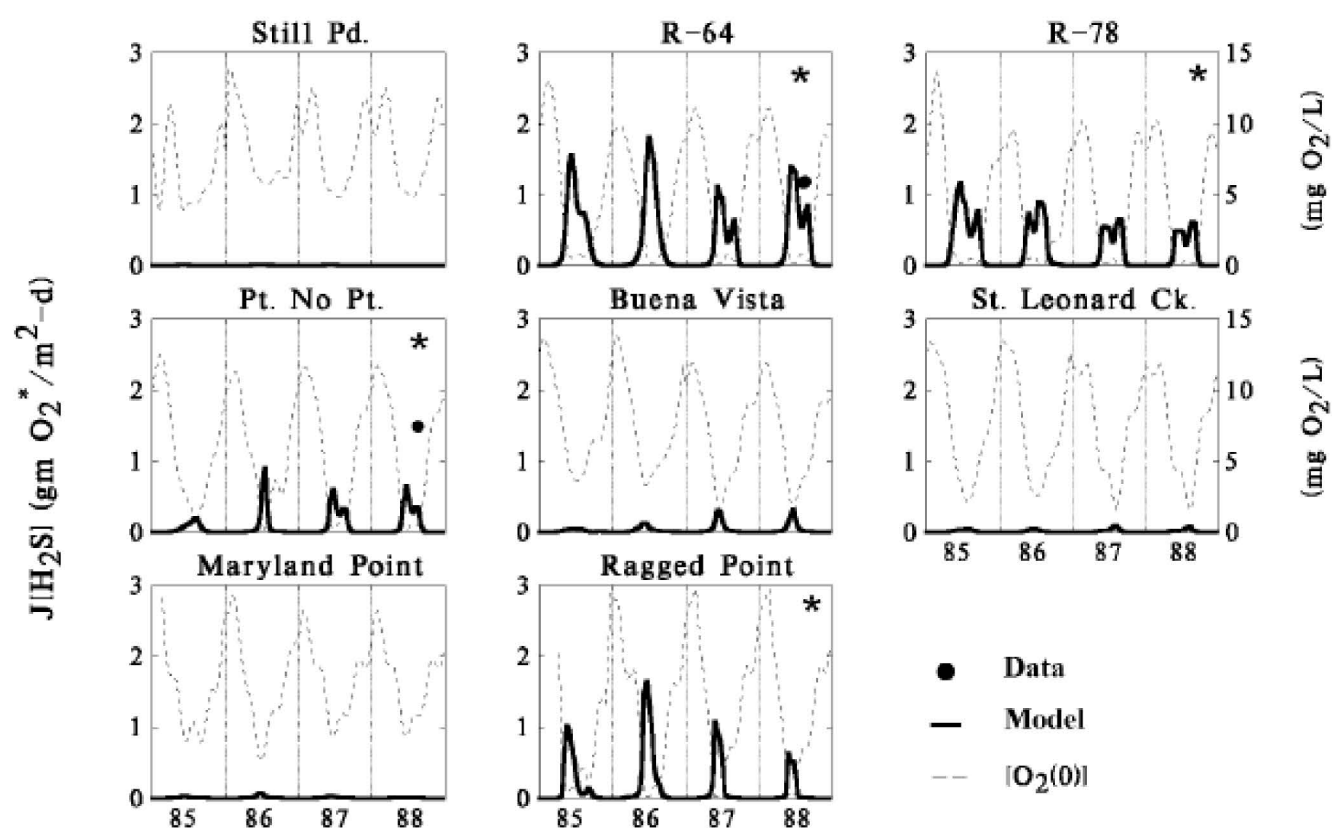
Legend



Nitrate Flux Model Calibration



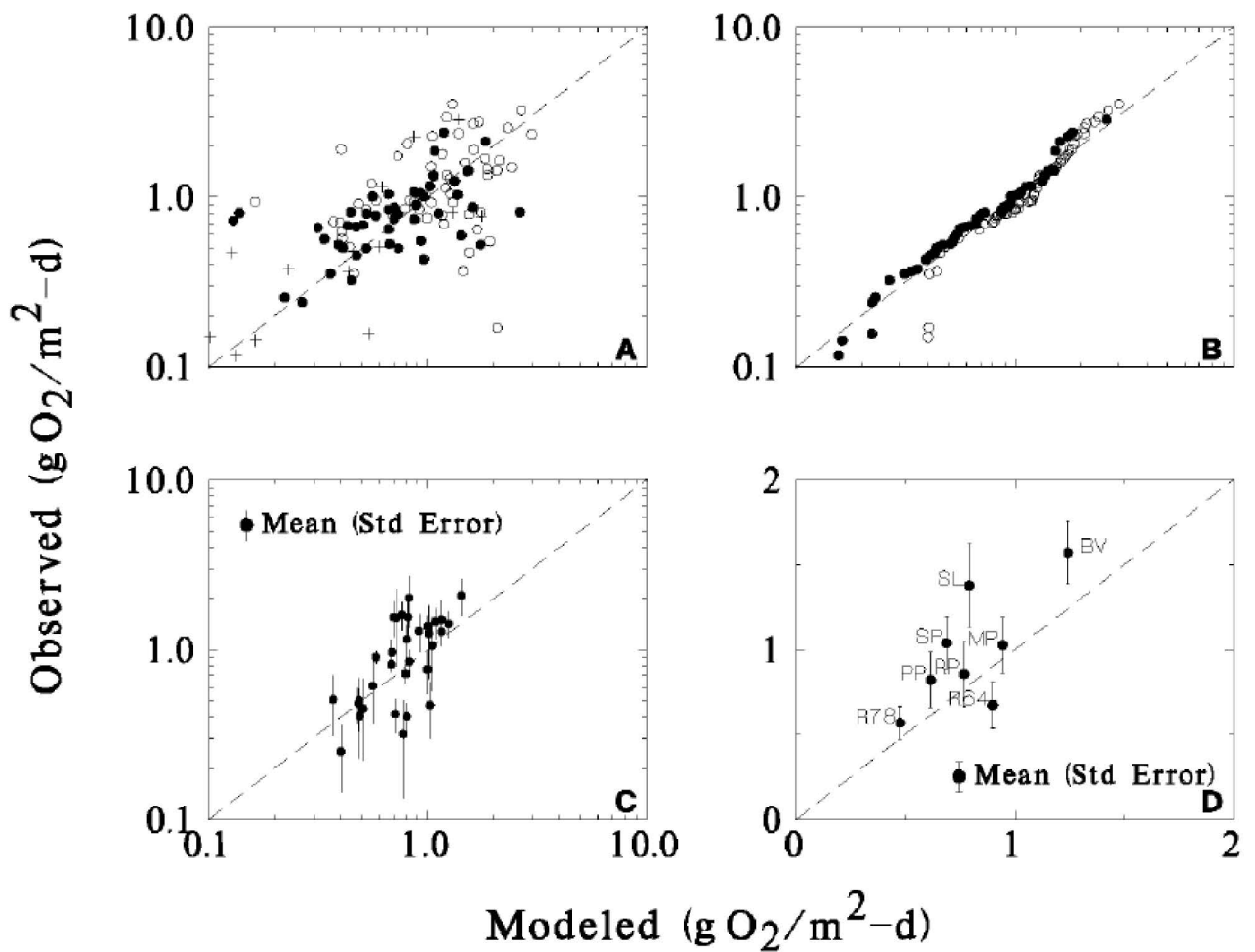
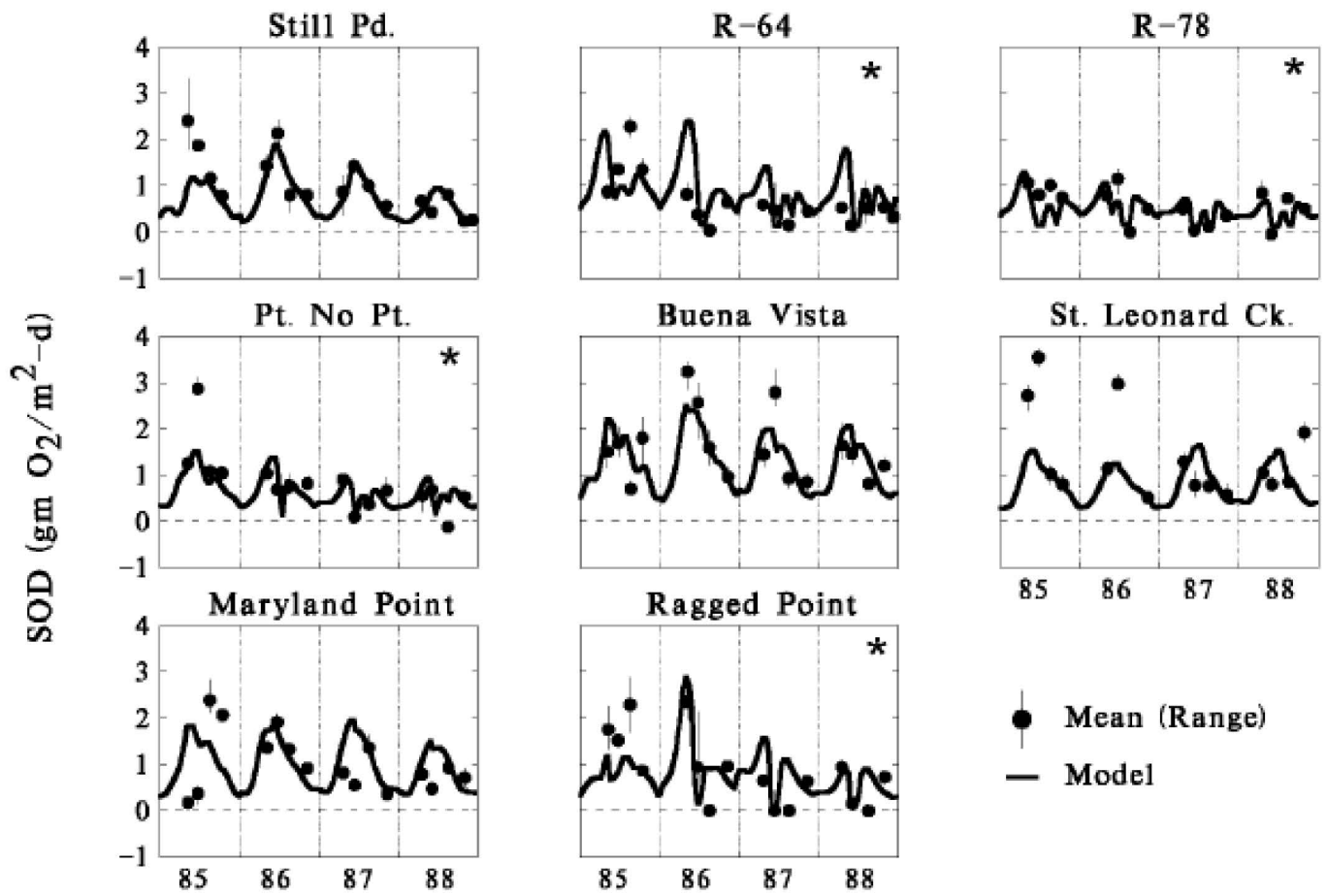
Hydrogen Sulfide Flux Model



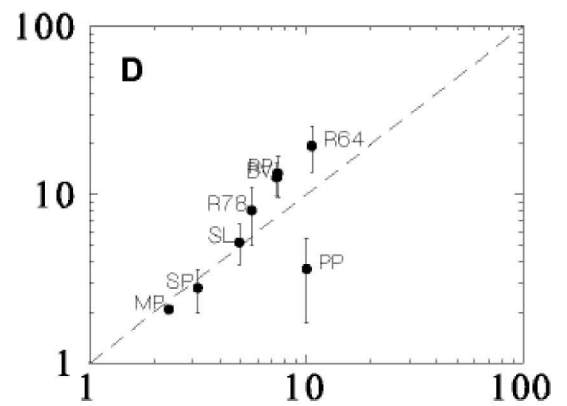
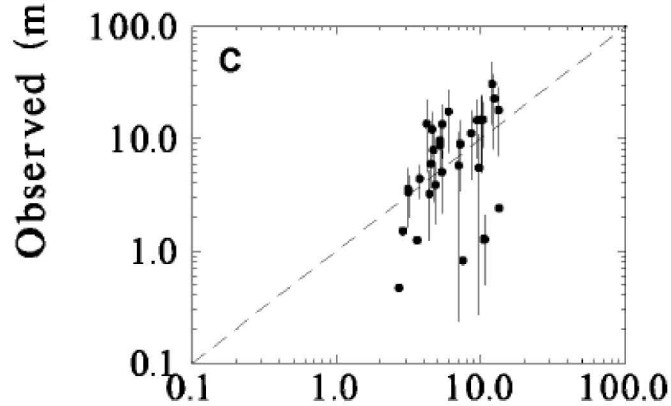
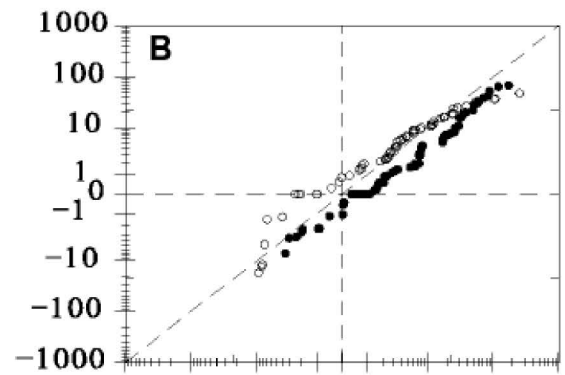
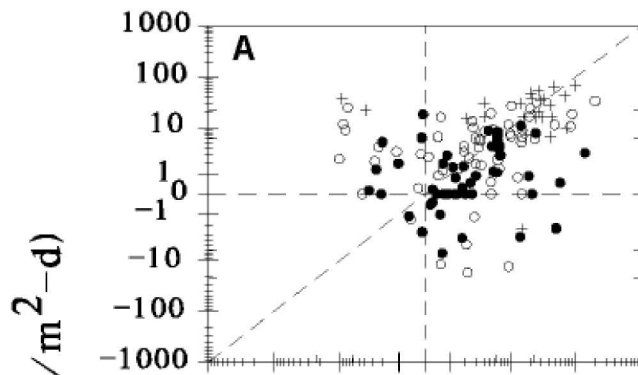
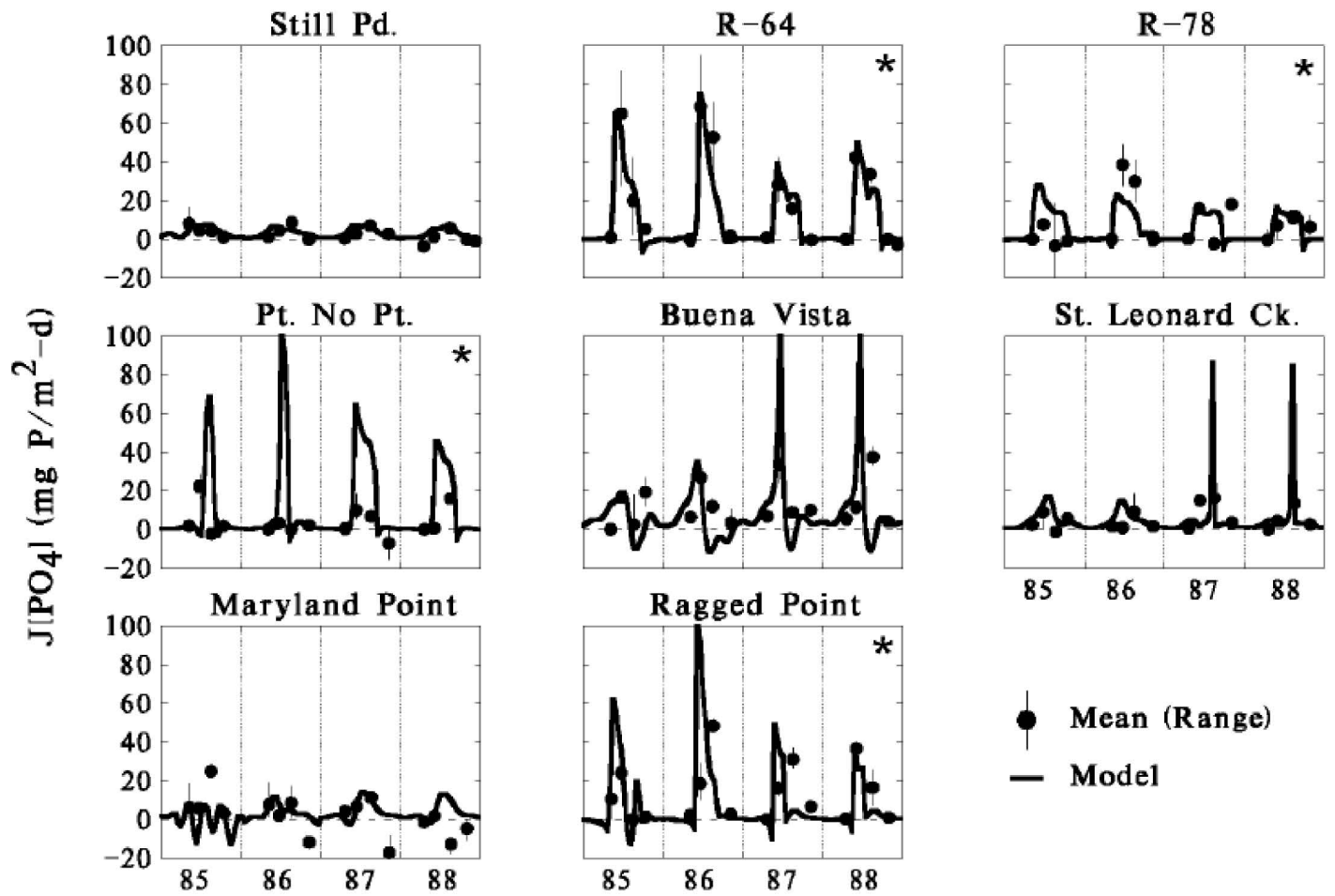
Legend

- J_{POC}
- $w_2 \text{ POC}$
- $[\text{SiNO}_3]$
- $\kappa \text{H}_2\text{S}$
- $w_2 \text{ PS}$
- $J[\text{H}_2\text{S}]$

SOD Model

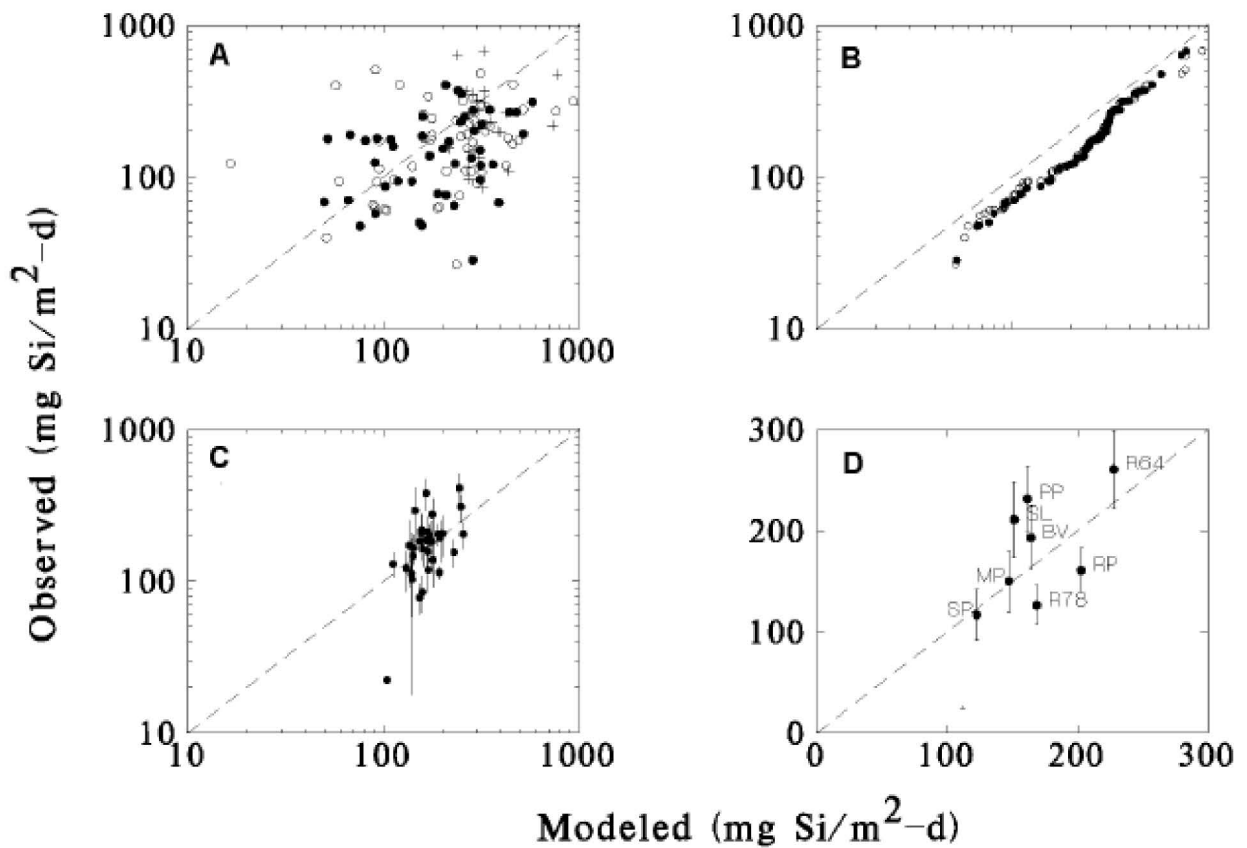
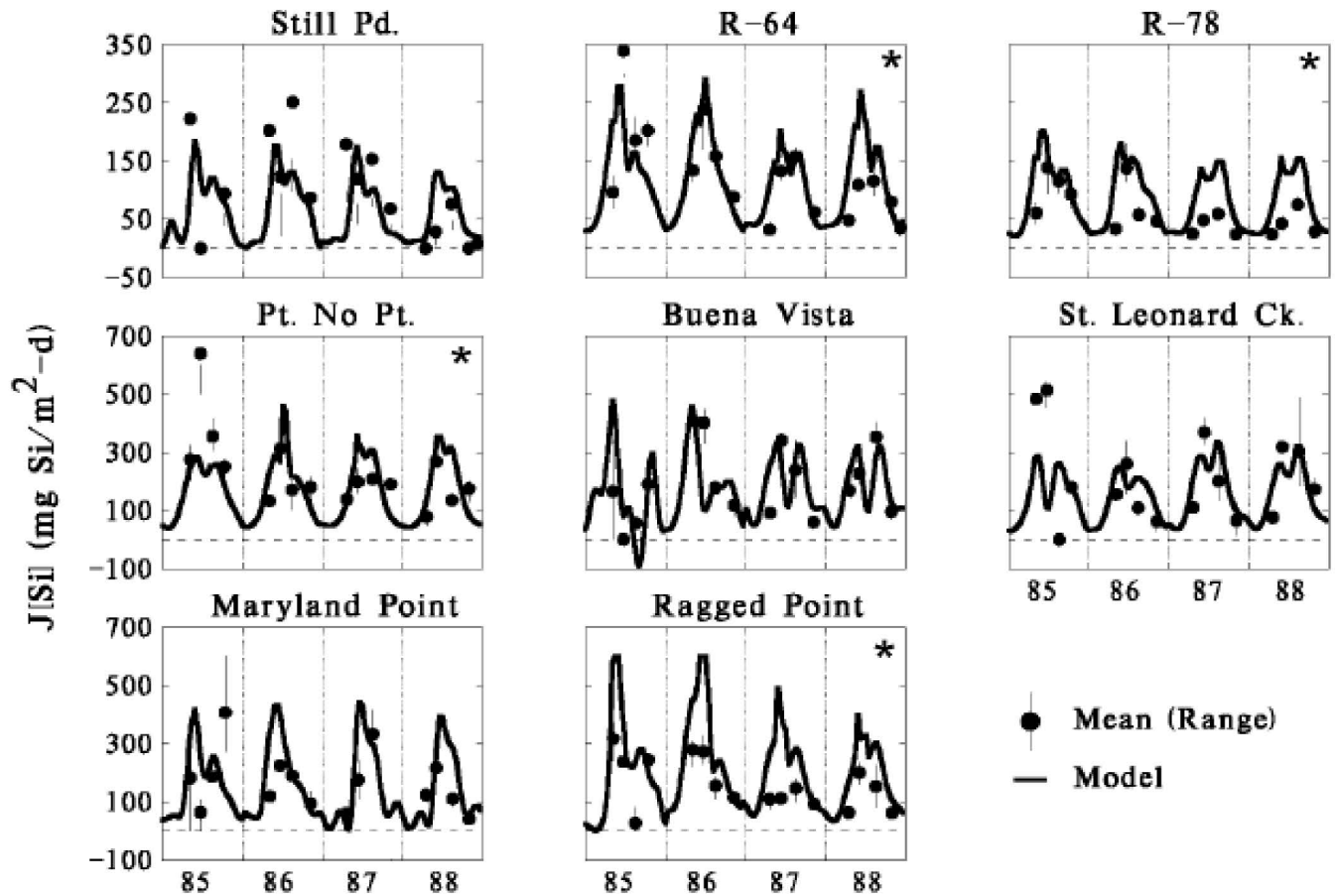


Phosphate Flux Model



Modeled (mg P/m²-d)

Silica Flux Model



Di Toro, D.M., 2001. Sediment Flux Modeling.
Wiley-Interscience, New York ISBN: 0-471-13535-6

Contents

<i>Preface</i>	<i>xv</i>
<i>Acknowledgments</i>	<i>xxi</i>
 <i>Part I Preliminaries</i>	
<i>1 Properties of Sediments</i>	<i>3</i>
1.1 <i>Physical Characteristics</i>	<i>3</i>
1.2 <i>Chemical Preliminaries</i>	<i>9</i>
1.3 <i>Chemical Characteristics</i>	<i>14</i>
1.4 <i>Biological Characteristics</i>	<i>20</i>
1.5 <i>Conclusion</i>	<i>24</i>
 <i>2 Model Formulation</i>	 <i>27</i>
2.1 <i>Framework</i>	<i>27</i>
2.2 <i>Mass Balance Equations</i>	<i>29</i>
2.3 <i>Sedimentation and Burial</i>	<i>33</i>
2.4 <i>Mixing Processes and Mass Transfer Coefficients</i>	<i>37</i>
2.5 <i>Two-Layer Mass Balance</i>	<i>42</i>
	 <i>vii</i>

viii CONTENTS

2.6	<i>Particulate Organic Nitrogen and Ammonia</i>	43
2.7	<i>Continuous Models</i>	48
	<i>Appendix 2A: Solution of Mass Balance Equations</i>	53
2A.1	<i>First-Order Equation</i>	53
2A.2	<i>Second-Order Equation</i>	54
	<i>Appendix 2B: MACSYMA Solutions</i>	55

Part II Nutrients

3	<i>Ammonia</i>	63
3.1	<i>Introduction</i>	63
3.2	<i>Model Components</i>	63
3.3	<i>Mass Balance Equations</i>	65
3.4	<i>Data Analysis</i>	75
3.5	<i>Observations of Chesapeake Bay Nitrification</i>	81
3.6	<i>Nonsteady State Features</i>	82
3.7	<i>Conclusions</i>	84
	<i>Appendix 3A: Solution of Ammonia Mass Balance Equations</i>	84
	<i>Appendix 3B: Ammonia and Dissolved Oxygen Surface Mass Transfer Coefficients</i>	85
	<i>Appendix 3C: Regression Analysis</i>	90
4	<i>Nitrate</i>	93
4.1	<i>Introduction</i>	93
4.2	<i>Model Formulation and Solution</i>	93
4.3	<i>Nitrate Source from the Overlying Water</i>	98
4.4	<i>Nitrate Source from Nitrification</i>	102
4.5	<i>Model Applications</i>	102
4.6	<i>Flux Normalization and Parameter Estimation</i>	106
4.7	<i>Application to Chesapeake Bay</i>	110
4.8	<i>Estimate of the Denitrification Reaction Velocities</i>	111
4.9	<i>Observations of Chesapeake Bay Denitrification</i>	113
4.10	<i>Extent of Denitrification and the Nitrogen Balance</i>	115
4.11	<i>Conclusions</i>	116
	<i>Appendix 4A: MACSYMA</i>	117

5	<i>Steady State Model</i>	119
5.1	<i>Introduction</i>	119
5.2	<i>Modeling Framework</i>	121
5.3	<i>Mass Balance Equations</i>	121
5.4	<i>Solution For Anaerobic Layer Source</i>	123
5.5	<i>Solution For Aerobic Layer Source</i>	127
	<i>Appendix 5A: MACSYMA</i>	129
6	<i>Phosphorus</i>	131
6.1	<i>Introduction</i>	131
6.2	<i>Model Components</i>	132
6.3	<i>Solutions</i>	133
6.4	<i>Simplified Phosphate Flux Model</i>	138
6.5	<i>Steady State Numerical Model</i>	140
6.6	<i>Conclusions</i>	143
	<i>Appendix 6A: Positive and Negative Logarithmic Scale for Plotting</i>	143
7	<i>Silica</i>	149
7.1	<i>Introduction</i>	149
7.2	<i>Model Components</i>	149
7.3	<i>Solutions</i>	151
7.4	<i>Final Model</i>	154
7.5	<i>Conclusions</i>	158
 <i>Part III Oxygen</i>		
8	<i>Oxygen Equivalents</i>	161
8.1	<i>Introduction</i>	161
8.2	<i>Proposed Modeling Frameworks</i>	162
8.3	<i>Oxygen Equivalents</i>	167
8.4	<i>Sediment Oxygen Demand</i>	172
8.5	<i>Oxygen Equivalents and SOD</i>	175
8.6	<i>Conclusion</i>	182
9	<i>Sulfide</i>	183
9.1	<i>Introduction</i>	183

x CONTENTS

9.2	<i>Sulfide Production</i>	183
9.3	<i>Sulfide Oxidation</i>	185
9.4	<i>Solutions</i>	186
9.5	<i>Sediment Oxygen Demand</i>	189
9.6	<i>Data Analysis</i>	191
9.7	<i>Commentary</i>	194
10	<i>Methane</i>	195
10.1	<i>Introduction</i>	195
10.2	<i>Stoichiometry and Oxygen Equivalents</i>	195
10.3	<i>Dissolved Methane Mass Balance</i>	197
10.4	<i>Dissolved Oxygen Mass Balance</i>	201
10.5	<i>SOD Equation</i>	204
10.6	<i>Data Analysis</i>	210
10.7	<i>Relationship to Sulfide Oxidation</i>	216
	<i>Appendix 10A: Positive and Negative Logarithmic Scale for Plotting</i>	217
	<i>Appendix 10B: Solution of Dissolved Oxygen Mass Balance Equations</i>	219
11	<i>Sulfide and Methane</i>	221
11.1	<i>Introduction</i>	221
11.2	<i>Sulfate Consumption</i>	222
11.3	<i>Layers and Mass Transfer Resistances</i>	224
11.4	<i>Multilayer versus Two-layer Models</i>	226
11.5	<i>Depth of Sulfate Reduction</i>	227
11.6	<i>Sulfate and Methane Mass Balance Equations</i>	231
11.7	<i>Numerical Examples</i>	235
11.8	<i>Upper Potomac Estuary</i>	237
11.9	<i>Anacostia River</i>	242
11.10	<i>Conclusions</i>	242
	<i>Appendix 11A: MACSYMA Solution for the Three-Layer Equations</i>	243
	<i>Appendix 11B: MACSYMA Solution of the Sulfate Mass Balance Equations</i>	243
	<i>Appendix 11C: MACSYMA Solution of the Sulfide-Sulfate Mass Balance Equations</i>	243

Part IV Time Variable Model Implementation

<i>12 Diagenesis</i>	<i>251</i>
12.1 <i>Introduction</i>	<i>251</i>
12.2 <i>Mass Balance Equations</i>	<i>252</i>
12.3 <i>Diagenesis Stoichiometry</i>	<i>254</i>
12.4 <i>Diagenesis Kinetics</i>	<i>259</i>
12.5 <i>Depositional Flux</i>	<i>267</i>
12.6 <i>Sediment Composition</i>	<i>269</i>
12.7 <i>Sediment Algal Carbon</i>	<i>270</i>
12.8 <i>Conclusions</i>	<i>273</i>
 <i>13 Mass Transport and Numerical Methods</i>	 <i>275</i>
13.1 <i>Introduction</i>	<i>275</i>
13.2 <i>Transport Parameters</i>	<i>275</i>
13.3 <i>Sediment Solids</i>	<i>282</i>
13.4 <i>Effect of Varying Layer Thickness</i>	<i>284</i>
13.5 <i>Numerical Considerations</i>	<i>288</i>
<i>Appendix 13A: Fourier Series and the Boundary</i> <i>Conditions</i>	 <i>293</i>

Part V Model Calibration and Applications

<i>14 Chesapeake Bay</i>	<i>299</i>
14.1 <i>Introduction</i>	<i>299</i>
14.2 <i>Ammonia</i>	<i>301</i>
14.3 <i>Nitrate</i>	<i>308</i>
14.4 <i>Sulfide</i>	<i>311</i>
14.5 <i>Oxygen</i>	<i>313</i>
14.6 <i>Phosphate</i>	<i>318</i>
14.7 <i>Silica</i>	<i>324</i>
14.8 <i>Station Composite Plots</i>	<i>328</i>
14.9 <i>Conclusions</i>	<i>332</i>
 <i>15 MERL, Long Island Sound, and Lake Champlain</i>	 <i>335</i>

xii CONTENTS

15.1	<i>Introduction</i>	335
15.2	<i>MERL</i>	335
15.3	<i>Long Island Sound</i>	349
15.4	<i>Lake Champlain</i>	355
15.5	<i>Summary of Parameter Values Used in All Applications</i>	361
16	<i>Steady State and Time Variable Behavior</i>	367
16.1	<i>Introduction</i>	367
16.2	<i>Steady State Model</i>	367
16.3	<i>Model Sensitivity</i>	371
16.4	<i>Time to Steady State</i>	379
16.5	<i>Conclusions</i>	387
	<i>Appendix 16A: Model Equations</i>	389
 <i>Part VI Metals</i>		
17	<i>Calcium and Alkalinity</i>	395
17.1	<i>Introduction</i>	395
17.2	<i>Calcium Carbonate</i>	395
17.3	<i>Chemistry and Simplifications</i>	396
17.4	<i>Closed System</i>	398
17.5	<i>Sediment Model Equations and Solutions</i>	401
17.6	<i>Application to Long Island Sound</i>	406
17.7	<i>Conclusion</i>	408
18	<i>Manganese I: Sediment Flux</i>	409
18.1	<i>Introduction</i>	409
18.2	<i>Steady State Model</i>	413
18.3	<i>Time Variable Model</i>	426
18.4	<i>Effect of pH</i>	439
	<i>Appendix 18A: MACSYMA</i>	449
19	<i>Manganese II: Overlying Water-Sediment Interaction</i>	453
19.1	<i>Introduction</i>	453
19.2	<i>Model Formulation</i>	456
19.3	<i>Time Variable Model</i>	464

19.4	<i>Calibration</i>	467
	Appendix 19A: MACSYMA	475
20	<i>Iron Flux Model</i>	479
20.1	<i>Introduction</i>	479
20.2	<i>Iron Chemistry</i>	479
20.3	<i>Model Configuration</i>	482
20.4	<i>Application to Onondaga Lake</i>	485
20.5	<i>Application to the Croton Reservoir</i>	501
20.6	<i>Model Framework</i>	503
20.7	<i>Summary</i>	506
21	<i>Cadmium and Iron</i>	509
21.1	<i>Introduction</i>	509
21.2	<i>Toxicity of Metals</i>	510
21.3	<i>Model Structure</i>	511
21.4	<i>Model Framework</i>	512
21.5	<i>Solution Method</i>	520
21.6	<i>Applications</i>	521
21.7	<i>Conclusions</i>	535
	Appendix 21A: Partitioning Equations	536
A.1	<i>FeS Partitioning</i>	536
A.2	<i>Cadmium Partitioning</i>	537
	Appendix 21B: MACSYMA	539
	<i>Appendix A: Data Tables</i>	541
A.1	<i>Chesapeake Bay</i>	542
A.2	<i>MERL</i>	542
A.3	<i>Lake Champlain</i>	543
	<i>Appendix B: Computer Program</i>	567
	<i>Nomenclature</i>	581
	<i>Bibliography</i>	593
	<i>Index</i>	613

Nitrate Source from the Overlying Water

$$J[\text{NO}_3] = -s \left(1 - \frac{s}{\kappa_{\text{NO}_3,1}^2/s + s + \kappa_{\text{NO}_3,2}^*} \right) [\text{NO}_3(0)]$$

Normalized nitrate flux

$$\frac{J[\text{NO}_3]}{[\text{NO}_3(0)]} = -s \left(1 - \frac{s}{\kappa_{\text{NO}_3,1}^2/s + s + \kappa_{\text{NO}_3,2}^*} \right)$$

For large s

$$\frac{J[\text{NO}_3]}{[\text{NO}_3(0)]} = -\kappa_{\text{NO}_3,2}^* = - \left(\frac{1}{\kappa_{\text{NO}_3,2}} + \frac{1}{K_{\text{L}12}} \right)^{-1}$$

Constant, limited by either mass transfer $K_{\text{L}12}$ or denitrification rate $\kappa_{\text{NO}_3,2}$

Nitrate Source from the Overlying Water

For small s

$$\frac{J[\text{NO}_3]}{[\text{NO}_3(0)]} = -s \quad s \rightarrow 0$$

$$\frac{J[\text{NO}_3]}{[\text{NO}_3(0)]} = -s = -\frac{\text{SOD}}{[\text{O}_2(0)]} = \frac{J[\text{O}_2]}{[\text{O}_2(0)]}$$

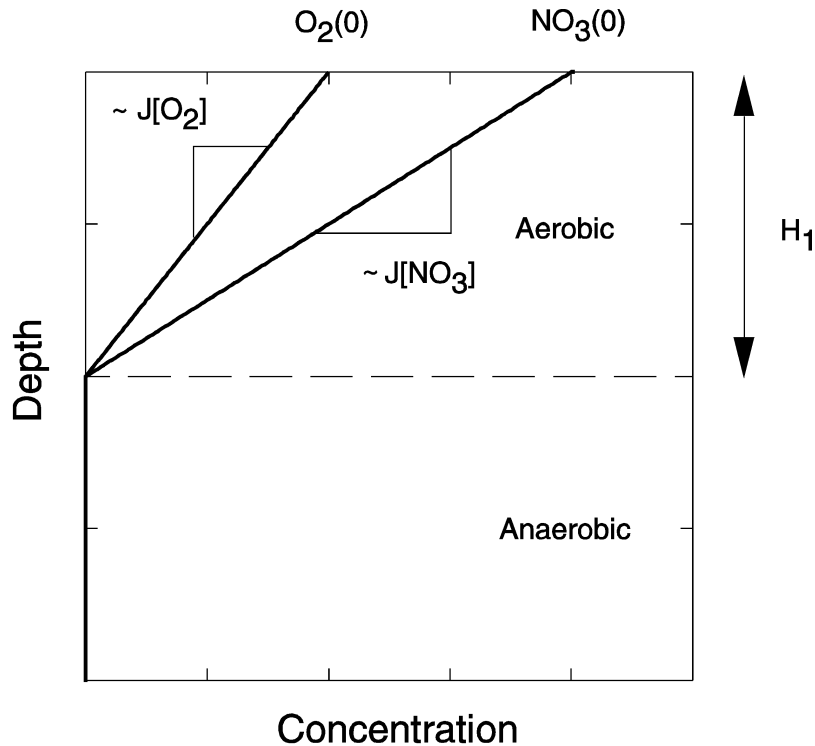


Figure 2: Vertical profiles of oxygen and nitrate.